TECHNICAL UNIVERSITY OF CRETE
DEPART. OF PRODUCTION ENGINEERING & MANAGEMENT

APPLICATION OF THE MOTORWAY TRAFFIC SURVEILLANCE

TOOL RENAISSANCE TO THE ITALIAN A3 MOTORWAY:

ESTIMATION AND PREDICTION ASSESSMENT

A thesis submitted for the satisfaction of the partial requirements for the degree of

MASTER OF OPERATIONAL RESEARCH

of the Department of

Production Engineering & Management

by

Tzimitsi Athina

Chania, 2007

This thesis is approved by:

1. Professor Markos Papageorgiou (supervisor):_____

2. Assistant Professor Elias Kosmatopoulos:_____

3. Lecturer Ioannis Papamichail:_____

Table of Contents

List of Figures

List of Tables

8

ACKNOWLEDGMENTS

I would like to thank my supervisor Prof. Markos Papageorgiou for the opportunity that he gave me to work on this subject.

I wish to express my gratitude to Dr. Yibing Wang for his guidance throughout this work.

I would also like to thank my colleagues in the Dynamic Systems and Simulation Laboratory for their friendship and the interesting and useful discussions.

Finally, I thank all the six members of my family for their love and for always supporting my decisions.

SHORT CURRICULUM VITAE

Athina Tzimitsi was born in Naoussa in March 26, 1974. At 2005 she took the diploma of Production Engineering and Management at the Technical University of Crete. Her diploma thesis was about neural network training on the tic tac toe game using evolutionary algorithms. Since 2005 she has been working as an associated partner in the Dynamic Systems and Simulation Laboratory. In the frames of this partnership she has been involved in several research programs and has come by experience to the development and simulation of traffic control strategies. She has taught, as a teaching assistant, to undergraduates of the department.

ΠΕΡΙΛΗΨΗ

Η εκτίμηση σε πραγματικό χρόνο της κυκλοφοριακής κατάστασης ενός αυτοκινητόδρομου αναφέρεται στην εκτίμηση των μακροσκοπικών μεταβλητών της κυκλοφοριακής ροής (ροές, μέσες ταχύτητες και πυκνότητες) ενός οδικού δικτύου με επαρκή χωρική και χρονική ανάλυση (π.χ. 500m και 10sec), βασισμένη σε ένα περιορισμένο αριθμό διαθέσιμων μετρήσεων από τους κυκλοφοριακούς φωρατές. Ας σημειωθεί ότι ο αριθμός των υπό εκτίμηση μεταβλητών κυκλοφοριακής ροής μπορεί να είναι πολύ μεγαλύτερος από τον αριθμό των άμεσα μετρούμενων μεταβλητών και αυτή είναι η ουσιαστική συμβολή της εκτίμησης κυκλοφοριακής κατάστασης αυτοκινητόδρομου. Η εκτίμηση κυκλοφοριακής κατάστασης σε πραγματικό χρόνο είναι μια θεμελιώδης προϋπόθεση για την επιτήρηση και τον έλεγχο της κυκλοφορίας ενός αυτοκινητόδρομου. Με την υποστήριξη ενός Ευρωπαϊκού προγράμματος, αναπτύχθηκε τελευταία το εργαλείο RENAISSANCE για την επιτήρηση κυκλοφορίας αυτοκινητόδρομου σε πραγματικό χρόνο. Το RENAISSANCE βασίζεται στη μακροσκοπική μοντελοποίηση κυκλοφοριακής ροής οδικού δικτύου και στο επεκταμένο φίλτρο Kalman, για την εκτίμηση της κυκλοφοριακής κατάστασης (καθώς και άλλων στοιχείων κυκλοφοριακής επιτήρησης πραγματικού χρόνου) σαν μια καθολική πρότυπη προσέγγιση.

Αυτή η εργασία αναφέρεται στην εφαρμογή του RENAISSANCE σε πραγματικό χρόνο στον αυτοκινητόδρομο Α3 (Νάπολη - Σαλέρνο, 50 km διπλής κατεύθυνσης) στην Ιταλία και συγκεκριμένα, στα αποτελέσματα εκτίμησης της κυκλοφοριακής κατάστασης του αυτοκινητόδρομου με βάση το εργαλείο RENAISSANCE. Στην εργασία αρχικά γίνεται μια εισαγωγή ενός μακροσκοπικού μοντέλου κυκλοφοριακής ροής οδικού δικτύου και ενός μοντέλου μέτρησης κυκλοφορίας σε πραγματικό χρόνο, για κάθε ένα από τα οποία εφαρμόζεται ένα ολοκληρωμένο δυναμικό μοντέλο για οδικό δίκτυο κυκλοφορίας. Κατά την

κατασκευή αυτού του δυναμικού μοντέλου δίνεται ιδιαίτερη προσοχή στη διαχείριση μερικών σημαντικών παραμέτρων του. Ακολουθεί μια παρουσίαση του εκτιμητή κυκλοφοριακής κατάστασης RENAISSANCE βασισμένο στο επεκταμένο φίλτρο Kalman καθώς και στη λειτουργική αρχιτεκτονική του RENAISSANCE. Εν συνεχεία, παρουσιάζεται ο αυτοκινητόδρομος Α3 (Νάπολη - Σαλέρνο) στην Ιταλία, ο τρόπος τοποθέτησης των φωρατών, η μακροσκοπική μοντελοποίηση δικτύου κυκλοφοριακής ροής και η αντίστοιχη διαμόρφωση του RENAISSANCE για την εφαρμογή του στην εκτίμηση κυκλοφοριακής κατάστασης στον Α3. Κατόπιν, η εργασία επικεντρώνεται στα αποτελέσματα της εκτίμησης της κυκλοφοριακής κατάστασης στον Α3. Ο διπλής κατεύθυνσης αυτοκινητόδρομος Α3 χωρίζεται σε 10 διαδοχικά μέρη (καθένα και για τις δύο κατευθύνσεις). Στο σημείο αυτό παρουσιάζονται κάποια αντιπροσωπευτικά αποτελέσματα ελέγχου από ορισμένα μέρη, κυρίως αυτών που είναι κοντά στη Νάπολη (στην κατεύθυνση προς Νάπολη) που είναι γενικά τα πιο κορεσμένα σε όλο τον Α3. Τα επιτευχθέντα αποτελέσματα κρίνονται αρκετά ικανοποιητικά και ελπιδοφόρα για την περαιτέρω εφαρμογή του εργαλείου. Τέλος, καταλήγει σε κάποια απορρέοντα συμπεράσματα και συστάσεις βασισμένες στην εμπειρία που αποκτήθηκε.

ABSTRACT

A generic macroscopic model-based approach to real-time freeway network traffic surveillance has recently been investigated and a software tool RENAISSANCE has been developed to implement the approach for field applications. On the basis of stochastic macroscopic freeway network traffic flow modeling, extended Kalman filtering, and a limited amount of traffic measurements, RENAISSANCE enables a number of real-time freeway network traffic surveillance tasks, including traffic state estimation and prediction, travel time estimation and prediction, queue tracking, and incident alarms. RENAISSANCE can be employed as an intermediate layer between real-time traffic measurements and various traffic operations and aims to deliver a complete real-time image of the current and future network traffic conditions, especially in case of sparse detector installation. RENAISSANCE has been operating in the Naples motorway traffic control center since early April of 2006 to supervise in real time traffic conditions in the A3 motorway between Naples and Salerno. This thesis first introduces the macroscopic freeway network traffic flow model and real-time traffic measurement model employed by RENAISSANCE, describes the tool's various traffic surveillance algorithms, and outlines its functional architecture. The thesis then focuses on real-time large-scale field application of the RENAISSANCE traffic state estimation and prediction functions to the A3 motorway. The obtained results are deemed quite satisfactory and promising for further application of the tool. A number of representative testing results are presented in the thesis. Finally, some recommendations based on the experience gained from thorough testing are given.

Στις Μαρία και Θωμαή

It is a concern in traffic engineering that on one hand traffic operators in traffic control centers can hardly handle manually a flood of traffic measurement data arriving at a frequency of at most a couple of minutes so as to extract significant information in real time for various use; on the other hand, even if traffic operators could deal promptly with available measurement data, the noisy measurements from a limited number of locally installed detectors may still not suffice to provide complete information that would be needed; this is typically the case when traffic detectors are relatively sparsely installed within motorway networks. In other words, the available local measurement data may already be too much in quantity to be processed manually in real time, but at the same time still too little, in terms of its spatial coverage, for further applications [1].

A number of traffic surveillance approaches [1-11] have been developed to address such problems. Real-time motorway network traffic surveillance is essentially a dynamic information extraction process, whereby a large amount of raw traffic measurement data is appropriately processed in real time leading to the complete, succinct, and reliable information that traffic operators can definitely base their decisions on. Normally, such processed information includes:

- estimation of **traffic flow variables** (flows, mean speeds, and densities) with an adequate spatial resolution (e.g. 500 m or less) based on a limited amount of real-time local and noisy traffic measurements (**traffic state estimation**);

- prediction of traffic flow variables with the same spatial resolution over a future time horizon of e.g. 20 minutes from each current time instant (**traffic state prediction**);

- prediction of travel time to be experienced along specific routes within a considered motorway network if the trip is started at each current time instant (**travel time prediction**);

- estimation/prediction of queue (congestion) lengths currently existing/to appear over a future time horizon within a considered motorway network (**queue length estimation/prediction**);

- alarms regarding any abnormal traffic event (**incident alarm**).

The software tool **RENAISSANCE** [1] has recently been developed to implement all these traffic surveillance tasks in a unified macroscopic model-based approach (Figure 1). As depicted in Figure 2, RENAISSANCE can be employed as an intermediate layer between real-time traffic measurements and various traffic operations and aims to deliver a **complete real-time image** of the current and future network traffic conditions, especially in case of sparse detector installation. The different colors and widths of links inside the estimated network block in Figure 2 represent different kinds of traffic condition (e.g. free, dense, congested, etc.) identified in the corresponding links. Such a global image of the estimated network traffic conditions is updated at least as frequently as traffic measurements (usually 30 seconds to 1 minute). All real-time information, extended and enriched by RENAISSANCE, may either be provided to traffic operators as a decision support or be exploited for more efficient operations in motorway networks, e.g. driver information and guidance, traffic control, etc.

As indicated in Figure 1, the traffic state estimation is the most fundamental task of RENAISSANCE as all other surveillance tasks (including traffic state prediction) are
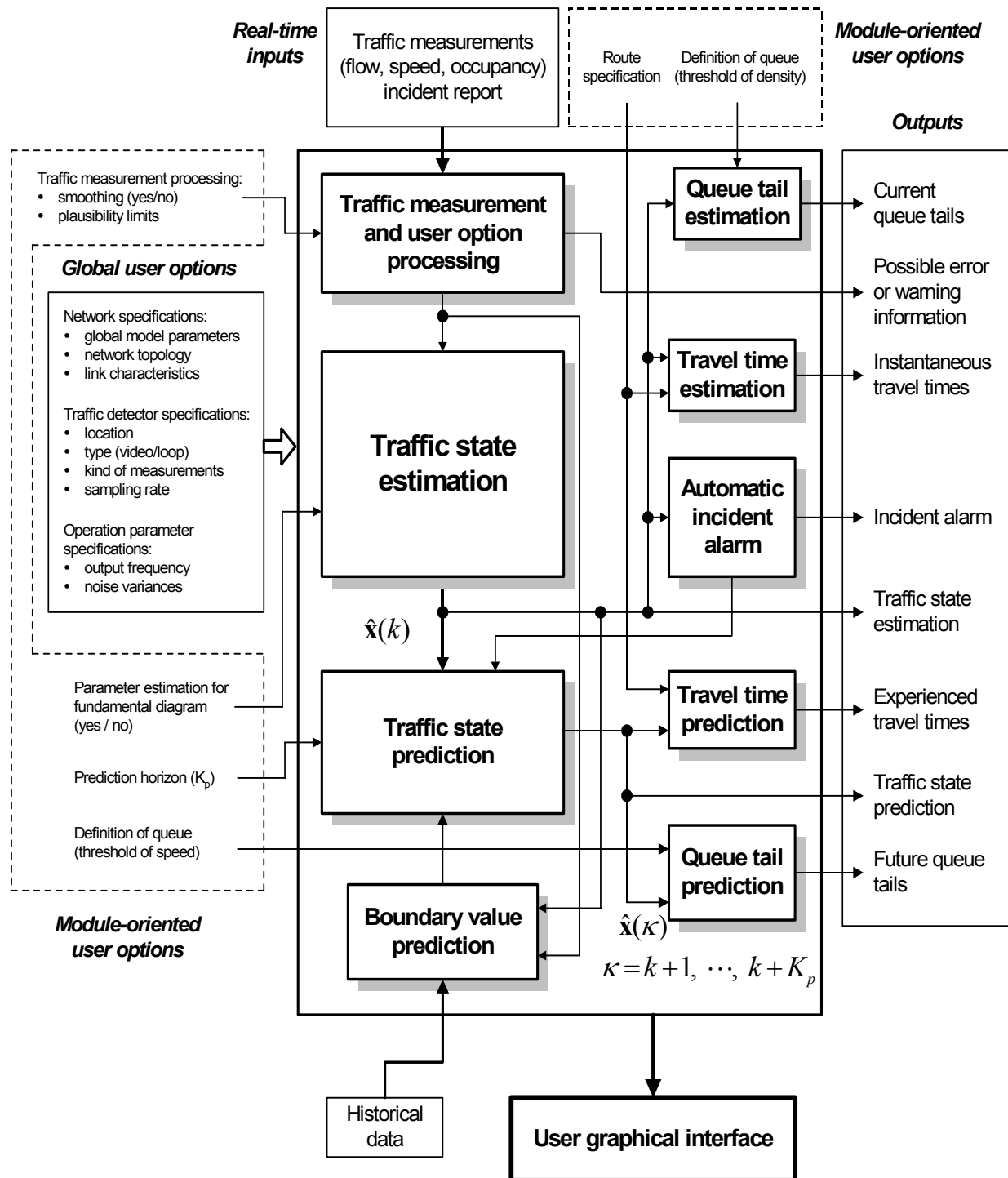
Figure 1: Functional architecture of RENAISSANCE

performed on the basis of the traffic state estimation results. Note also that the number of traffic

flow variables to be estimated for a motorway network (represented in Figure 2 with the

colored links) may be much larger than those directly measured (represented in Figure 2 with

the red dots), especially in case of sparse detector installation, and this is in fact the essential
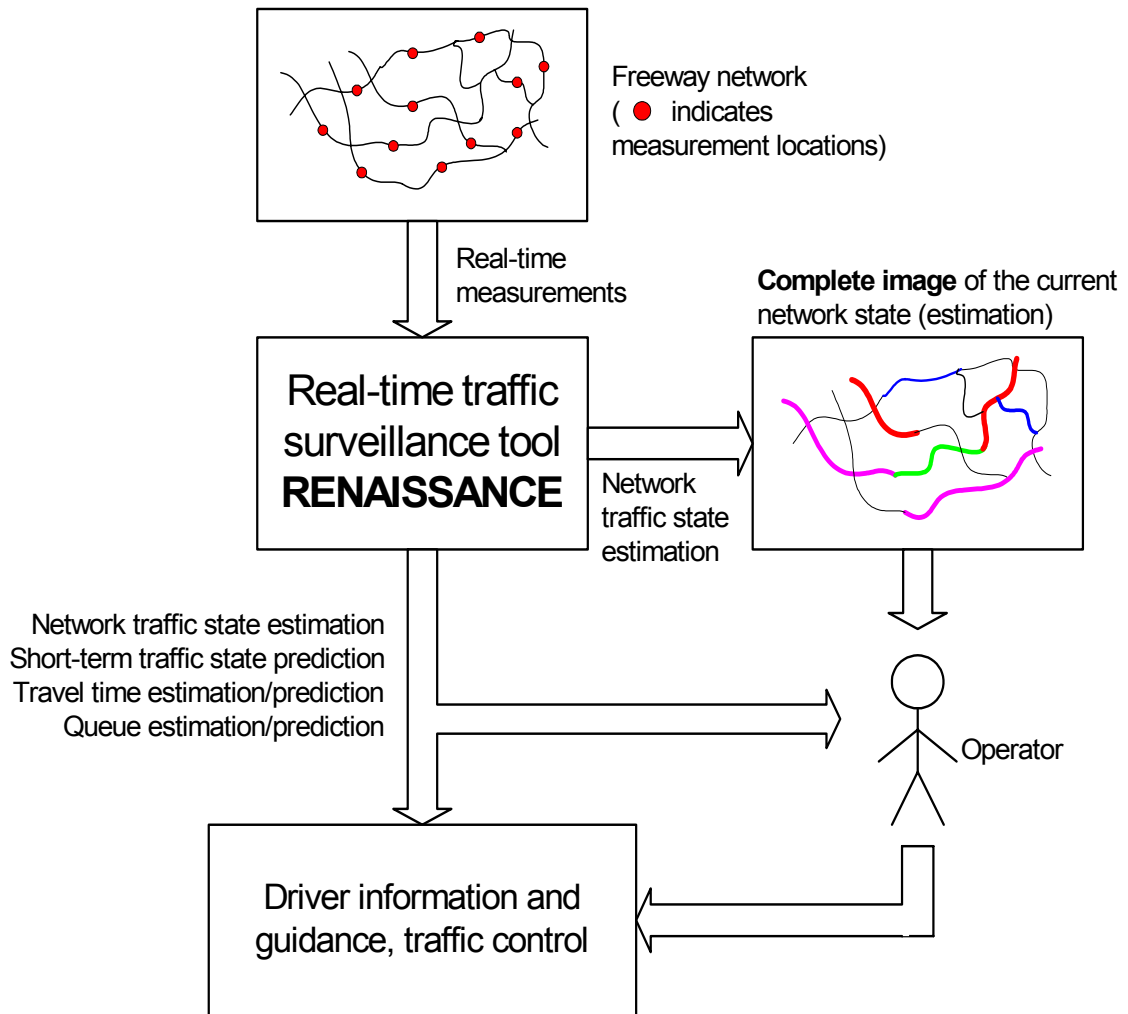
Figure 2: The role of the RENAISSANCE

contribution of the motorway traffic state estimation task. Investigations on traffic state estimation dates back to the early 1970s (see e.g. [3, 4]) and has attracted considerable efforts in the past 20 years (see e.g. [5-9]). Following the extended-Kalman-filter (**EKF**) avenue pursued in some previous work, this topic was recently investigated further, and a general approach to the design of motorway traffic state estimators was proposed in [10]. One major innovative feature of this recent work is the on-line model parameter estimation, which leads to some significant adaptive capabilities for the designed estimator [11]. The traffic state estimator developed in this general approach has been integrated into RENAISSANCE as one of its major functional modules.

Motorway traffic is a large-scale nonlinear dynamic process; in particular, traffic dynamics of motorway networks are more complex than single motorway stretches. So far, only **simulation investigation** of traffic state estimation and prediction has been reported for motorway **networks** [1]. Since early May of 2006, RENAISSANCE has been operating in the motorway traffic control center of Naples, Italy, supervising the A3 motorway between Naples and Salerno of 47.5 km. This thesis reports some representative traffic state estimation and prediction results of RENAISSANCE from A3. Due to its complex topological layout and measurement availability, the dual-direction A3 motorway is actually a motorway network, as seen from the point of view of system modeling. It would probably be the first time to report real-time traffic state estimation and prediction results of so large-scale a freeway network.

In what follows, Chapter 2 presents the dynamic system modeling of RENAISSANCE. Chapter 3 introduces various traffic surveillance tasks of RENAISSANCE and the corresponding algorithm design. Chapter 4 briefly describes the A3 motorway and its modeling with RENAISSANCE. The field tests of RENAISSANCE's traffic state estimation and prediction functions with regard to A3 are reported in Chapters 5 and 6. Chapter 7 addresses the issue of inner congestions with some countermeasures and recommendations given. Finally, some conclusive remarks are given in Chapter 8.

2.1 Stochastic Macroscopic Motorway Network Traffic Flow Model

A motorway network may be represented as a directed graph. More precisely, bifurcations, junctions, on-ramps, and off-ramps are represented by the **nodes**, whereas the motorway stretches between these locations are represented by the **links** of the graph. The two directions of a motorway stretch are modeled as separate links with opposite directions. Inside each link we suppose homogeneous geometric characteristics such as number of lanes, grade, curvature, etc. A geometrically inhomogeneous motorway stretch is represented by two or more consecutive links separated by nodes at the locations where geometrical changes occur. At the bounds of the network, origins or destinations are added where traffic enters or leaves, respectively, the simulated network.

A stochastic version of a validated second-order macroscopic traffic flow model [12-15] is employed in RENAISSANCE to describe the traffic flow dynamics in considered motorway networks of any topology, size, and characteristics. More precisely, the dynamic behavior of traffic flow along motorway links is described in terms of appropriate aggregated **traffic flow variables** (space mean speeds, traffic densities, and flows), while the distribution of traffic flow at bifurcation nodes is modeled in terms of **turning rates**. This traffic flow model can simulate all kinds of traffic conditions (free-flow, dense, and congested) and capacity-reducing events (incidents) with prescribed characteristics (location, intensity, and duration).

2.1.1 Modeling of motorway links

The utilized macroscopic traffic flow model defines three main types of links for any considered motorway network, which are normal links, origin links, and destination links. Ordinary motorway stretches are modeled with the normal links, whereas the origin links and destination links address network origins and destinations, respectively. For the convenience of modeling and digital computation, the model is presented in a space-time discretized form. More specifically, for the space discretization any normal link m is sub-divided into a number N_m of segments each with a length Δ_m, while the time discretization is based on a model time step T and the discrete time index $k = 0, 1, 2, \cdots$. The macroscopic aggregated traffic flow variables are accordingly defined in this discrete space-time frame as follows:

1. traffic density $\rho_{m,i}(k)$ (in veh/km/lane) is the number of vehicles in segment i of link m at time instant kT, divided successively by the segment length Δ_m and number of lanes λ_m;

2. space mean speed $v_{m,i}(k)$ (in km/h) is the average speed of all vehicles included in segment i of link m at time instant kT;

3. traffic flow $q_{m,i}(k)$ (in veh/h) is the number of vehicles leaving segment i of link m during the time period $[kT, (k+1)T]$, divided by T.

It is shown by Papageorgiou *et al*. [12] that the macroscopic model works pretty accurately with segment lengths Δ_m in the order of 500 m (or less) and model time step T in the order of 10 s. For a segment i of a link m the stochastic nonlinear difference equations of the second-order macroscopic traffic flow model are as follows:

$$\rho_{m,i}(k+1) = \rho_{m,i}(k) + \frac{T}{\Delta_m \lambda_m}[q_{m,i-1}(k) - q_{m,i}(k)], \tag{1}$$

$$v_{m,i}(k+1) = v_{m,i}(k) + \frac{T}{\tau}[V_m(\rho_{m,i}(k)) - v_{m,i}(k)] + \frac{T}{\Delta_m} v_{m,i}(k)[v_{m,i-1}(k) - v_{m,i}(k)]$$

$$- \frac{\nu T}{\tau \Delta_m} \frac{[\rho_{m,i+1}(k) - \rho_{m,i}(k)]}{\rho_{m,i}(k) + \kappa} + \xi^v_{m,i}(k), \tag{2}$$

$$V_m(\rho) = v_{f,m} \exp\left[-\frac{1}{a_m}\left(\frac{\rho}{\rho_{cr,m}}\right)^{a_m}\right], \tag{3}$$

$$q_{m,i}(k) = \rho_{m,i}(k) \cdot v_{m,i}(k) \cdot \lambda_m + \xi^q_{m,i}(k), \tag{4}$$

where equations (1)-(4) are the well-known conservation equation, dynamic speed equation, stationary speed equation, and transport equation, respectively; τ, ν, κ, $v_{f,m}$, $\rho_{cr,m}$, and a_m are model parameters; in particular, τ, ν, κ are given the same values for the whole network, whereas $v_{f,m}$ denotes the free speed, $\rho_{cr,m}$ the critical density, and a_m the exponent in the stationary speed equation (3) for link m; $\xi^v_{m,i}(k)$ and $\xi^q_{m,i}(k)$ denote noise acting on the empirical speed equation and approximate transport equation, respectively. Note that (1) is not corrupted by noise as it reflects the conservation of vehicles, which holds strictly in any case. The model parameter values are normally unknown beforehand and may be identified via an off-line model calibration procedure (see e.g. [16]), but they may change in real-time due to changing external conditions (weather and light conditions, percentage of trucks, variable speed limits, etc.); hence it would be best to estimate them on-line (based on real-time traffic measurements). On the other hand, it was demonstrated in [12] that the model results are most sensitive to the variations of the free speed, critical density, and exponent values. Therefore, this work only regards the free speed, critical density, and exponent as the unknown model parameters (for on-line estimation), while the values of the other model parameters are determined by off-line model calibration. Based on the fundamental diagram $Q_m(\rho) = \rho \cdot V_m(\rho)$ the capacity of link m (per lane) may be deduced from (3) as

$$q_{cap,m} = v_{f,m} \cdot \rho_{cr,m} \cdot \exp[-1/a_m].$$

With (4) replaced in (1) and (3) in (2), the above segment model is reduced to two equations with two segment variables $\rho_{m,i}(k)$ and $v_{m,i}(k)$; and three segment boundary variables $q_{m,i-1}(k)$, $v_{m,i-1}(k)$, and $\rho_{m,i+1}(k)$. If any link m is considered as a tandem connection of its segments, then the complete macroscopic model of link m can be built upon a chain of interconnected segment models with a total of $2N_m$ dynamic equations with the **segment variables** $\rho_{m,1}$, $v_{m,1}$, $\rho_{m,2}$, $v_{m,2}$, …, ρ_{m,N_m}, v_{m,N_m}; this model includes three link **boundary variables**: (a) flow $q_{m,0}$ at the upper boundary of link m (needed in (1) for $i=1$); (b) speed $v_{m,0}$ at the upper boundary of link m (needed in (2) for $i=1$); (c) density ρ_{m,N_m+1} at the lower boundary of link m (needed in (2) for $i=N_m$). These boundary variables are exogenous variables for the link model, which are determined by the node model (6)-(8).

The other two types of links are origin and destination links. Each origin link is modeled as a waiting queue that receives traffic demand and forwards it into the simulated motorway network; the outflow of an origin link is determined based on the current demand and queue length, its capacity, and the downstream traffic conditions. On the other hand, each destination link is characterized by its density; in the case of congestion spillback from downstream of the network, traffic densities at the destination links are used to limit the corresponding network outflows.

2.1.2   Modeling of motorway nodes

Links are interconnected by nodes. Traffic enters a node n through a number of inflowing links according to

$$Q_n(k) = \sum_{\mu \in I_n} q_{\mu, N_\mu}(k),$$ (5)

where I_n denotes the set of the links entering node n, q_{μ, N_μ} represents the flow in the last segment of an entering link μ, and $Q_n(k)$ is the total traffic flow reaching node n during time period $[kT, (k+1)T]$. On the other hand, traffic leaves a node n via an outgoing link m according to

$$q_{m,0}(k) = Q_n(k) \cdot \beta_n^m(k), \qquad \forall m \in O_n,$$ (6)

where O_n is the set of links leaving node n, $q_{m,0}(k)$ is the traffic flow leaving node n via an exiting link m during time period $[kT, (k+1)T]$, and **turning rate** $\beta_n^m(k)$ is defined as the percentage of $Q_n(k)$ that leaves node n via link m during the same time period. The turning rate at the bifurcation node immediately upstream of an off-ramp is also called the **exiting rate** at the off-ramp.

For a merging node n, the impact of the upstream-segment speeds on the downstream traffic conditions is considered via the flow-weighted average

$$v_{m,0}(k) = \sum_{\mu \in I_n} v_{\mu, N_\mu}(k) \cdot q_{\mu, N_\mu}(k) \cdot [\sum_{\mu \in I_n} q_{\mu, N_\mu}(k)]^{-1}$$ (7)

where $v_{m,0}(k)$ is the virtual upstream speed of a leaving link m of node n while q_{μ, N_μ}, respectively, v_{μ, N_μ} represent the flow, respectively, mean speed in the last segment of an entering link μ of the node.

For a bifurcation node n, the influence of the downstream-segment densities on the upstream traffic conditions is considered via the quadratic average

$$\rho_{m, N_m+1}(k) = \sum_{\mu \in O_n} \rho_{\mu,1}^2(k) \cdot [\sum_{\mu \in O_n} \rho_{\mu,1}(k)]^{-1}$$ (8)

where ρ_{m,N_m+1} is the virtual downstream density of an entering link m and $\rho_{\mu,1}$ is the traffic density in the first segment of a leaving link μ. This quadratic form accounts for the fact that, even if one leaving link is strongly congested, it could be sufficient for the congestion to spill back towards the entering links.

The overall traffic flow model of a motorway network can be built upon the link models and node models. Note that the boundary variables of each normal link are delivered by the node model (6)-(8). Therefore, the **traffic flow variables** involved in the overall network model include:

4. **Segment variables**: space mean speed and density (as well as flow) of each segment.

5. **Network boundary variables**: (a) inflow at each origin link, (b) inflow speed at each origin link, (c) density at each destination link, and (d) turning rate (or exiting rate) at each bifurcation node.

Besides, the model is also related to

6. **Important model parameters**: (a) free speed, (b) critical density, and (c) exponent or capacity of each normal link.

For information regarding the validation, efficiency, and accuracy of the deterministic version of this macroscopic traffic flow model, the reader is referred to [12, 13] for the case of motorway stretches and [15] for the case of motorway networks.

2.2   Model of Traffic Measurements

Traffic detectors are installed along motorway stretches at a separation up to several kilometers as a main device for obtaining real-time traffic measurements. Consider a traffic detector

installed at the boundary of two adjacent segments i and $i+1$ of a link m. For the flow measurements, we have via (4)

$$y^q_{m,i}(k) = \rho_{m,i}(k) \cdot v_{m,i}(k) \cdot \lambda_m + \xi^q_{m,i}(k) + \gamma^q_{m,i}(k), \qquad (9)$$

where $y^q_{m,i}(k)$ denotes the flow measurement during the period $[kT,\ (k+1)T]$ and $\gamma^q_{m,i}(k)$ the flow measurement noise. For the mean speed measurements, we have

$$y^v_{m,i}(k) = v_{m,i}(k) + \gamma^v_{m,i}(k), \qquad (10)$$

where $y^v_{m,i}(k)$ denotes the space mean speed that may be calculated as the harmonic mean of individual-vehicle speed measurements collected during the period $[kT,\ (k+1)T]$ and $\gamma^v_{m,i}(k)$ the corresponding measurement noise. Regarding on-ramps and off-ramps, only flow measurements are needed. The flow measurement $y^q_o(k)$ at an on-ramp o during the period $[kT,\ (k+1)T]$ can be expressed as

$$y^q_o(k) = q_o(k) + \gamma^q_o(k), \qquad (11)$$

where $\gamma^q_o(k)$ denotes the corresponding measurement noise. For an off-ramp d with its upstream bifurcation node n, the off-ramp flow measurement $y^q_d(k)$ during the period $[kT,\ (k+1)T]$ can be modeled via (6) as

$$y^q_d(k) = \beta^d_n(k) \cdot Q_n(k) + \gamma^q_d(k), \qquad (12)$$

where $\gamma^q_d(k)$ denotes the corresponding measurement noise.

It should be noted that the utilized real-time measurements must reflect a feasible detector configuration that guarantees observability of any flow variable within the network. For example, a bifurcation node is not flow-observable if only one out of three adjacent links is equipped with traffic detectors. Flow observability in this case calls for flow measurements (or estimates) at least for two (out of three) adjacent links (even if the corresponding detectors are

31

placed relatively far from the bifurcation node). Once flow observability is guaranteed, the density of available detectors on motorway stretches was found to have a moderate impact on the estimation quality [1].

2.3   Dynamic System Model of RENAISSANCE

The overall motorway network traffic flow model can be expressed in a compact state-space form:

$$\mathbf{z}(k+1) = \mathbf{h}[\mathbf{z}(k), \mathbf{d}(k), \mathbf{p}(k), \xi_1(k)], \tag{13}$$

where $\mathbf{h}$ is a nonlinear differential vector function that corresponds to (1)-(4) for each involved segment and (5)-(8) for each involved node, vector $\mathbf{z}$ includes all segment variables, vector $\mathbf{d}$ includes all network boundary variables, vector $\mathbf{p}$ includes all interested model parameters, vector ξ_1 includes all modeling noise. Considering that $\mathbf{d}(k)$ may not be fully measured (or measurable) in real time and that $\mathbf{p}(k)$ are normally unknown, two random-walk equations are introduced for them: $\mathbf{d}(k+1) = \mathbf{d}(k) + \xi_2(k)$ and $\mathbf{p}(k+1) = \mathbf{p}(k) + \xi_3(k)$, and the combination of (13) and both random-walk equations leads to the following augmented state-space model

$$\mathbf{x}(k+1) = \mathbf{f}[\mathbf{x}(k), \xi(k)], \tag{14}$$

where $\mathbf{x} = \begin{bmatrix} \mathbf{z}^T & \mathbf{d}^T & \mathbf{p}^T \end{bmatrix}^T$, $\xi = \begin{bmatrix} \xi_1^T & \xi_2^T & \xi_3^T \end{bmatrix}^T$, and the nonlinear differentiable vector function $\mathbf{f}$ can be determined accordingly. In this thesis, the **state vector** $\mathbf{x}$ is referred to as the **traffic state** of a considered motorway network (to be estimated).

On the other hand, all network traffic measurements formulated by (9)-(12) can be expressed via

$$\mathbf{y}(k) = \mathbf{g}[\mathbf{x}(k), \ \eta(k)], \tag{15}$$

where vector $\mathbf{y}$ consists of all available real-time measurements of flow and space mean speed; $\mathbf{g}$ is a nonlinear differentiable vector function; vector $\boldsymbol{\eta}$ is a function of state noise $\boldsymbol{\xi}$ and measurement noise $\boldsymbol{\gamma}$. Equations (14) and (15) constitute a complete dynamic system model $\Sigma(\mathbf{x}, \mathbf{y}, \boldsymbol{\xi}, \boldsymbol{\eta})$ of motorway network traffic that is essential for RENAISSANCE to perform its traffic surveillance tasks. The reader is referred to [17] for further detail of the presented model.

The real-time motorway network traffic surveillance tasks addressed by RENAISSANCE include traffic state estimation and prediction, travel time estimation and prediction, queue tail/head/length estimation and prediction, and incident alarm. These traffic surveillance tasks are presented in this section under a unified macroscopic model-based framework.

3.1 Traffic State Estimation and Prediction

The **traffic state estimation** refers to estimating all traffic state variables of a considered motorway network (i.e. the elements of vector $\mathbf{x}$ in (14)) at each current time instant based on a limited amount of real-time traffic measurements, whereas the (short-term) **traffic state prediction** refers to predicting at each current time instant the segment variables (i.e. the elements of vector $\mathbf{z}$ in (13)) over a future time horizon (normally 15-60 min). Note that **the number of traffic flow variables to be estimated and predicted within a motorway network may be much larger than those that can be directly measured**, especially when the detectors are sparsely installed within the network.

3.1.1 Traffic state estimation algorithm

Considering that the model $\Sigma(\mathbf{x}, \mathbf{y}, \boldsymbol{\xi}, \boldsymbol{\eta})$ is highly nonlinear, the extended Kalman filter [18] is employed to design the traffic state estimator as

$$\hat{\mathbf{x}}(k+1/k) = \mathbf{f}[\hat{\mathbf{x}}(k/k-1),\ 0] + \mathbf{K}(k)[\mathbf{y}(k) - \mathbf{g}(\hat{\mathbf{x}}(k/k-1),\ 0)], \qquad (16)$$

where $\hat{\mathbf{x}}(k+1/k)$ denotes the traffic state estimation for time instant $k+1$ based on the traffic measurements available up to time instant k; $\mathbf{K}(k)$ is the gain matrix calculated on-line based on the linear Taylor expansion of $\mathbf{f}$ and $\mathbf{g}$ at $\hat{\mathbf{x}}(k/k-1)$. Because these calculations are recursive, $\mathbf{K}(k)$ is actually calculated based (implicitly) on traffic measurements at all previous time instants $k-1,\ k-2, \ldots$ The reader is referred to [10] for more details on (16). For the sake of simplicity, we will denote $\hat{\mathbf{x}}(k/k-1)$ by $\hat{\mathbf{x}}(k)$ in the sequel.

Keeping in mind the constitution of vector $\mathbf{x}$, (16) delivers the estimates of the involved segment variables simultaneously with those of the model parameters and network boundary variables. In fact, with (16), each model parameter can actually be handled in two alternative approaches: (a) keep the parameter value constant at a pre-specified value; (b) estimate the parameter value on-line. With approach (a), the values of the corresponding model parameters have to be pre-specified accurately; else the segment variable estimates may be biased [1, 10, 11]. With approach (b), initial parameter values (used for on-line parameter estimation) can be given quite arbitrarily, because the traffic state estimator (16) based on real-time traffic measurements is capable of identifying the actual model parameter values and even tracking their changes in real time [1, 10, 11].

Based on the canonical form $\Sigma(\mathbf{x}, \mathbf{y}, \boldsymbol{\xi}, \boldsymbol{\eta})$, (16) actually leads to a straightforward, unique, and simple formulation of the traffic state estimator for motorway networks of arbitrary topology, size, and characteristics, and with any suitable detector configuration; an extensive discussion can be found in [10] for the case of motorway stretches but the same underlying ideas and arguments apply to the case of motorway networks as well. It should also be mentioned that

(16) delivers a suboptimal solution to the nonlinear state estimation problem, as an optimal solution to this problem is infinitely dimensional.

3.1.2 Traffic state prediction algorithm

Neglecting the impact of unpredictable noise ξ_1, the network model (13) is written as

$$\mathbf{z}(k+1) = \mathbf{h}[\mathbf{z}(k), \mathbf{d}(k), \mathbf{p}(k), \mathbf{0}], \qquad (17)$$

Let $\hat{\mathbf{z}}(k)$, $\hat{\mathbf{d}}(k)$, and $\hat{\mathbf{p}}(k)$ denote, respectively, the estimates of $\mathbf{z}(k)$, $\mathbf{d}(k)$, and $\mathbf{p}(k)$. Let $\hat{\mathbf{d}}(\kappa)$, $\kappa = k+1,\ k+2,\cdots,\ k+\mathrm{K}_{\mathrm{p}}-1$, denote the prediction of $\mathbf{d}$ for the future $\mathrm{K}_{\mathrm{p}}-1$ steps. Note that at each time instant k,

1. The values $\hat{\mathbf{z}}(k)$, $\hat{\mathbf{d}}(k)$, and $\hat{\mathbf{p}}(k)$ are available with the traffic state estimator (16).

2. The model parameters are not strongly time-varying, so $\hat{\mathbf{p}}(\kappa)$ may be set equal to $\hat{\mathbf{p}}(k)$, for $\kappa = k+1,\cdots,\ k+\mathrm{K}_{\mathrm{p}}-1$;

3. $\hat{\mathbf{d}}(\kappa)$ is available for $\kappa = k+1,\cdots,\ k+\mathrm{K}_{\mathrm{p}}-1$ via the boundary value prediction (see section 3.1.3).

Thus, running (17) for K_{p} steps produces $\hat{\mathbf{z}}(\kappa)$, $\kappa = k+1,\cdots,\ k+\mathrm{K}_{\mathrm{p}}$, i.e. the pursued traffic state prediction.

3.1.3 Boundary value prediction

The boundary value prediction is indispensable to the traffic state prediction and can be performed based on historical data, or on extrapolation of the boundary variable estimates available up to the current time instant, or by an appropriate combination of both [1, 17].

3.2 Travel Time Estimation and Prediction

A **route** within a motorway network is a sequence of consecutive links that connect two specific network nodes. The **instantaneous** travel time along a route is an ideal travel time spent by an ideal vehicle traveling along that route under the currently prevailing traffic conditions. In other words, the instantaneous travel time is calculated based on an assumption that the segment speeds along the whole route are 'frozen' at the values they have, when a vehicle traverses the route. Consider a route including M consecutive links (each link m with N_m segments). Then the instantaneous travel time along the route at time instant k can be expressed as

$$\tau_1(k) = \sum_{m=1}^{M} \sum_{i=1}^{N_m} \frac{\Delta_m}{v_{m,i}(k)}.$$
(18)

The travel time **estimation** refers to estimating at each time instant k the **instantaneous** travel time along any specified route based on segment speed estimation. For the same route addressed in (18), we have

$$\hat{\tau}_1(k) = \sum_{m=1}^{M} \sum_{i=1}^{N_m} \frac{\Delta_m}{\hat{v}_{m,i}(k)},$$
(19)

where $\hat{v}_{m,i}(k)$ denotes the estimation of $v_{m,i}(k)$ obtained via (16) and $\hat{\tau}_1(k)$ the travel time estimation.

Experienced travel time along a route at a time instant k is the real travel time that vehicles leaving the origin of the route at k will actually experience on that route. With regard to the route already considered (with a total length $\sum_{m=1}^{M} N_m \Delta_m$), we denote by $\tau_2(k)$ the experienced travel time at time instant k, and by $v_k(t)$, $t \geq k$, the speed trajectory of addressed vehicles during the trip. Then we have

$$\sum_{m=1}^{M} N_m \Delta_m = \int_{k}^{k+\tau_2(k)} v_k(t)\,dt\,. \tag{22}$$

Travel time **prediction** means predicting the **experienced** travel time along any specified route at each current time instant. Corresponding to (22), we have

$$\sum_{m=1}^{M} N_m \Delta_m = \int_{k}^{k+\hat{\tau}_2(k)} \hat{v}_k(t)\,dt\,. \tag{23}$$

where $\hat{\tau}_2(k)$ and $\hat{v}_k(t)$ denote, respectively, the travel time prediction at time instant k and the prediction of $v_k(t)$ over a future time horizon.

It is difficult to express $\hat{\tau}_2(k)$ explicitly. However, based on the segment speed prediction (a part of traffic state prediction) conducted at time instant k along the route, $\hat{v}_k(t)$ is available over a future time horizon; then it is not difficult to calculate $\hat{\tau}_2(k)$ numerically with the aid of virtual cars [20]. More precisely, a virtual car is generated (inside the prediction model (17)) at the beginning of the route at time instant k, and moved segment after segment along the route according to the predicted speed prevailing in each segment at the time of the presence of the virtual car. After the virtual car arrives at the route end, the travel time prediction along that route for time instant k becomes known. Note that the utilized prediction horizon K_p should be sufficiently long so that a virtual car starting its trip at time instant k can complete its trip within this prediction horizon, i.e. $K_p \geq \tau_2(k)$, $\forall k$.

3.3 Queue Tail/Head/Length Estimation and Prediction

A vehicle queue (stop-and-go congestion) is defined for RENAISSANCE as a portion of the motorway where vehicles are moving at a speed below a user-selectable speed threshold. The tail of a vehicle queue is usually a congestion shockwave, while the head of a vehicle queue is

normally the location where the traffic congestion originates, e.g. a bottleneck, a traffic incident location, etc. Once a queue is built up within a motorway network, operators in the traffic control center (TCC) need to track in real time the dynamic evolution of the queue and, in particular, track how the queue tail is propagating. Such information allows operators to inform drivers, through VMS or other means, of the existence, extent and propagation of the queue. The drivers can then make their corresponding route choice or be instructed to use a speed that would prevent shockwave crashes. Moreover, accurate information on the length and position of the queue may help operators or automatic control algorithms to make more confident decisions on possible control actions to improve the traffic conditions. To this end, queue tail/head estimation (prediction) aims at estimating (predicting) the location of any queue tail/head existing (to appear) at the current (future) time instant(s). With the identified locations of queue tails and heads, the queue lengths are readily estimated and predicted. The queue tail/head estimation and prediction are based on the segment speed estimation and prediction. When the estimated/predicted mean speeds of some segments along a route are below a threshold value, one (or several) vehicular queue(s) is (are) considered to exist/to appear within the corresponding segments in that route.

3.4   Incident Alarm

The incident alarm intends to issue a warning regarding an abnormal traffic phenomenon, which could be due to a traffic incident. The underlying idea for the incident alarm is that any abnormal traffic flow behavior may be reflected in the drastically abrupt changes of some critical model parameter values that may be identified or even tracked in real-time via on-line model parameter estimation. Therefore, the real-time model parameter estimates may be used as indicators of abnormal traffic phenomena, the consequence of traffic incidents. Such an

approach to incident alarm was tested in simulation [10, 19] and with real data [11], and quite encouraging results were obtained.

3.5   The RENAISSANCE Architecture

A number of real-time motorway network traffic surveillance tasks have been presented in the preceding sections under a unified macroscopic model-based framework. To implement this unified approach for field applications, the software tool **RENAISSANCE** (**RE**al-time motorway **N**etwork tr**A**ff**I**c **S**tate **S**urveill**ANCE**) has recently been developed with the support of the European Project RHYTHM [19]. As already shown, with this unified approach, all surveillance tasks other than traffic state estimation and prediction are performed on the basis of the traffic state estimation or prediction results. Therefore, the traffic state estimation and prediction functions build the operating foundation of RENAISSANCE.

Figure 1 displays a schematic diagram of the functional architecture of RENAISSANCE. The highlighted central block represents the main body of the tool; whereas the included sub-blocks represent its various functional modules, most of which correspond to the aforementioned traffic surveillance tasks. The directed lines between the modules represent the signal flows. The external inputs to the tool include real-time traffic measurements (flow and mean speed or occupancy) and, possibly, incident reports from the TCC operators, while the outputs correspond to the tool's various functionalities. In addition, RENAISSANCE provides the users with quite a few options in order for the traffic surveillance tasks to be performed according to the specific user needs and application requirements. RENAISSANCE also includes a graphical user-friendly interface (GUI).

As depicted in Figure 2, RENAISSANCE can be employed as an intermediate layer between real-time traffic measurements and various traffic operations. The real-time information, extended and enriched by RENAISSANCE, may either be provided to traffic operators as a decision support or be exploited for more efficient operations in motorway networks, e.g. driver information and guidance, traffic control, etc. RENAISSANCE is a generic tool that is applicable in real time to motorway networks of arbitrary size, topology and characteristics, with any suitable traffic detector configuration; it is able to handle real-time measurements collected via inductive loops, radar detectors, video sensors, or via any combination of those. RENAISSANCE is actually the first and unique software tool so far developed that enables all addressed real-time motorway network traffic surveillance tasks in a systematic and unified way.

4.1   Site description

RENAISSANCE is currently operating in the South Italian motorway traffic control center in Naples to supervise the traffic conditions in both directions of the A3 motorway of about 47.5 km between Naples and Salerno (Figure 3). The A3 motorway was opened to traffic in the early 1960s to connect the municipalities of the coastal strip along the southern slope of Mount Vesuvius with Naples, the main city of the region. In the last decades, these municipalities have grown considerably despite the limited space between the coast and Vesuvius. Nowadays, this narrow area is among the most densely populated regions in Italy and, because most of the population commutes daily towards Napoli, the A3 motorway actually serves one of the most congested metropolitan areas in southern Italy. As a consequence, recurrent congestions occur in the A3 motorway, typically within the last 15 km in the Naples direction during the morning peak period (6:30 AM–9:30 AM); this is mainly due to the high inflows from the on-ramps there. Within the outlined traffic context, the implementation of RENAISSANCE is expected to enhance considerably the traffic surveillance ability of the traffic control center.

A3 currently has 2 lanes in each direction, except for some short stretches, where it has three lanes. The motorway has generally small slopes, with some strong curvatures only in the section between Vietri sul Mare and Salerno (Figure 3). Figure 4 presents a schematic diagram of A3 in both directions: Naples (North) and Salerno (South). The utilized detector configuration is also presented in Figure 4, where each black dot represents a video detector
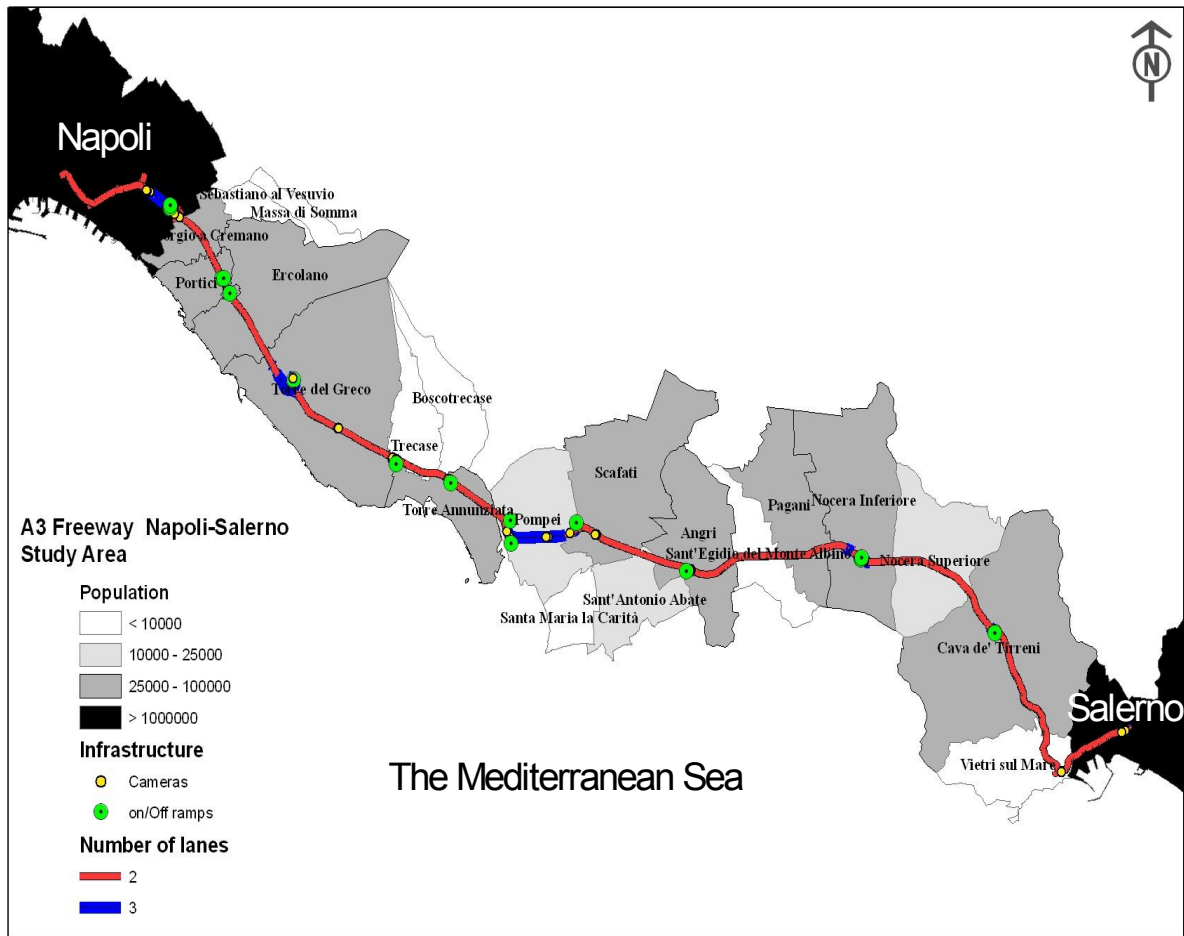
Figure 3: The A3 freeway between Naples and Salerno

that offers flow and speed measurements, while each black triangle just upstream of each pair of on-ramps represents a toll station that records only the number of passing vehicles. The measurement interval was irregular but of 30 seconds on average (while the RENAISSANCE model time step was set equal to 5 s). The detectors are rather sparsely installed in the mainstream, with an average spacing of 4 km within the first 20 km and of about 7 km within the next 27.5 km.

4.2 RENAISSANCE Setup

From the modeling point of view, this test site, including a number of internal bifurcations at the immediate downstream of some toll stations, has to be modeled as a motorway network. In
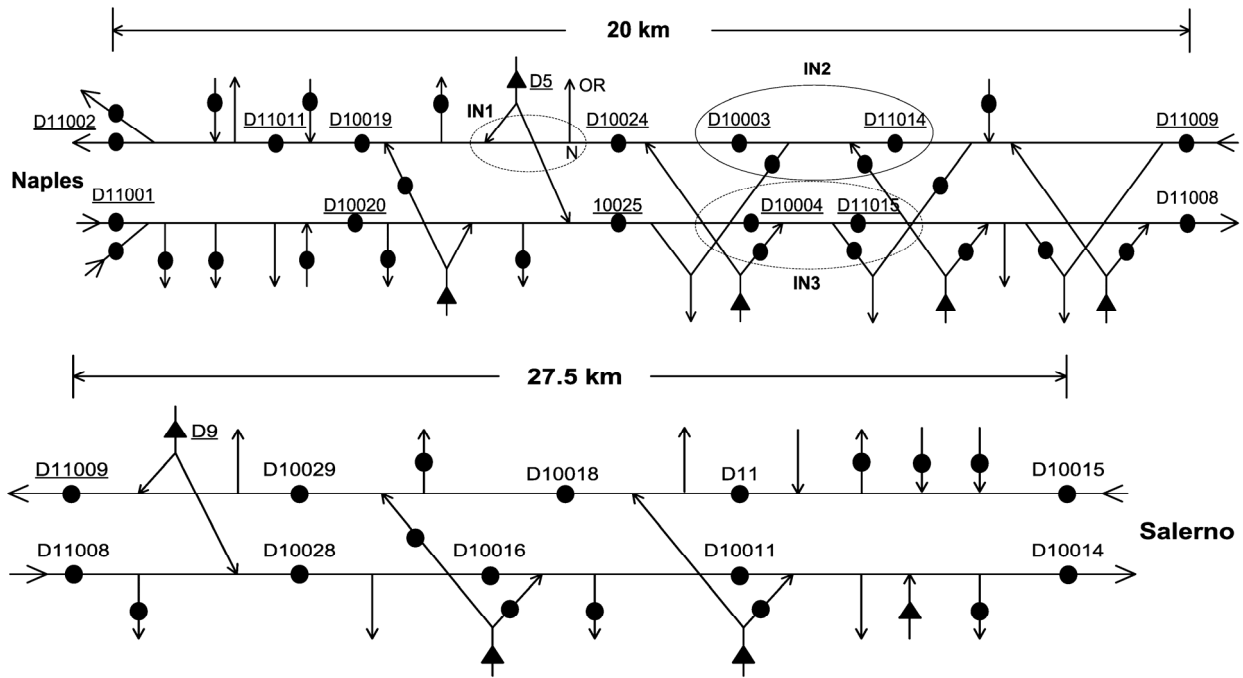
Figure 4: The considered detector configuration in the A3 Motorway

other words, both motorway directions must be considered by RENAISSANCE simultaneously, because otherwise the partial missing of independent on-ramp and off-ramp measurements would lead to lack of observability of the A3 traffic dynamic system and thus render infeasible the estimation task and hence all other tasks built upon it [1]. In Figure 4, any motorway stretch between a pair of neighboring on/off-ramps is defined as a motorway link, if it is geometrically homogeneous (without any lane drop or significant curvature/slope change). Moreover, each motorway link is sub-divided into a number of segments of about 500 m.

Significant spatial difference of speed measurements can be observed from daily mainstream speed measurements (see e.g. Figure 5). Generally speaking, such spatial speed difference could be due to traffic flow inhomogeneity, i.e. the free-speed value may change over a long motorway stretch because of the involved curvature, slope, tunnels, etc. In this case multiple fundamental diagrams may be introduced to the model (with each fundamental diagram addressing each separate section of the considered motorway network) and thus the on-line

estimation of multiple groups of model parameters (e.g. the on-line estimation of more than one free speed value) can be performed, still under the modeling and methodological framework (14)-(16). RENAISSANCE allows for such on-line calibration of multiple fundamental diagrams; and more precisely, 17 fundamental diagrams were employed by RENAISSANCE for A3, each addressing a directional stretch generally between two mainstream detectors. Thus, more than 500 state variables are involved in the RENAISSANCE-A3 model, while the detectors and toll stations deliver 59 flow measurements and 46 speed measurements.

This section reports on the RENAISSANCE traffic state estimation results. The estimator was fed with real traffic measurement data and the results were obtained by one simulation of 24 hours. Five different days, May 25, May 28, June 10, October 9 and October 10, 2006, with available data, are presented below.

5.1 May 25

The measurements were available from all detectors and toll stations along the A3 motorway, except for the last 4 km of the Naples-bound stretch (between D10019 and D11002) and the first 4 km of the Salerno-bound stretch (between D11001 and D10020). All available flow and speed measurement data was used by RENAISSANCE to produce the estimated complete image of real-time traffic conditions in the major part of the A3 network covered by the measurements.

5.1.1 Measurement Data Analysis

Figures[1] 5a and 5b display 24-hour speed measurements collected in the Salerno and Naples directions, respectively. Obviously, free-flow conditions were prevailing the whole day in the Salerno direction except for some temporarily local speed drops before 9:00 PM. On the other hand, sharp speed drops in the Naples direction were recorded by detectors D10019, D10024,

---

[1] See Appendix A

D10003, and D11014 (see these detectors in the upper part of Figure 4) that morning; the speed

drops are seen more clearly in Figure 5c that zooms on Figure 5b for the congestion period.

Figure 5c reveals that:

- Oscillatory (stop-and-go) speed behavior was dominating at D10024, D10003, and D11014 during 7:30 AM to 10:30 AM.

- The speed-drop dynamics observed at D10019 is quite different from that observed at the upstream detectors; also, the speed at D10019 dropped down to e.g. 20 km/h later than this occurred at D10024 (further upstream).

Furthermore, by comparing the oscillatory speed curves in the figure, it is reasonable to assume that it was the propagation of the same shockwave that lead to the stop-and-go behavior at D10024, D10003, and D11014, which, however, may not be much related to the speed drop at D10019. In fact, the RENAISSANCE traffic state estimation results also show that a strong shockwave was propagating from D10024 until several segments after D11014 during those stop-and-go hours, while a slight shockwave was also triggered by the speed drop at D10019 and propagated upstream but dissipated before reaching D11009. For this reason, we concentrate on the results of the stretch between D10024 and D11009 (Figure 4). In addition, as aforementioned, significant traffic flow inhomogeneities in terms of spatial speed unbalance is reflected in Figure 5.

5.1.2   Traffic State Estimates at Measurement Locations

RENAISSANCE is fed with all available measurements to produce estimates of the complete network traffic state, including estimates of the measured variables and fundamental diagram parameters. This sub-section presents the estimation results for the variables that are measured[2]. Figures 6 and 8 compare, respectively, the flow measurements with the flow estimates at

---

[2] As a convention, throughout the thesis, the flow and speed estimates are presented in the downstream-upstream order, as congestion shockwave, if arising, propagates upstream. In addition, model parameter estimates are also presented in the downstream-upstream order.

D10019 and D10024, while Figures 7 and 9 presents a similar comparison for speed at the same detectors. Figures 10 and 11 zoom, respectively, on Figures 8 and 9 for the stop-and-go time period. Figures 12-15 present similar curves for D10003, while Figures 16-19, respectively, for D11014 and D11009. Figures 9, 13, 17, and 19 depict the propagation, evolution, and eventually dissipation of the stop-and-go shockwave from D10024 until D11009.

Although the whole motorway is quite inhomogeneous as illustrated by the distinct free-flow speed levels in Figures 7, 9, 13, 17, and 19, the speed estimates track the corresponding measurements perfectly at each detector location, thanks to the employment of multiple fundamental diagrams and on-line simultaneous calibration of multiple fundamental diagrams (the interested reader is referred to [21] for the case that only one fundamental diagram is defined for the whole A3). Some representative free speed and capacity estimates are presented in Figure 20 for the downstream half of the Naples-bound stretch between D10019 and D11009; more specifically, Figures 20e and 20f correspond to the section including D11014 (the speed measurements of D11014 are much lower than those at the neighboring detectors D10024, D10003, and D11009). The free speed and capacity estimates for the stretch upstream of D11009 looks as regular as those in Figures 20g-20h.

The flow estimates at the toll stations D5 and D9 in the Naples direction are presented in Figure 21 and 22. In terms of the RENAISSANCE modeling, the flows at both toll stations are regarded as boundary variables, and the corresponding estimation is actually the sum of the estimated flows at their respective downstream on-ramps. Figures 21 and 22 indicate that both on-ramp inflows related to each toll station are probably well estimated. In addition, the flow (and speed) estimates match the corresponding measurements at all other measurement locations (not presented here).

5.1.3   Traffic State Estimates at Non-Measuring Locations

Figures 23 and 24 display speed measurements and speed estimates along the whole motorway in the Naples direction. More precisely, the omitted detector legends for Figure 23 are: red (D10024), pink (D10003), black (D11014), and gray (D11009), and for Figure 24 are: red (D11009), blue (D10029), yellow (D10018), and gray (D10015). In either figure, any curve of a color other than the above-mentioned corresponds to a certain segment located between two of those corresponding detectors. For Figure 25 we have: red (D10024), black (D10003), while any curve of another color addresses a segment located between these two detectors. Except for the stop-and-go time period, the segment speed estimates are seen to follow in general the estimated free speed, which is a reasonable result. On the other hand, focusing on the A3 stretch between D10024 and D10003 during the stop-and-go period, we see in Figure 25 a plausible and realistic shockwave propagating sequence between the two detectors; more precisely, the following rule for determining the plausibility and correctness of the estimated shockwave propagation can be used:

[Rule 1] The estimated speed drop at any segment without measurements (the green, blue, pink, and light blue curves in the case Figure 25) should not appear later than the speed drop observed at an upstream detector (the black curve-D10003 in the case of Figure 7h) and should not appear before the speed drop is observed at a downstream detector (the red curve in the case of Figure 25).

According to the "complete image" target illustrated in Figure 2, RENAISSANCE has a graphical user interface (GUI), see also Figure 1. For the reported testing, some illustrative GUI views of RENAISSANCE are presented in Figures 26-28, following the time sequence between 7:00 AM and 12:30 PM. The GUI view corresponds to the traffic state estimation results for the considered motorway network and is therefore updated each time RENAISSANCE performs its

traffic state estimation based on the latest measurement data (since the measurement data is updated around 30 seconds on average, so the GUI view is updated at a similar frequency). As can be seen in each GUI view, any link (headed by an arrow) is separated into a number of segments, each with a length of approximately 500 m. The width of each segment is proportional to the estimated segment flow, while the color of each segment corresponds to its estimated speed level (see e.g. Figure 26 for the three utilized colors):

- green or free-flow: the segment speed is more than 80 km/h;

- yellow or dense: the segment speed is between 80 km/h and 40 km/h;

- red or congested: the segment speed is less than 40 km/h.

These threshold values are user-specific. With the same convention used in Figure 4, a black dot represents a video camera while a triangle denotes a toll station. By clicking on any black dot, triangle, or segment, a corresponding diagram window pops up. For any measurement location, both measurements (in red) and estimates (in green) are displayed in the corresponding window (see e.g. the four windows above the motorway in Figure 26a); for a non-measurement location, only estimates are displayed (see e.g. the left three windows below the motorway in Figure 26a). Each window display can be switched between flow and speed except for toll-charging locations where the speed values are of no interest. Moreover, each diagram window displays the corresponding estimates (and measurements) over a certain time period until now; the time period length is user-specific (, which is 10 minutes in this work). All GUI views in Figures 26-28 address the motorway section including D10024, D10003, D11014, and D11009, as this part of the A3 motorway is the focus of interest as the stop-and-go traffic behavior is only observed therein. To see hidden parts of the whole motorway network, however, the user can simply pan the screen over to them.

As shown in Figure 26, the displayed motorway section was generally under free-flow conditions at 7:22 AM on May 25, 2006. A congestion was observed by D10019 at 7:36 AM (Figure 26b), which propagated upstream (Figure 26c). When the estimated congestion reached

the on-ramp (Figure 26c), one segment at its upstream has already turned dense, while the traffic further upstream is still under free-flow conditions. Later in time, the estimated congestion shockwave reaches D10024 around 8:03 AM (Figure 27a) and D10003 at 8:23 AM (Figure 27c). The estimated speed is seen to be similar to the available speed measurement at D10003, which demonstrates that the estimated shockwave propagation is correct. With the downstream flow increasing, the congestion at D10024 is dissolved before 8:32 AM (Figure 28a), while the congestion shockwave continues propagating upstream to reach D11014 before 8:42 AM (Figure 27b). The estimated upstream propagation of congestion is seen to match reasonably well the local speed measurements of the encountered detector locations (see also Figures 6-19). At around 8:50 AM, a second congestion was observed at D10019 and D10024, which initiates a second bottleneck moving upstream; later, a third congestion was recorded by D10024 and so forth. These observed shockwaves are quite consistent with the oscillatory stop-and-go speed measurements in Figure 5c for D10024, D10003, and D11014. In any case, that morning no congestion shockwave reached D11009 and beyond. Finally, Figure 28c presents the GUI view after the congestion is fully dissolved.

Since no independent measurements were available for evaluating the estimation results, another rule can be used to assess the plausibility and correctness of the estimation results:

[Rule 2] A congestion shockwave should be visible at a certain detector approximately at the same time as the estimated speed drop appears at the same location; moreover, if a congestion is already dissolved at a certain measurement location, this should be reflected by the speed estimates at the same location as well.

It is interesting to notice in Figures 26-28 that the temporal and spatial relationship between the estimated shockwave propagation (i.e. the dynamic evolution of the segment colors) and the measured speed drops (in the pop-up windows) matches this rule quite well. According to Rules

1 and 2, we conclude that the traffic state estimator of RENAISSANCE delivers satisfactory traffic state estimates for this test example. The GUI display presents a spatially global view for the whole motorway network under consideration at each time instant, while most diagrams in Figures 6-25 deliver a temporally global view for each user-specified location over a whole time horizon. The GUI display is more suitable for use in traffic control centers by traffic operators in real time, while the diagrams in Figures 6-25 are suitable for post-evaluation/investigation.

5.2 May 28

Like May 25, the data of May 28 was not available for the last 4 km of the Naples-bound stretch and the first 4 km of the Salerno-bound stretch. The speed measurements in both directions are displayed in Figures 29 and 30. May 28, 2006, was a Sunday; this may partially explain why serious congestion was dominating in the Naples-bound stretch until late in the night. Some representative flow and speed estimation results at the detector locations are presented in Figures 31-42. It is obvious that estimates track well the corresponding measurements. These estimation results were obtained with online estimation of multiple groups of fundamental diagram parameters. Some multi-fundamental-diagram-addressed parameter estimates are presented in Figure 43 for the Naples-bound stretch between D10019 and D11009 (in the downstream-upstream order), more specifically, Figures 43e and 43f corresponds to the section including D11014.

5.3 June 10

The measurement availability is exactly the same as that on May 25 and 28. The speed measurements of June 10, 2006 are displayed in Figures 44 and 45. Some representative flow

and speed estimation results at the detector locations are presented in Figures 46-53. As shown in Figure 45, a sharp speed drop was recorded only by D11014, and actually a sharp flow drop was observed only at D11014 (Figure 50). This indicates the occurrence of a local incident; which was partially confirmed with the model parameter estimation for the motorway section including D11014; see the peculiar capacity drop estimate in Figure 54f.

With a more careful look in Figure 54 we will notice drastic changes in the capacity and free speed estimation results especially indicated in Figure 54d. One assumption for the reason of this behavior is the unbalance between the inflow and the outflow measurements (see section 7.1) in the part of the network including D10003 and D11014, because of some faulty detector measurements (see section 5.4). More specifically, from the beginning of that day's simulation at 0:00 AM, the inflow is observed to be rather low than the outflow and for the whole duration until about 5:30 AM. This difference causes continuously decrease of density which could have the same impact in capacity. Obviously, bad quality measurements can cause unexpected strange behavior to the estimator. Another assumption is that the initial values used for the model parameters are quite different than those in reality. Since the simulation begins early in the morning where low flows are dominating, the estimator needs considerably much time to converge to the real parameter values. However both these hypothesizes could not be more investigated due to the sparse detector installation, or the inefficient data.

Similar phenomena are observed in other days data too, depicted in Figures 56 and 86 which are still presented for completeness.

5.4   October 9

The measurement data on this day was available for the whole A3. Figures 55 and 56 display the speed measurements in Salerno and Naples directions, respectively. Some representative

flow and speed estimation results at the detector locations are presented in Figures 57-68. The free speed and capacity estimates for the Naples-bound stretch between D11002 and D10029 are presented in Figures 69 and 70 (in the downstream-upstream order). A speed decrease between 6:00 PM and midnight was recorded by D10024 (Figure 62), while the corresponding flow measurements are rather low (Figure 61). This indicates the occurrence of a kind of abnormal event, which is partially confirmed by the free speed and capacity estimates around (Figures 69c and 69d).

The testing with the data of this day offers a chance to see the impact of a disabled detector on the RENAISSANCE estimation performance. As shown in Figures 71a and 71b, D10025 in the Salerno direction broke down around 12:00 PM. Driven by the faulty measurements, both flow and speed estimates at D10025 kept on tracking the faulty measurements, which led to the drastic change of the free speed and capacity values in the section including D10025 (Figures 71c and 71d); consequently, a huge fictitious congestion was created at D10025 that propagated upstream until Naples for the rest of the day (The corresponding GUI picture is omitted). On the other hand, if the measurements of D10025 were not fed to RENAISSANCE (this doesn't violate flow observability, owing to the local detector configuration), then the faulty impact of D10025 is fully ignored by the flow and speed estimation (Figures 71e and 71f), while no false alarm is indicated with model parameter estimation (Figures 71g and 71h). Note that, in any case, the traffic state estimates in the Naples direction is little impacted by those in the Salerno direction which are strongly disturbed by the D10025 measurements. This interesting test example suggests that, if a reliable mechanism for detector fault diagnosis would be integrated into RENAISSANCE, RENAISSANCE would be able to exclude the impact of faulty detectors by reconfiguring the estimator in real time (provided that this is allowed in terms of flow observability [1]).

5.5   October 10

The speed measurements of October 10, 2006, are displayed in Figures 72 and 73. Some representative flow and speed estimation results at the detector locations are presented in Figures 74-85. The free speed and capacity estimates for the Naples-bound stretch between D11002 and D10029 are presented in Figures 86 and 87 (in the downstream-upstream order). A speed decrease at between 6:00 PM and midnight was again recorded by D10024 (Figure 79), while the corresponding flow measurements are rather low (Figure 78); a corresponding decrease of the free speed and capacity can also be seen in Figures 86c and 86d. Recalling that similar speed decrease was observed at the same detectors during the similar time period on October 9 (see also Figures 61-62 and 69c and 69d), some specific (e.g. seasonal) events could happen those days. Finally it is also interesting to see in Figures 88-91 the estimator behavior with regard to the measurement switch from a faulty to correct status, and vice versa.

Chapter 6
RENAISSANCE Traffic State Prediction Results

The traffic state prediction function of RENAISSANCE was also tested with respect to the A3 Motorway. The flow and speed prediction results of May 25 at some detector locations are displayed in Figures 92-101, while those of May 28 in Figure 102-111. Since the comparison between the estimates and measurements at the same detector locations are already presented in Figures 6-19 and Figures 31-42, each of Figures 92-111 displays the estimates and prediction results for a specific traffic flow variable over a number of prediction horizons. The prediction repetitive internal is 10 minutes starting from the corresponding current traffic state estimate, while the duration of each prediction horizon is 20 minutes.

Since the Italian freeway A3 is not an everyday congested freeway, the historical data of the boundary variable estimates are not representative. Thus, the obtained prediction results are based on extrapolation of the boundary variable estimates available up to the current time instant without using any historical data. It seems that the prediction results plot the evolving tendency of traffic dynamics, albeit with some individual faulty trajectories. This could be an indication for a not so accurate estimation at the non measured locations. However the extrapolation of the boundary data should be more investigated.

7.1 Problem description and analysis

It was observed in the RENAISSANCE testing that the network estimates present some inner congestions at three locations. Inner congestions are fictitious congestions created by RENAISSANCE. As illustrated in Figure 112, an inner congestion (in red) may arise at the downstream of detector D2, but eventually stays steadily between two neighboring mainstream detector locations D1 and D2 over a long time period. During an inner congestion, all segments covered by the congestion have very low speeds, while the neighboring detectors (e.g. D1 and D2 in Figure 112) assume high free-flow speeds. Since a congestion shockwave propagates upstream, a real congestion generally cannot stay steadily within a given motorway section, i.e. it either continues to propagate upstream, which contradicts the fact the immediate upstream detector (D2) delivers free-flow speed measurements during the inner congestion, or dissolves towards the downstream. Therefore, such inner congestions can hardly exist in reality.

In the A3 motorway, an inner congestion is either triggered by real congestions or created due to flow measurement unbalance. Three sections in A3 that are prone to inner congestions are encircled and marked with IN1, 2, and 3. The inner congestion IN 1 (Figure 113) is typically caused due to the tricky detector configuration between D10019 and D10024. This detector installation satisfies flow observability under non-congested conditions; under congestions, however, the inflow to the Naples direction from D5 and outflow at the upstream off-ramp can hardly be estimated instantaneously accurately, and then an inner congestion is triggered, which

stays between D10019 and D10024 for a long time, although the speed measurements at D10024 are rather high.

The inner congestions IN 2 and IN 3 are of a same type (Figure 114), which are due to local flow measurement unbalance. More precisely, either IN 2 or IN 3 is caused by the fact that the measurements of total inflow from the mainstream detector (D11014 or D10004) and on-ramp detector are bigger than that of total outflow at the mainstream detector (D10003 or D11015). For IN 2, Figure 115 shows the case of total flow balance, while Figure 116 shows the case that the total inflow is higher than the total downstream outflow but mainstream inflow at D11014 seems to be close to the total outflow; Figure 117 shows the case that the mainstream inflow itself is even bigger than the total outflow. Exactly the same cases have been noticed for IN 3 (Figures omitted). Table 1 summarizes the data checking results for IN 2 and IN 3, where "comparison 1" refers to the comparison between the total upstream inflow and total downstream outflow; "comparison 2" refers to the comparison between the mainstream inflow only with the total downstream outflow; "√" means OK, "×" means "not OK". In the case of "×", the in-out flow unbalance of "Comparison 1" is 700 veh/h on average for IN 2, while it is bigger for IN 3. It is noticed that all unbalance occurred each day (as listed in Table 1) during the same time period as displayed in Figures 116 and 117.

7.2   Countermeasures and results

The reason for IN 1 to stay steadily is that the on-ramp inflow downstream of D5 and off-ramp outflow at OR (see Figure 4) cannot be well estimated when congestions are dominating there. More precisely, in this case (see Figure 113), the segments at both upstream and downstream of the off-ramp OR are congested, and hence the off-ramp flow is assumed to be very low by

RENAISSANCE according to the flow conservation. As far as the flow conservation keeps, there is no motivation for the congestion to dissolve, and consequently, the inner congestion IN 2 is created and stays steadily there (Figure 113). With this understanding in mind, the simple approach to the dissolution of this inner congestion is to increase the outflow at OR. Since this outflow is determined by the turning rate at bifurcation node N, the key point is to increase the turning rate. Considering that the turning rate is a boundary variable modeled as a random walk (see section 2.3 and [1]), the solution is to increase the standard deviation (SD) of the random-walk-modeling noise of the turning rate so that eventually the out flow at OR can be more sensitive to the traffic situation changes. Using measurement data of some days, Table 2 compares the inner congestion durations resulting from two turning rate SD settings of RENAISSANCE: Basic (SD equal to 0.001 for all turning rates) and Improved (SD equal to 0.02 for the turning rate at node N and 0.01 for all other turning rates). Obviously, the improved turning rate SD setting largely reduces the inner congestion duration. The traffic state estimation and prediction results presented in previous sections were obtained with the improved setting. With this improved setting, the inner congestions observed on the days other than presented in Table 2 generally do not have longer durations. Regarding IN 2 and IN3, feasible solutions are limited; one possible solution is to specify bigger SD values for the measurement noise of the involved detectors, which intends to inform the estimator not to trust the measurements too much. However, this countermeasure is not really recommendable, as it may hide real detector faults behind.

7.3 Recommendations

Traffic flow inhomogeneity is revealed from spatial unbalance of speed measurements. As a representative example, the speed measurements at D11014 are much lower than those at its

neighboring detectors D10003 and D11009; this can be seen for each day with available data. However, there seems no significant curvature or slop around D11014, so the exact reason for the lower speed measurements there is not very clear. Via data checking, it was also found that sometimes two detectors placed in the opposite directions but geometrically at almost the same locations deliver free-flow speeds of obviously different levels. In addition, the flow measurement unbalance related to inner congestions IN 2 and IN 3 clearly indicates that some involved detectors have operational faults, but it is not easy to identify the faulty detectors. It is also noticed in the testing that some detectors deliver rather low flow and speed over certain time periods of some days. Considering all A3 detectors are of the video type and IN 2 and IN 3 occur almost daily (Table 1) at night (Figures 116 and 117), some of these observed flow or speed measurement unbalance, if due to detector faults, may be attributed to light condition changes, e.g. the cameras are not placed properly such that its view is prone to some negative impacts from neighboring environments. Therefore, it is suggested that some video cameras in A3 be carefully re-calibrated.

On the other hand, the creation of inner congestion IN 1 may probably be due to both flow measurement unbalance and the corresponding spare detector installation; and just because of the sparse detector installation, it is impossible to tell which detector involved may deliver faulty flow measurements; more specifically, if the Naples-bound on-ramp downstream of D5 and off-ramp OR were equipped with detectors, it would be readily to identify, simply via flow conservation, which detectors around IN 1 would be operationally faulty. As far as A3 is concerned, it is suggested that some extra detectors be placed at the site, e.g. at the Naples-bound on-ramp downstream of D5 or at its immediate upstream in the mainstream, at the off-ramp OR, the off-ramp immediately downstream of D11009, etc.

Chapter 8
Conclusive Remarks

A real-time motorway network traffic surveillance tool RENAISSANCE that was recently developed, aims at delivering a complete real-time image of network traffic conditions at each current time instant and over a future time horizon from every current time instant as well as other traffic information of interest, especially in case of sparse detector installation. Owing to the employed generic approach to system modeling, RENAISSANCE is applicable in real time to motorway networks of arbitrary size, topology, and characteristics, with any suitable traffic detector configuration. This thesis reports 24-hour testing results of the traffic state estimation, traffic state prediction and incident alarm functions of RENAISSANCE with respect to the A3 motorway in south Italy. The obtained testing results are quite satisfactory. As a matter of fact, this is the first time to report on so large-scale field applications of real-time traffic state estimation and prediction. According to the experience gained from this work, some suggestions regarding the detector configuration in the A3 motorway are given.

REFERENCES

1. Wang, Y., M. Papageorgiou, and A. Messmer. RENAISSANCE – A Unified Macroscopic Model-Based Approach to Real-Time Motorway Network Traffic Surveillance. *Transportation Research C*, Vol. 14, 2006, pp. 190-212.

2. Kachroo, P., K. Ozbay, and A. G. Hobeika. Real-time Travel Time Estimation Using Macroscopic Traffic Flow Models. *Proc. 4th IEEE Conference on Intelligent Transportation Systems*, 2001, pp. 134-139.

3. Szeto, M. W., and D. C. Gazis. Application of Kalman Filtering to the Surveillance and Control of Traffic Systems. *Transportation Science*, Vol. 6, 1972, pp. 419-439.

4. Nahi, N. E., and A. N. Trivedi. Recursive Estimation of Traffic Variables: Section Density and Average Speed. *Transportation Science*, Vol. 7, 1973, pp. 269-286.

5. Papageorgiou, M. *Application of Automatic Control Concepts to Traffic Flow Modeling and Control*. Springer Verlag, New York, 1983.

6. Cremer, M., and H. A. Schütt. A Comprehensive Concept for Simultaneous State Observation, Parameter Estimation And Incident Detection. *Proc. 11th International Symposium on Transportation and Traffic Theory*, Elsevier, Amsterdam, 1990, pp. 95-111.

7. Cremer, M. Flow Variables: Estimation. In *Concise Encyclopedia of Traffic and Transportation Systems*. Pergamon Press, 1991, pp. 143-148.

8. Kohan, R. R., and S. A. Bortoff. An Observer for Highway Traffic System. *Proc. 37th IEEE Conference on Decision and Control*, Tampa, Florida, 1998, pp. 1012-1017.

9. Meier, J., and H. Wehlan. Section-wise Modeling of Traffic Flow and Its Application in Traffic State Estimation. *Proc. 4th IEEE Conference on Intelligent Transportation Systems*, Oakland, California, 2001, pp. 442-447.

10. Wang, Y., and M. Papageorgiou. Real-time Motorway Traffic State Estimation Based on Extended Kalman Filter: A General Approach. *Transportation Research B*, vol. 39, 2005, pp. 141-167.

11. Wang, Y., M. Papageorgiou, and A. Messmer. Investigation of the Adaptive Features of A Real-Time Motorway Traffic State Estimator. *Transportation Research Board 85th Annual Meeting*, Washington, D. C., Paper No. 06-0239, 2006.

12. Papageorgiou, M., J.-M. Blosseville, and H. Haj-Salem. Modeling and Real-time Control of Traffic Flow on the Southern Part of Boulevard Périphérique In Paris − Part I: Modeling. *Transportation Research A*, Vol. 24, 1990, pp. 345-359.

13. Papageorgiou, M. Freeway Traffic Modelling. In: Papageorgiou, M. (Ed.), *Concise Encyclopedia of Traffic and Transportation, Systems*. Pergamon Press, 1991, pp. 162–167.

14. Messmer, A., and M. Papageorgiou. METANET: A Macroscopic Simulation Program for Motorway Networks. *Traffic Engineering & Control*, Vol. 31, 1990, pp. 466-470 and 549.

15. Kotsialos, A., M. Papageorgiou, C. Diakaki, Y. Pavlis, and F. Middelham. Traffic Flow Modeling of Large-Scale Motorway Networks Using the Macroscopic Modeling Tool METANET. *IEEE Trans. on Intelligent Transportation Systems*, Vol. 3, 2002, pp. 282-292.

16. Cremer, M., Papageorgiou, M. Parameter Identification for a Traffic Flow Model. *Automatica* 17, 1981, 837–843.

17. Wang, Y., Papageorgiou, M., Messmer, A. *RENAISSANCE – A Real-time Motorway Network Traffic State Surveillance Tool, User Manual*. Dynamic Systems and Simulation Laboratory, Technical University of Crete, Chania, Greece, 2004.

18. Jazwinsky, A. H. *Stochastic Processes and Filtering Theory*. Academic Press, New York, 1970.

19. Wang, Y., Papageorgiou, M., Messmer, A. *Algorithms and Preliminary Testing for Traffic Surveillance*. Deliverable D3.2 of the Project RHYTHM (IST-2000-29427), Report for the Information Society Technologies Office of the European Commission, Brussels, Belgium, 2003.

20. Wang, Y., Messmer, A., Papageorgiou, M. Freeway Network Simulation and Dynamic Traffic Assignment Using METANET Tools. *Transportation Research Record* 1776, 2001, 178–188.

21. Wang, Y., P. Coppola, A. Messmer, A. Tzimitsi, M. Papageorgiou, A. Nuzzolo. Extended Field Test of a Real-Time Freeway Network Traffic State Estimator, submitted for publication in *Transportation Research Record*, 2007.
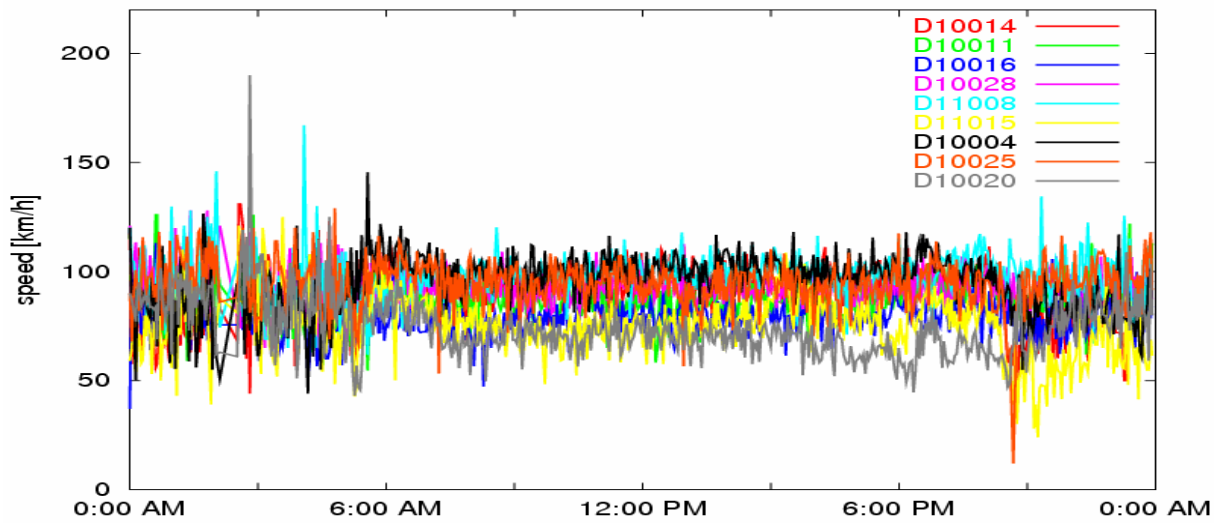
(a)
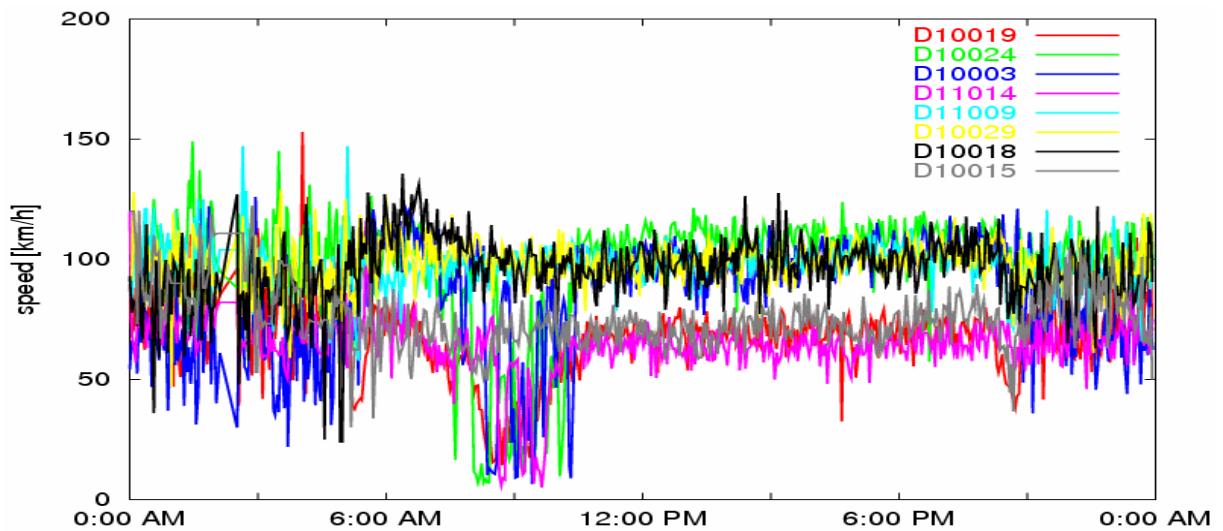
(b)
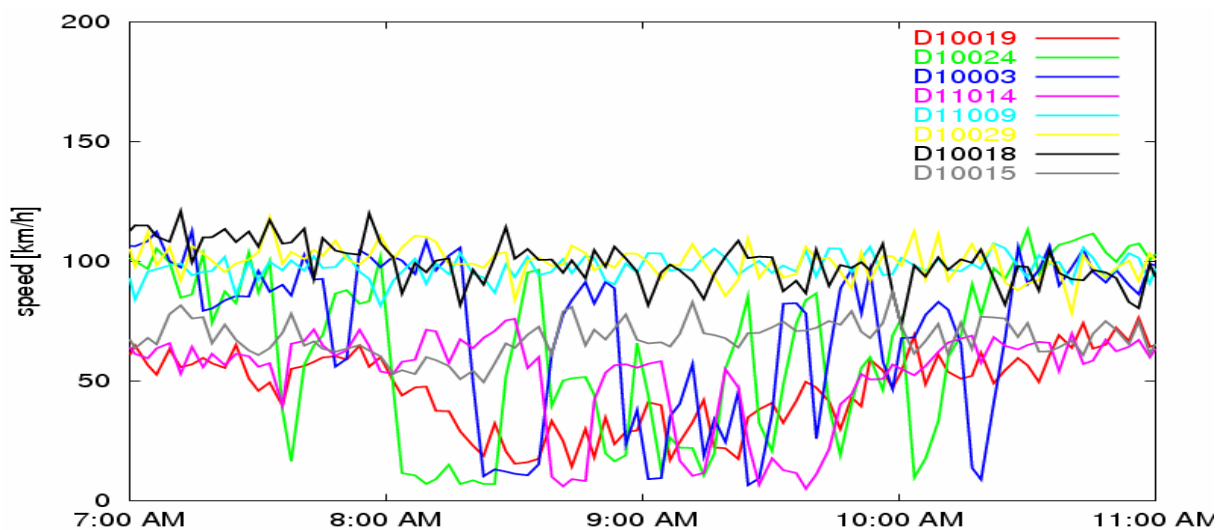
(c)

Figure 5: Speed measurements along A3 on May 25, 2006: (a) in Salerno direction; (b) in Naples direction; (c) zoom on (b)
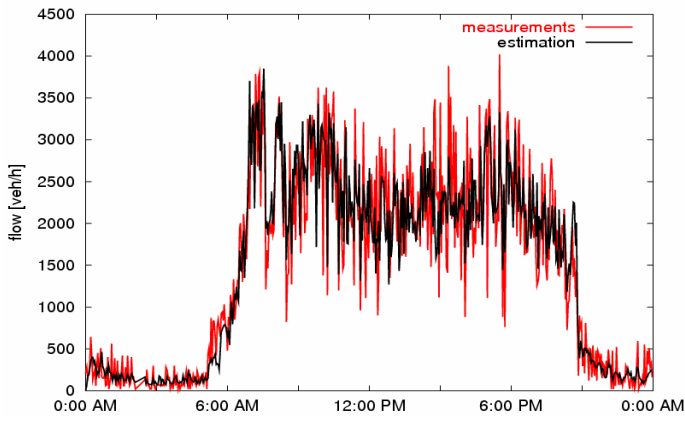
Figure 6: Flow at D10019, May 25
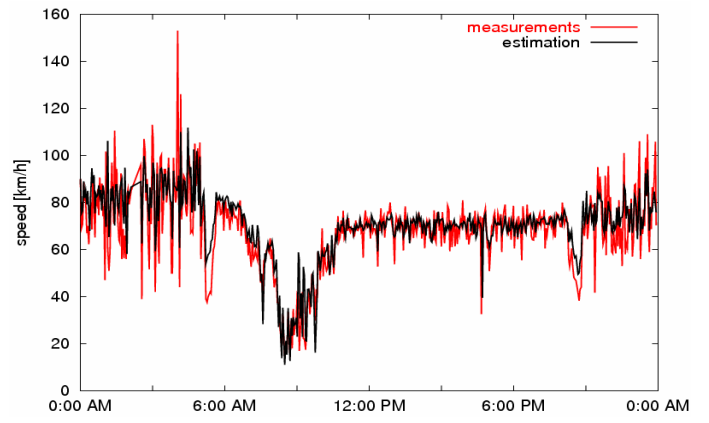
Figure 7: Speed at D10019, May 25
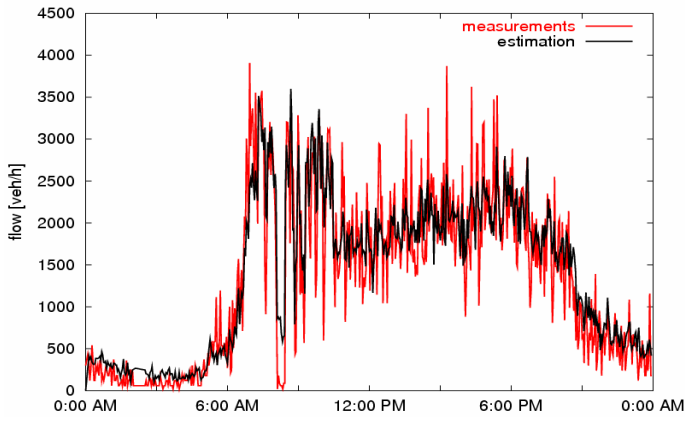
Figure 8: Flow at D10024, May 25
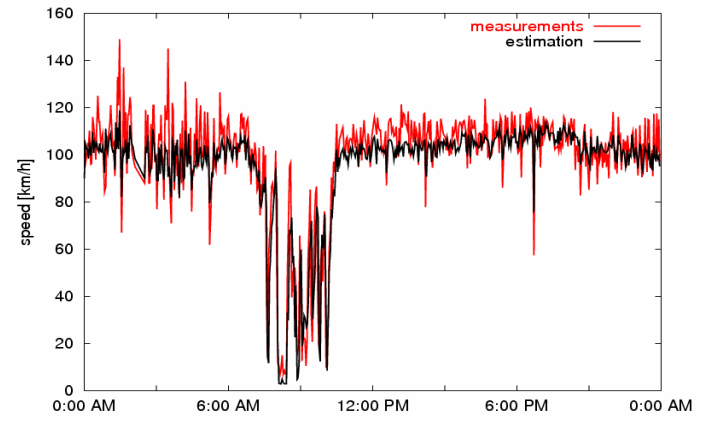
Figure 9: Speed at D10024, May 25
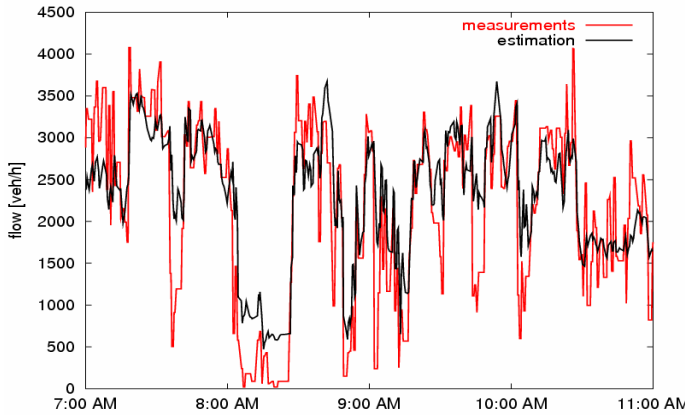
Figure 10: Zoom on Figure 8
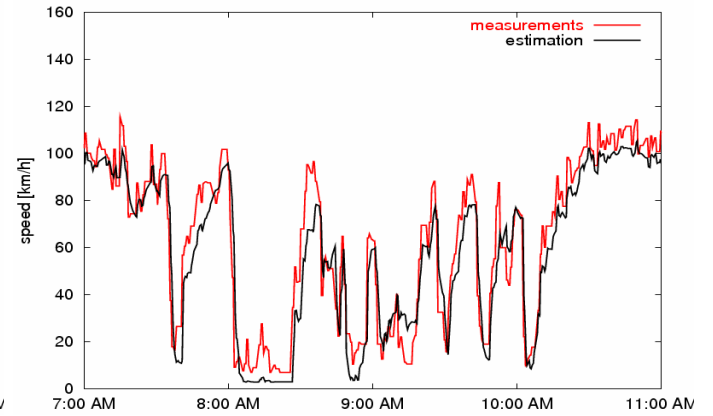
Figure 11: Zoom on Figure 9
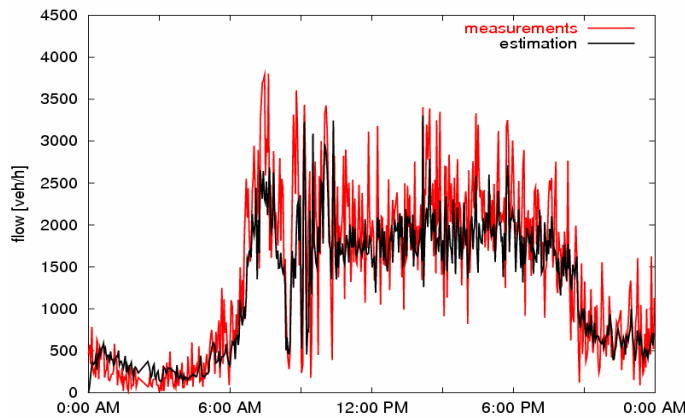
Figure 12: Flow at D10003, May 25
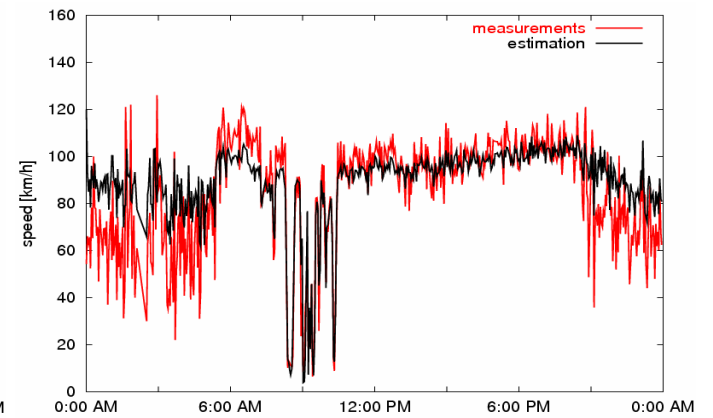
Figure 13: Speed at D10003, May 25
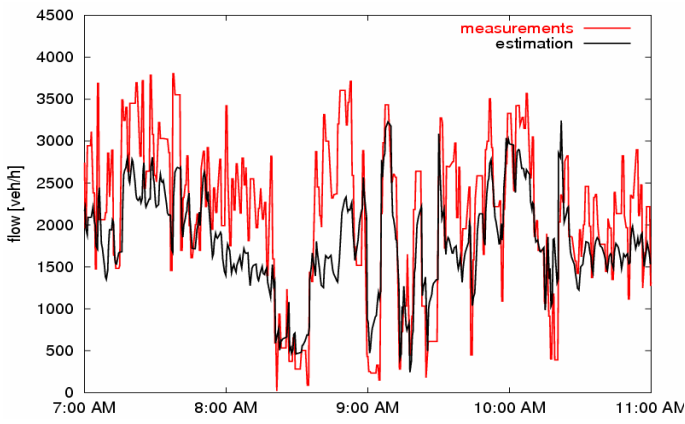
Figure 14: Zoom on Figure 12
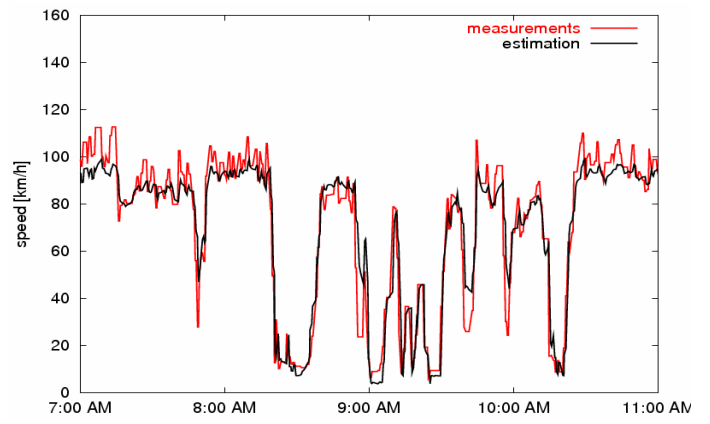
Figure 15: Zoom on Figure 13
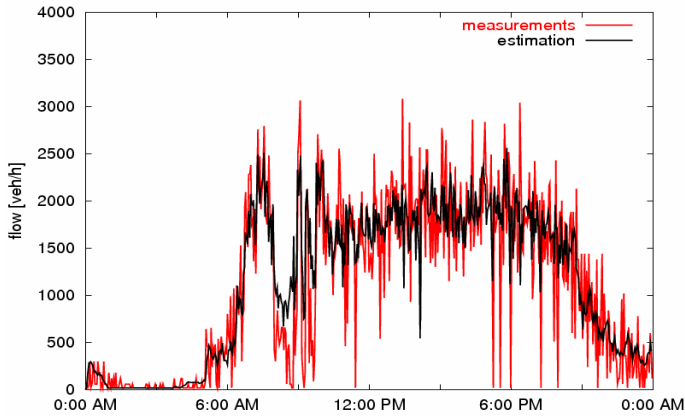
Figure 16: Flow at D11014, May 25
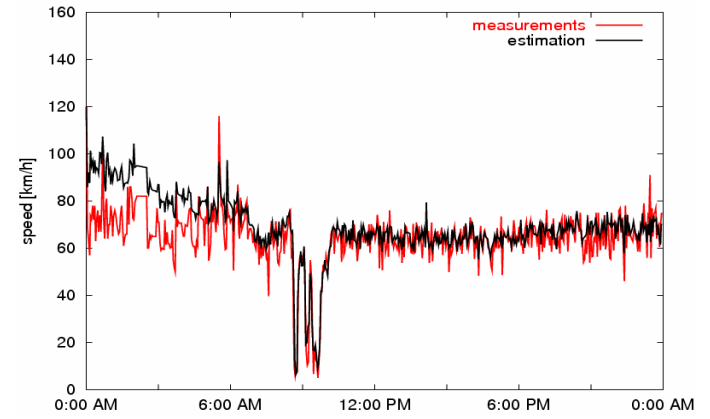
Figure 17: Speed at D11014, May 25
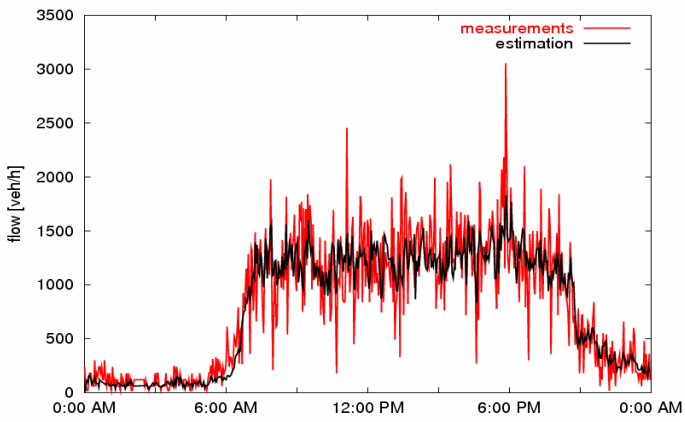
Figure 18: Flow at D11009, May 25
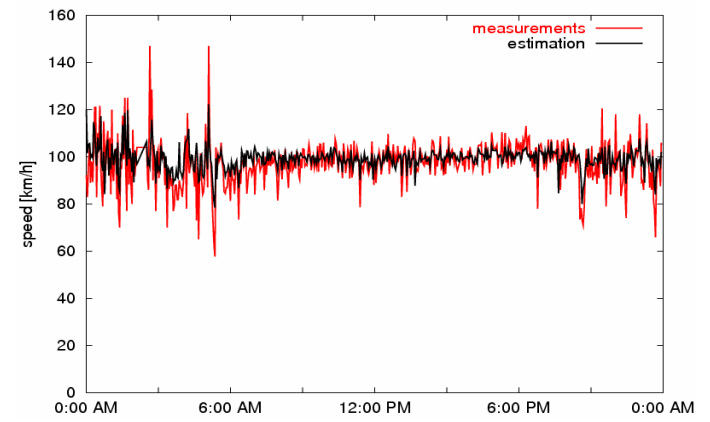
Figure 19: Speed at D11009, May 25

71
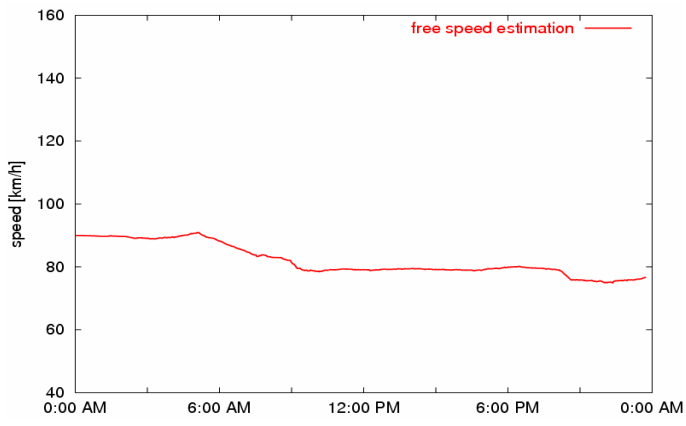
(a)
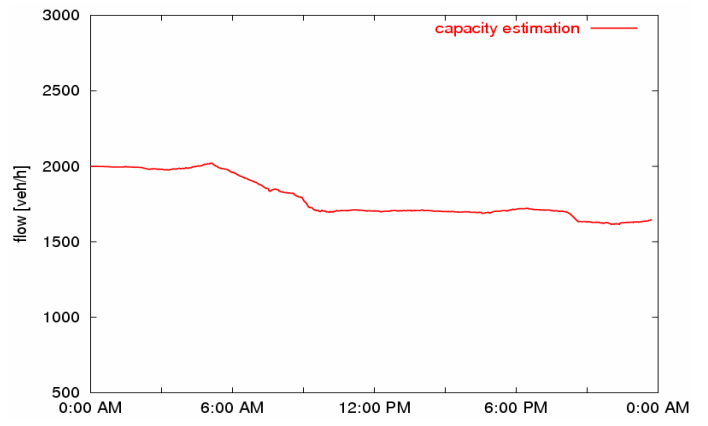
(b)
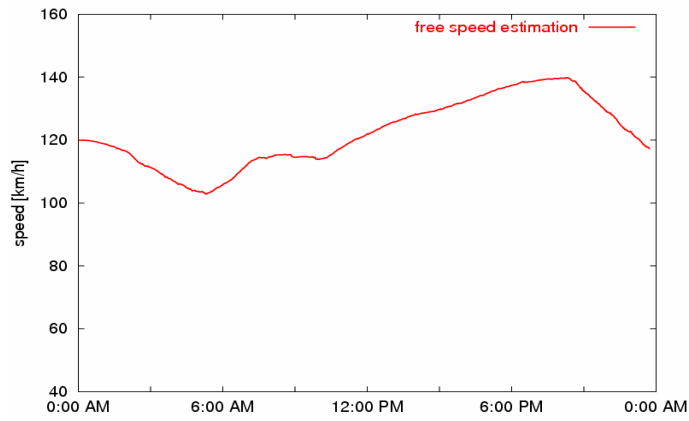
(c)
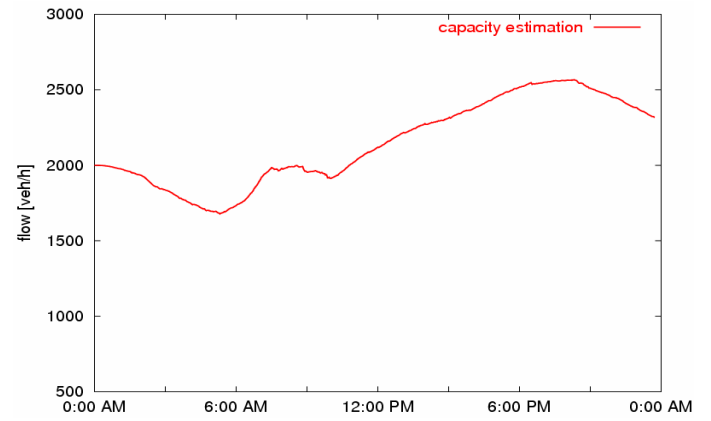
(d)
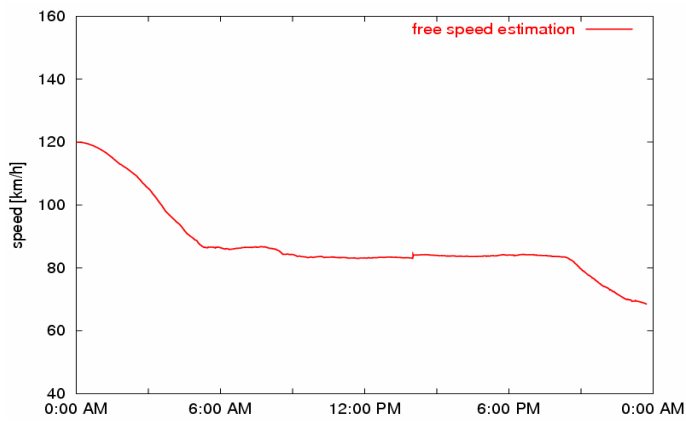
(e)
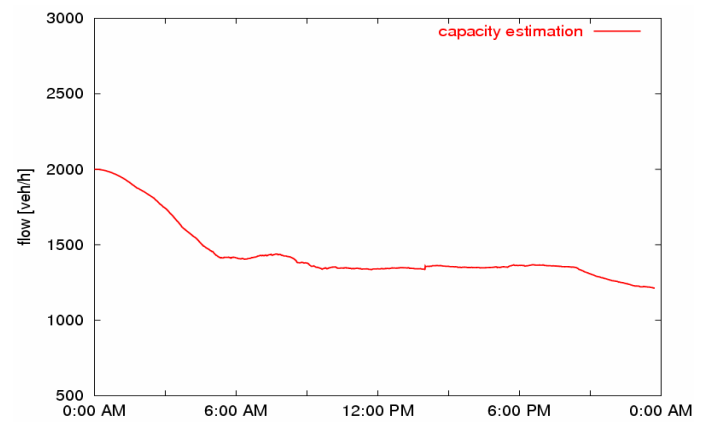
(f)
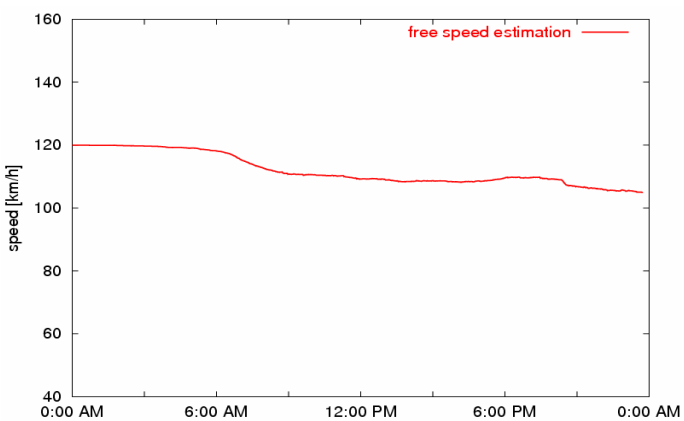
(g)
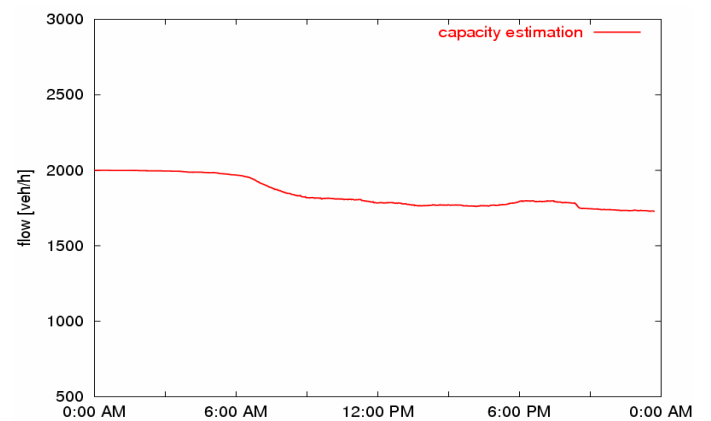
(h)

Figure 20: Free speed and capacity estimates along A3 in Naples direction on May 25, 2006
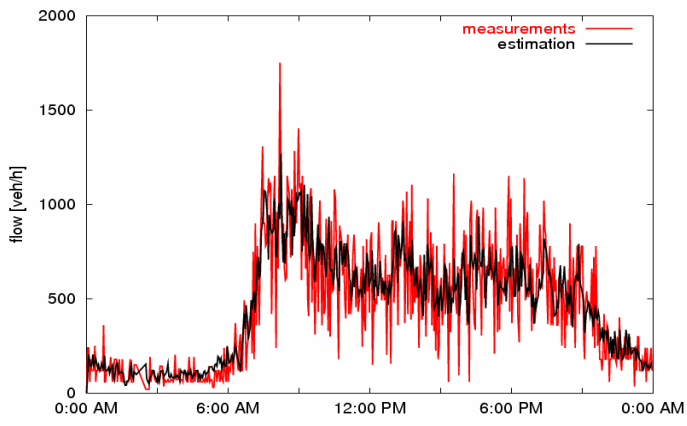
Figure 21: Flow at D5, May 25
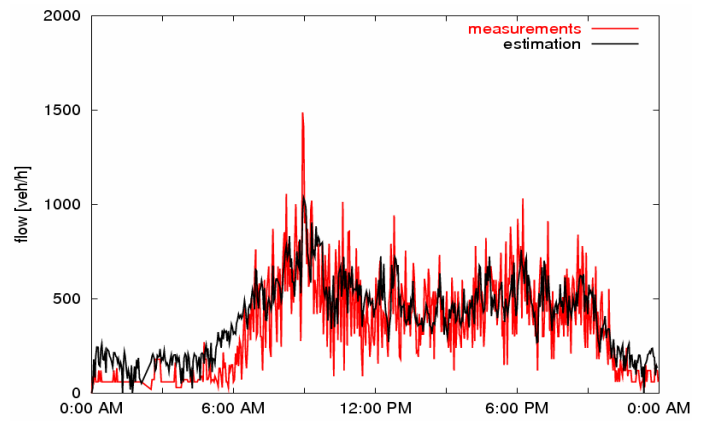
Figure 22: Flow at D9, May 25
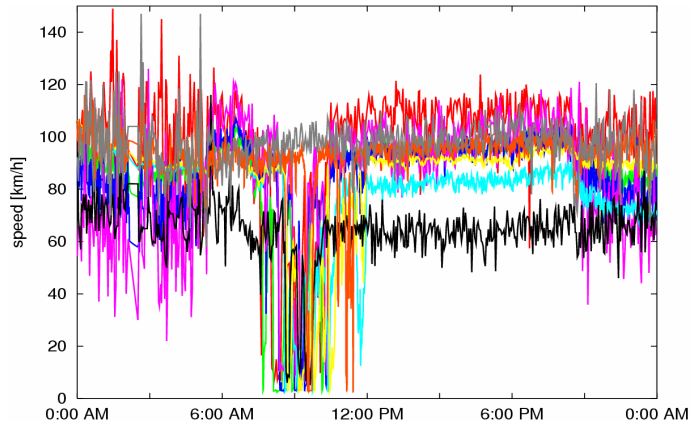
Figure 23: Speed estimation along A3 in Naples direction, May 25
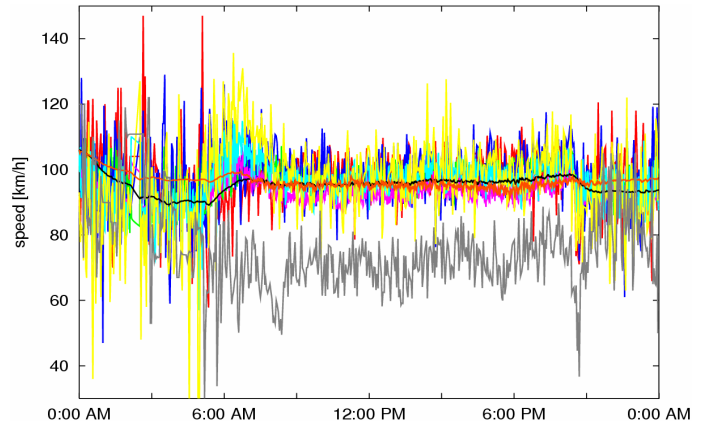
Figure 24: Speed estimation along A3 in Naples direction, May 25
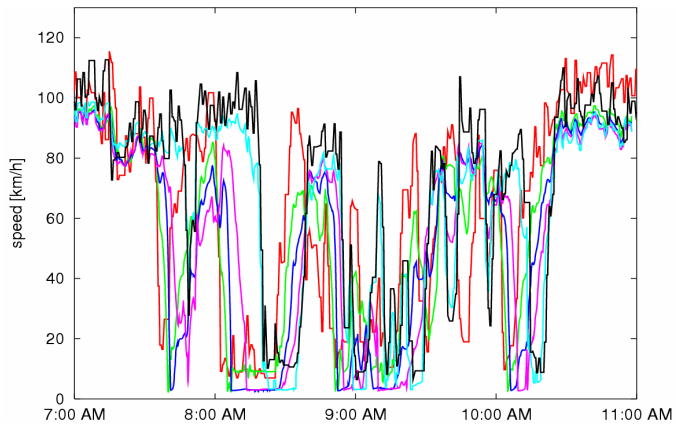
Figure 25: Zoom on Figure 23
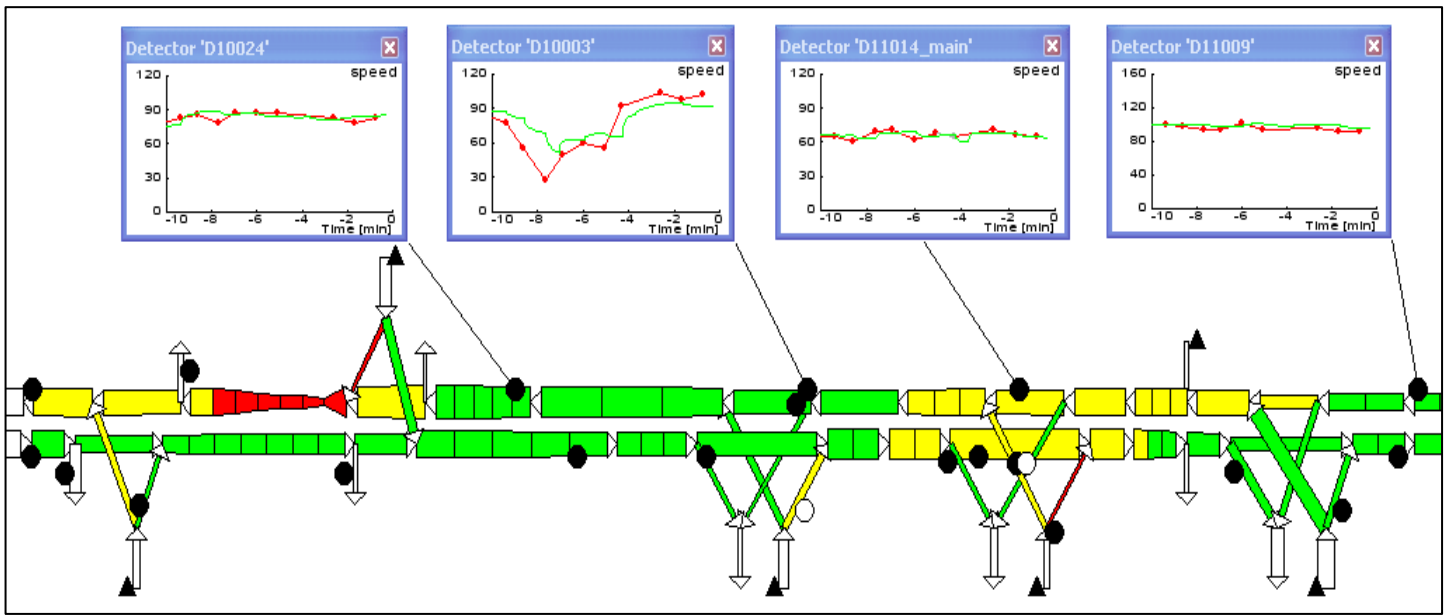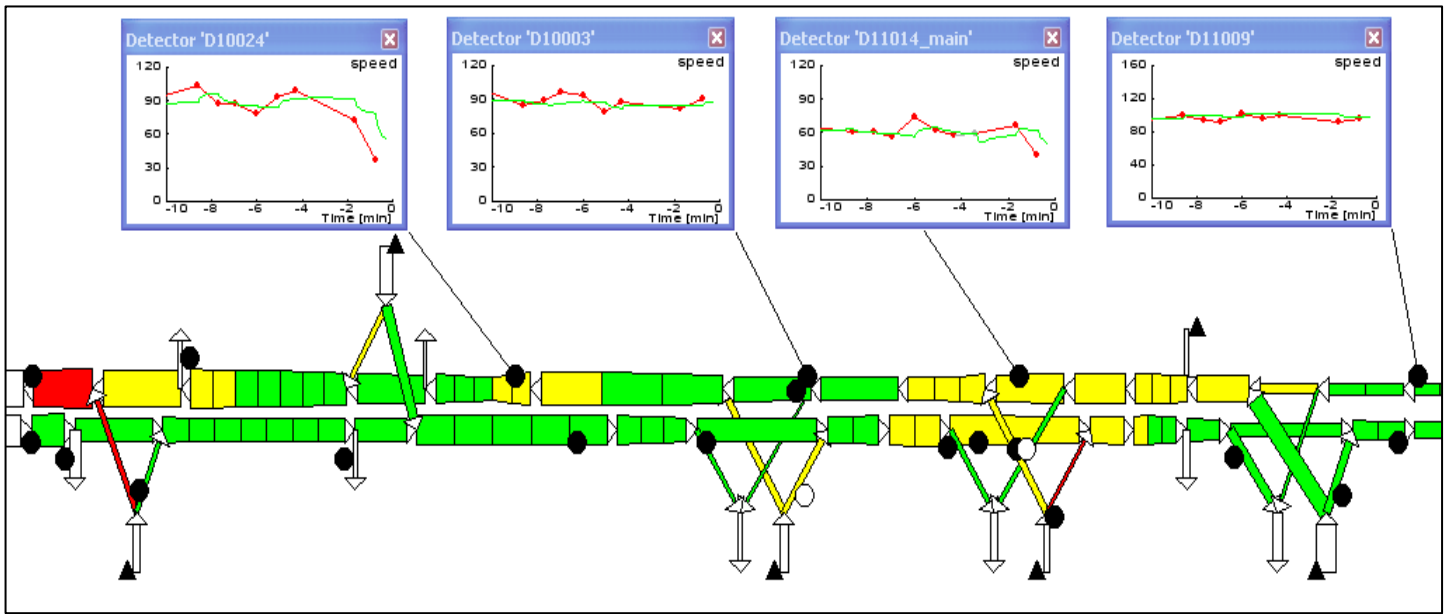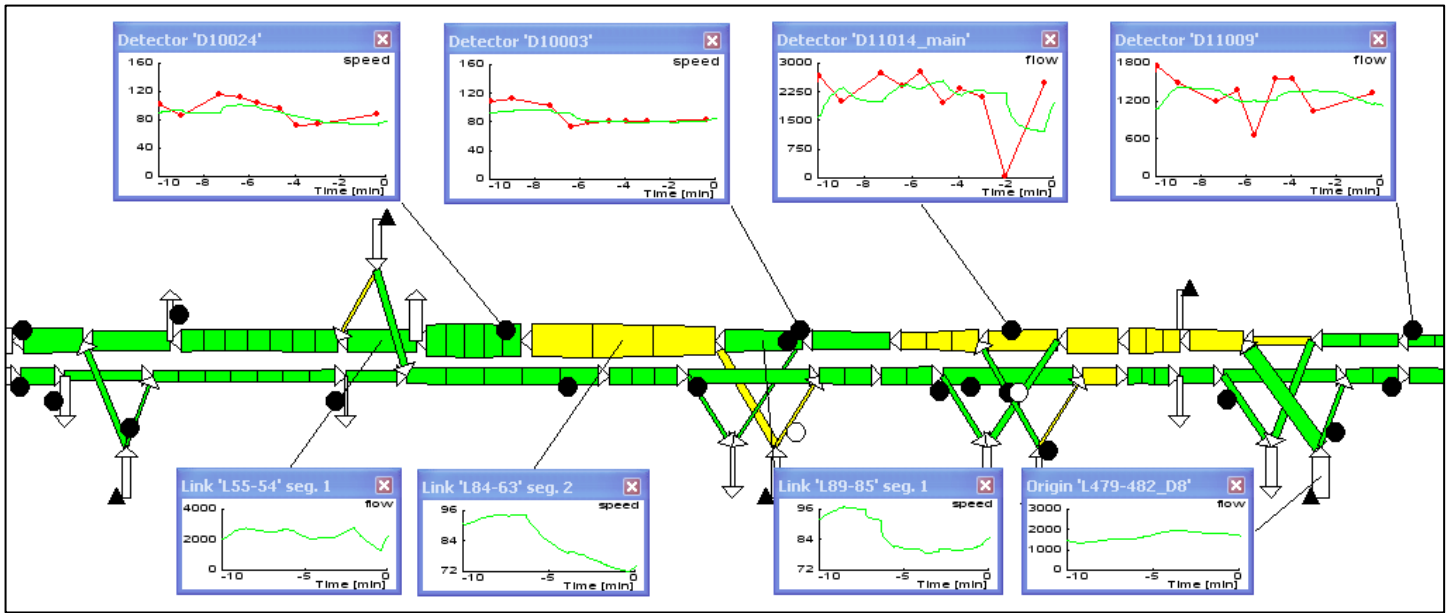
Figure 26: Traffic state estimation results displayed with the RENAISSANCE GUI (top to bottom): (a) 7:22 AM; (b) 7:36 AM; (c) 7:56 AM
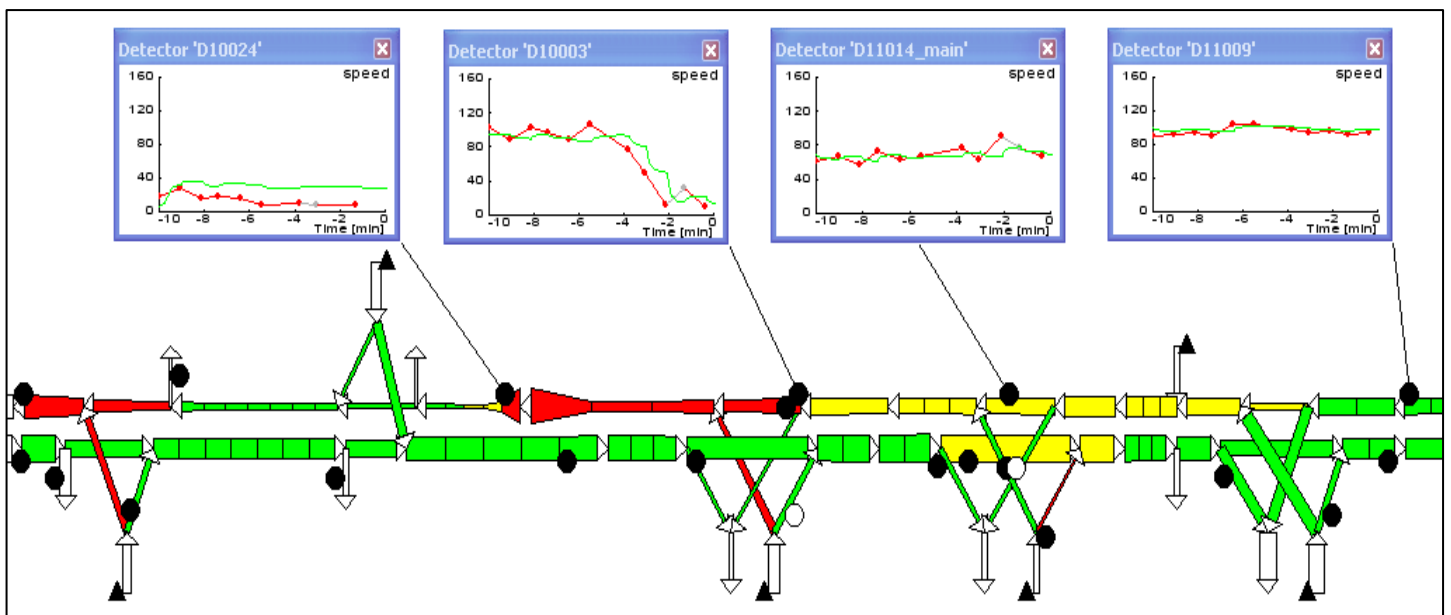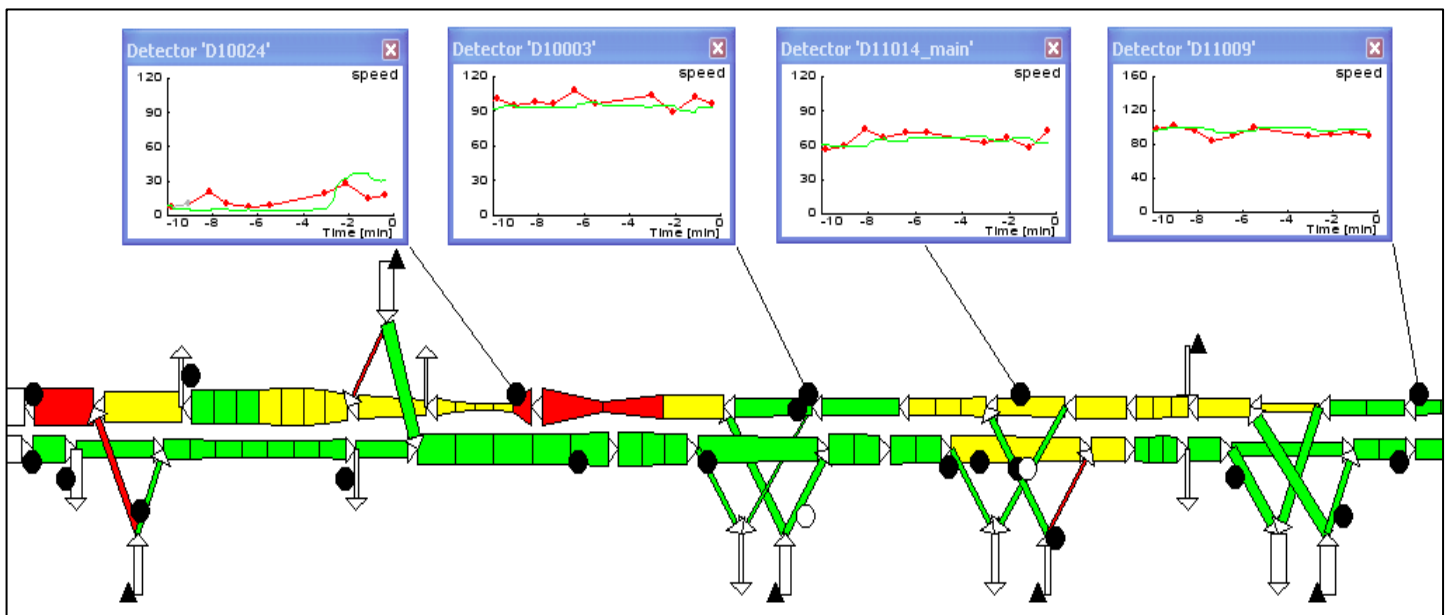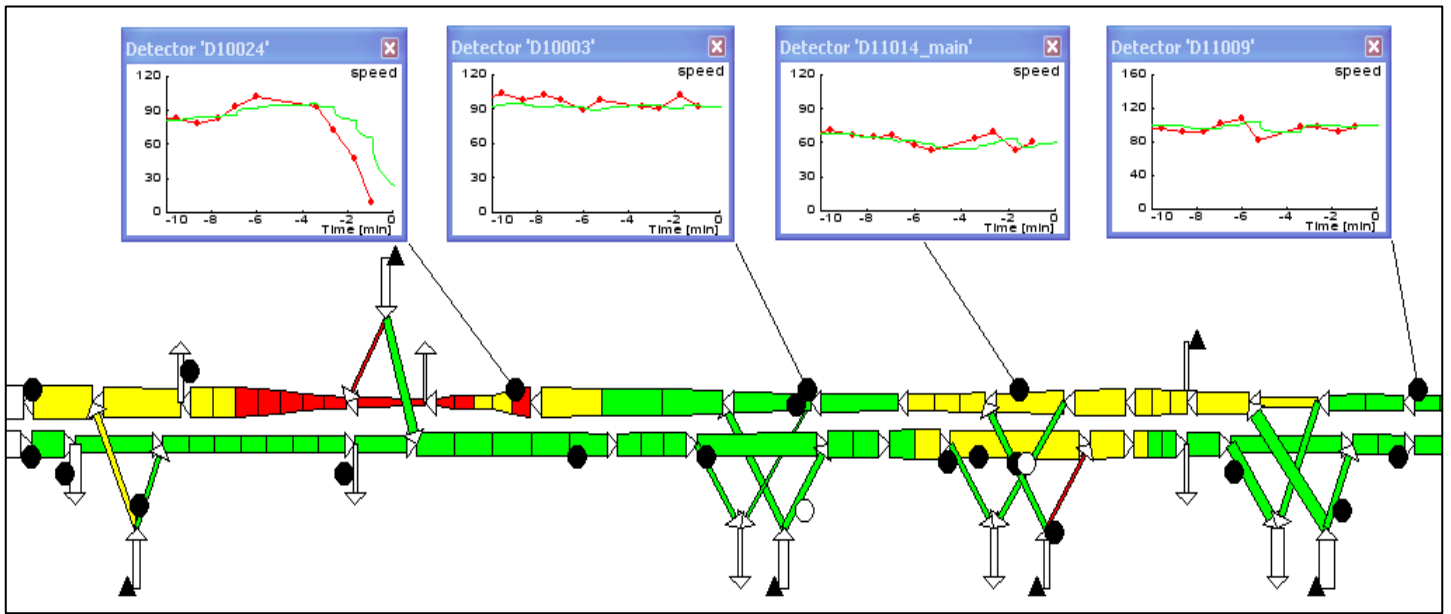
Figure 27: Traffic state estimation results displayed with the RENAISSANCE GUI (top to bottom): (a) 8:03 AM; (b) 8:15 AM; (c) 8:23 AM
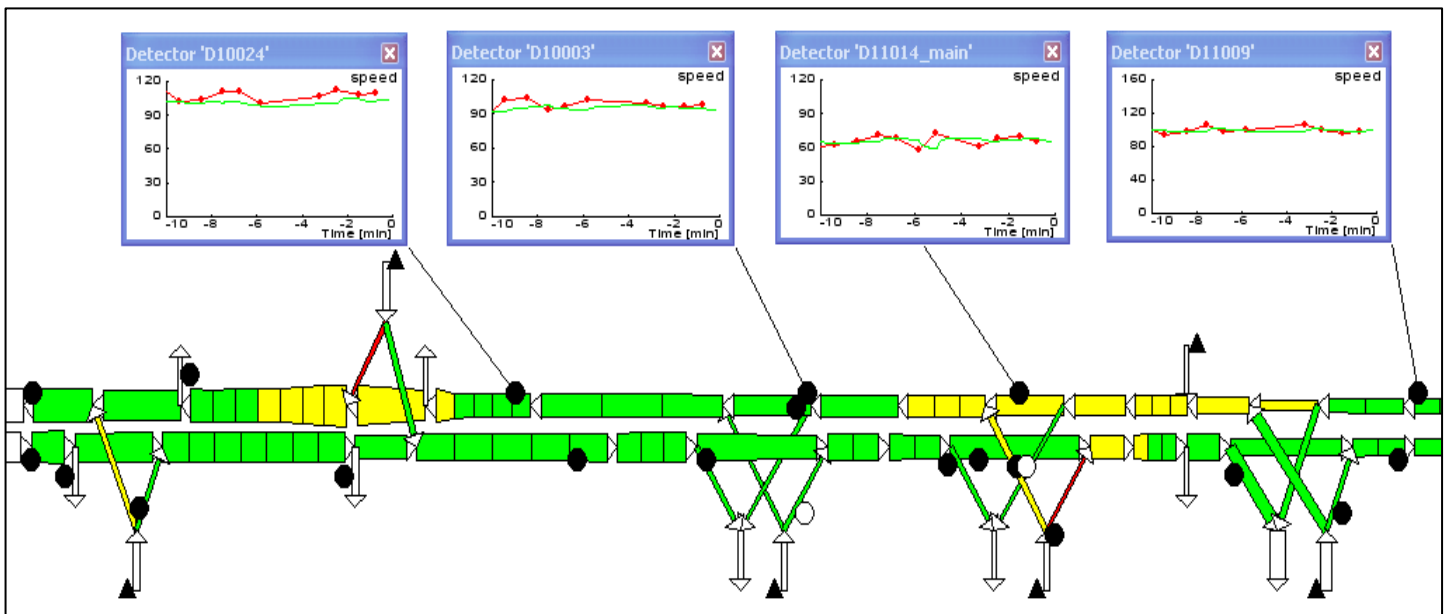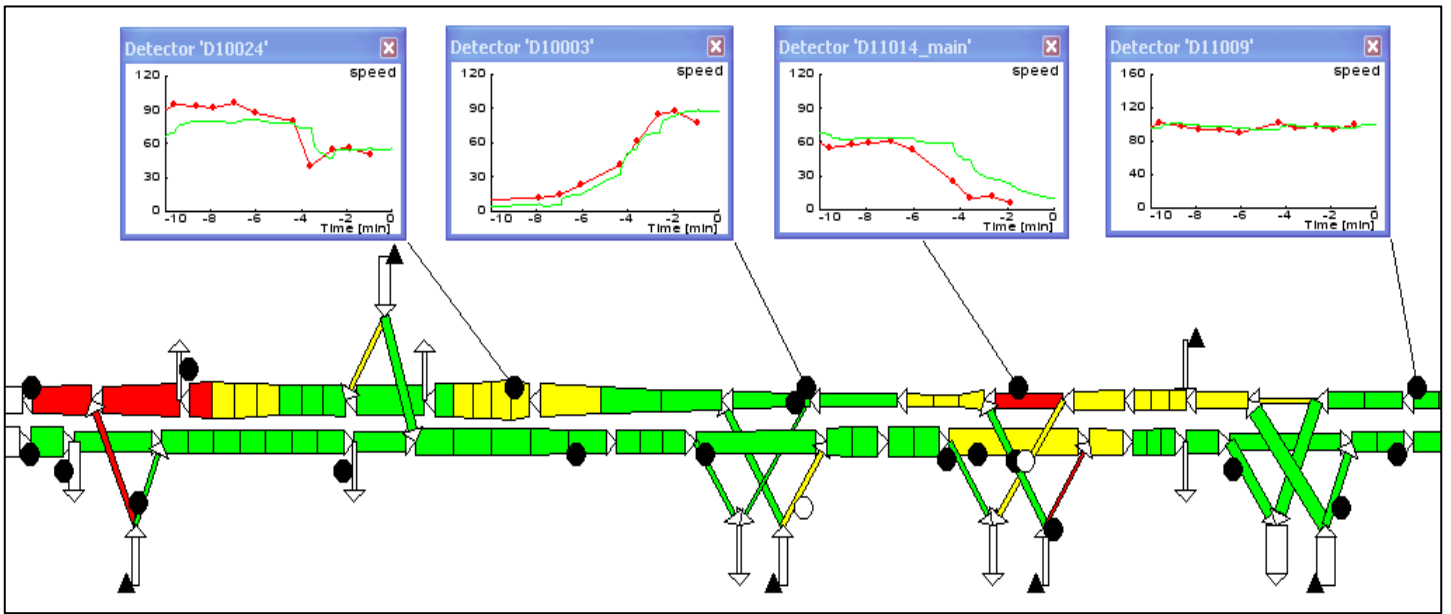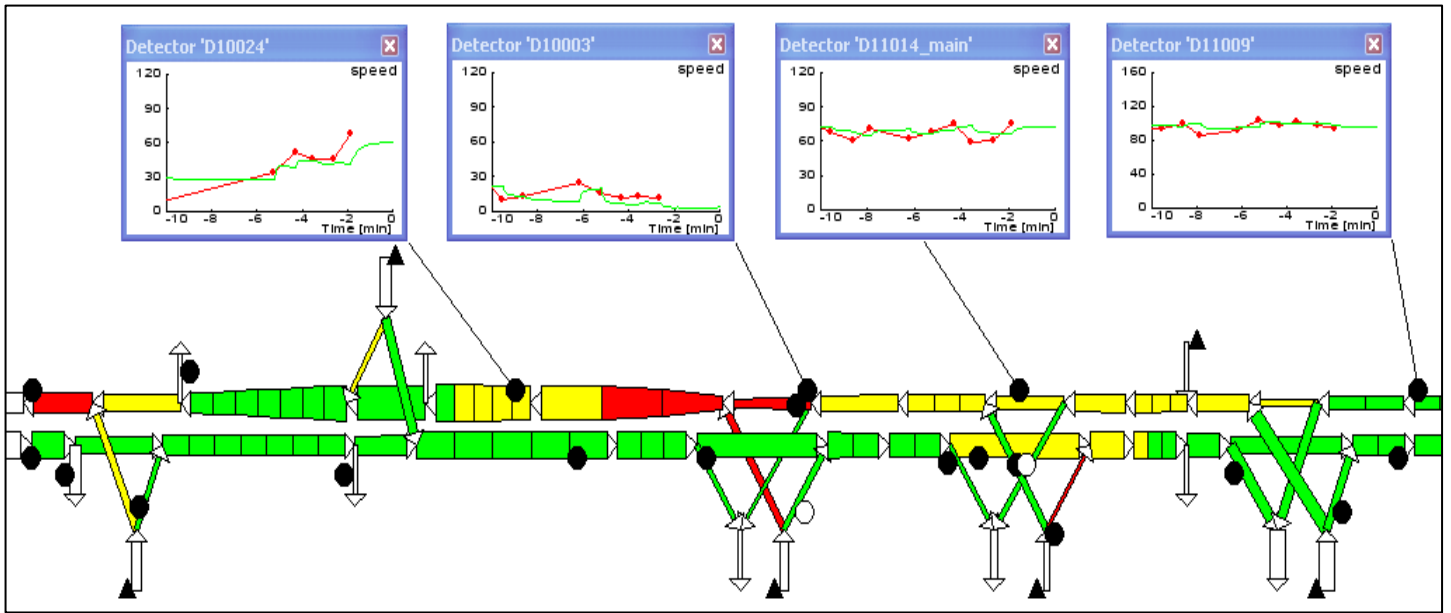
Figure 28: Traffic state estimation results displayed with the RENAISSANCE GUI (top to bottom): (a) 8:32 AM; (b) 8:42 AM; (c) 12:23 AM
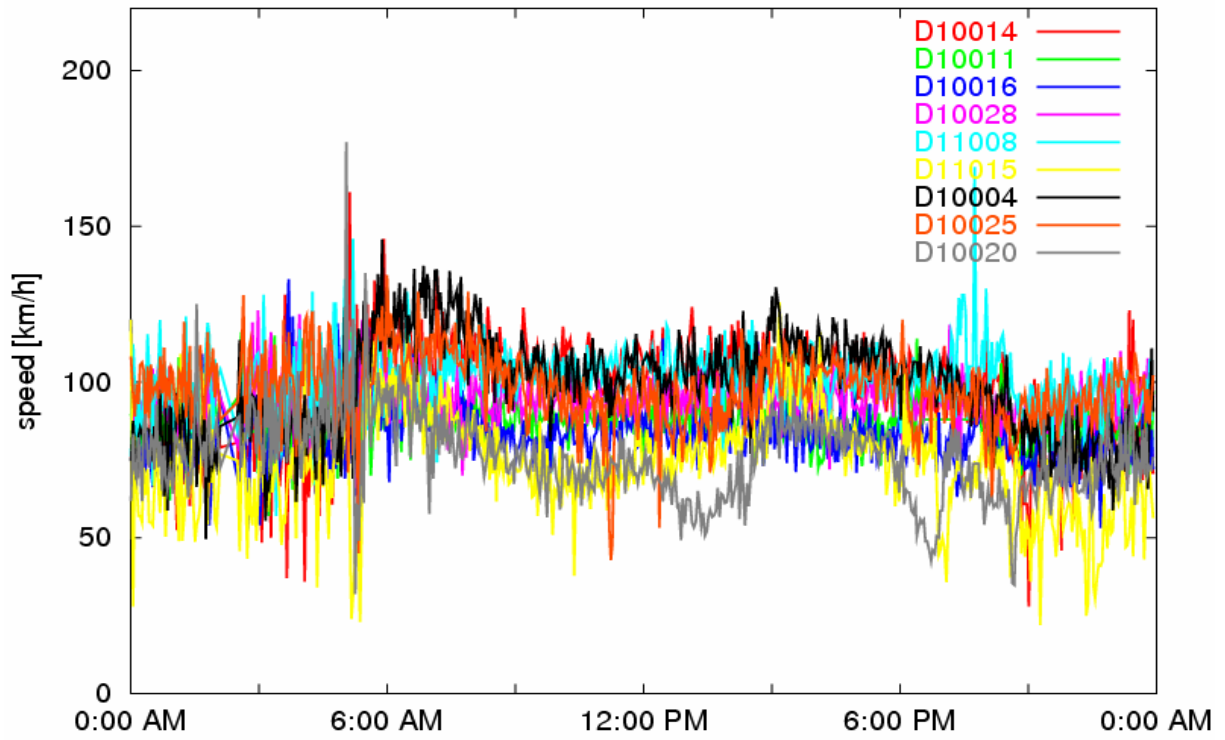
Figure 29: Speed measurements along A3 in Salerno direction on May 28, 2006
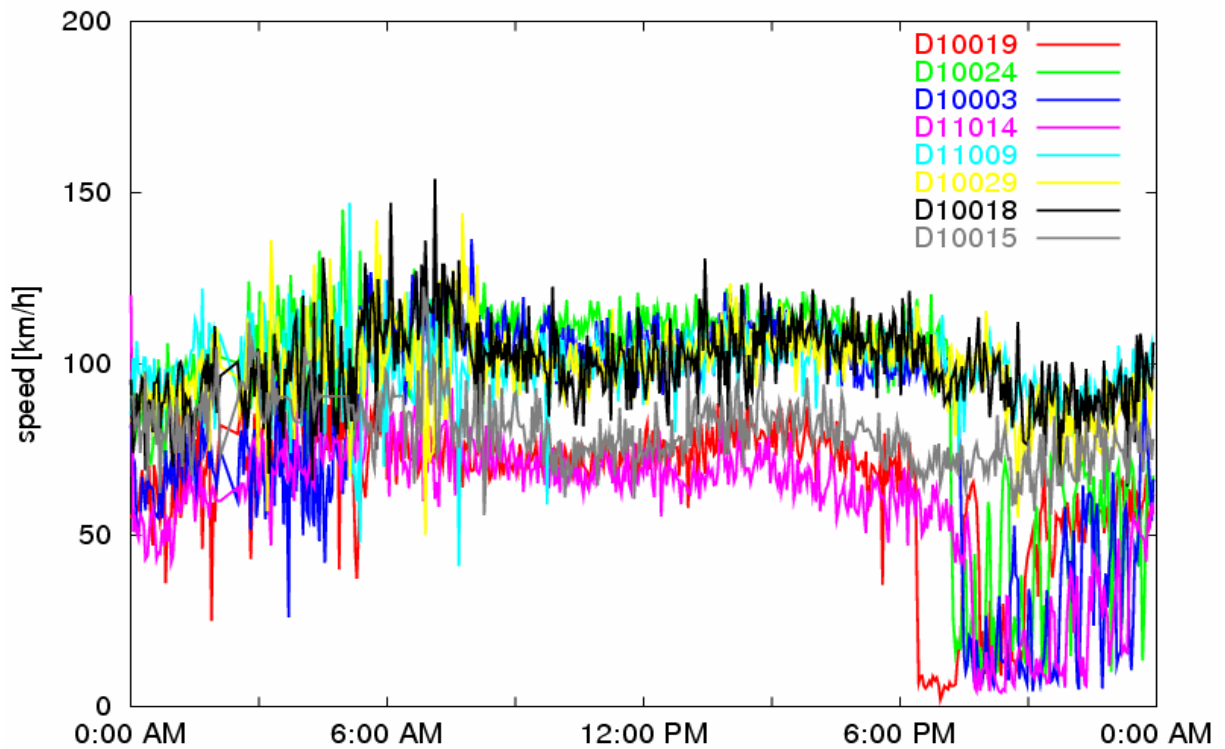
Figure 30: Speed measurements along A3 in Naples direction on May 28, 2006
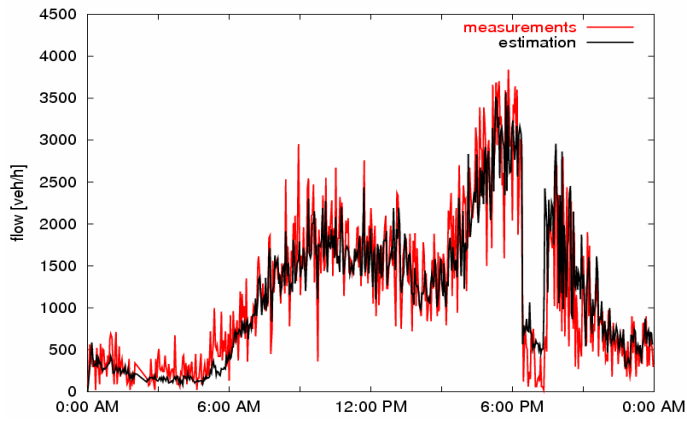
Figure 31: Flow at D10019, May 28
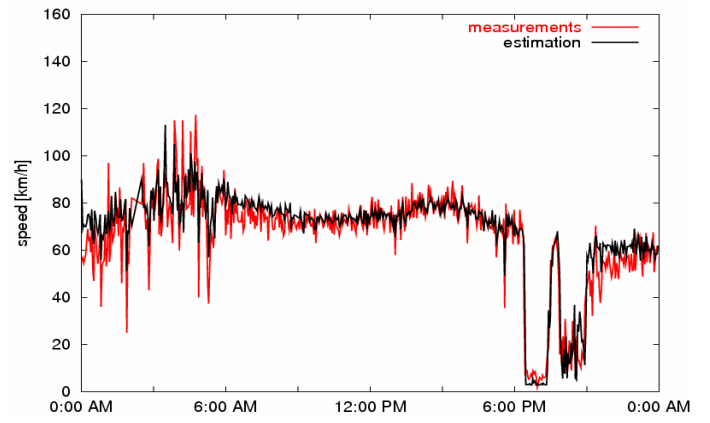
Figure 32: Speed at D10019, May 28
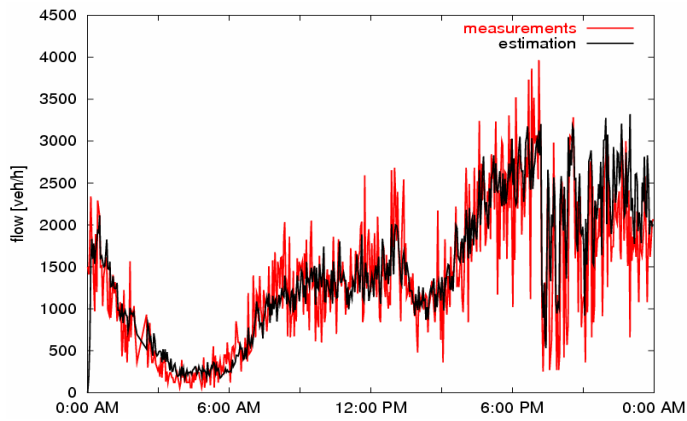
Figure 33: Flow at D10024, May 28
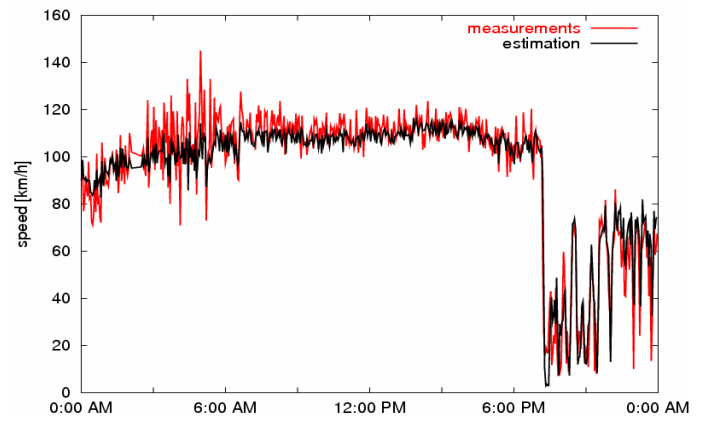
Figure 34: Speed at D10024, May 28
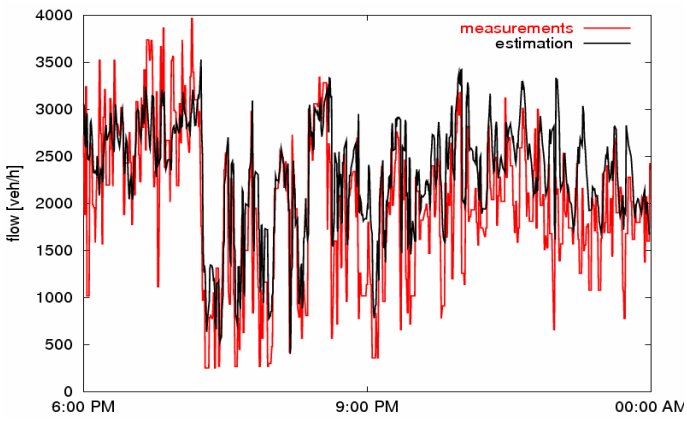
Figure 35: Zoom on Figure 33, May 28
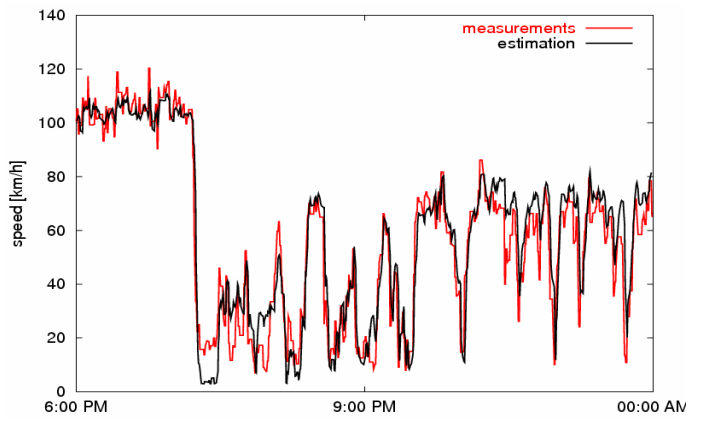
Figure 36: Zoom on Figure 34, May 28
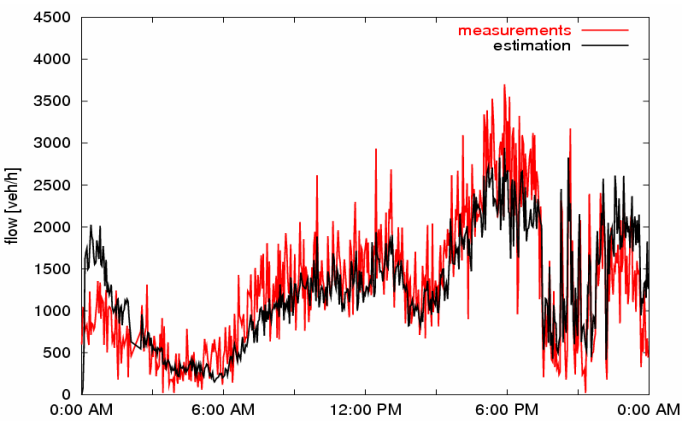
Figure 37: Flow at D10003, May 28
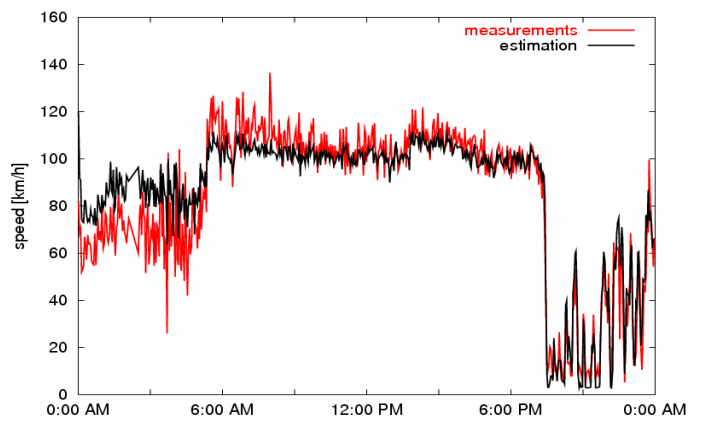
Figure 38: Speed at D10003, May 28

78
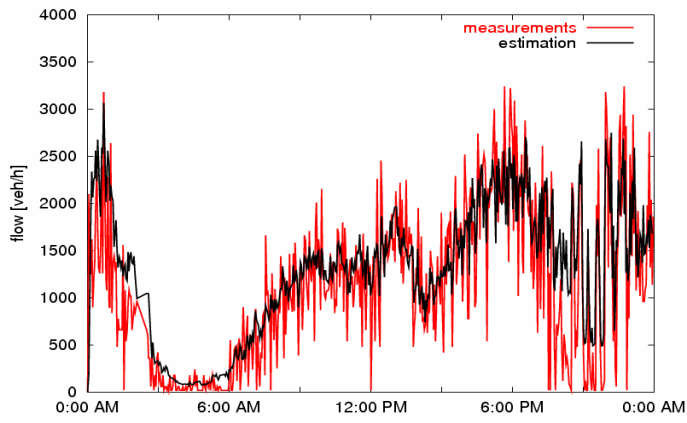
Figure 39: Flow at D11014, May 28
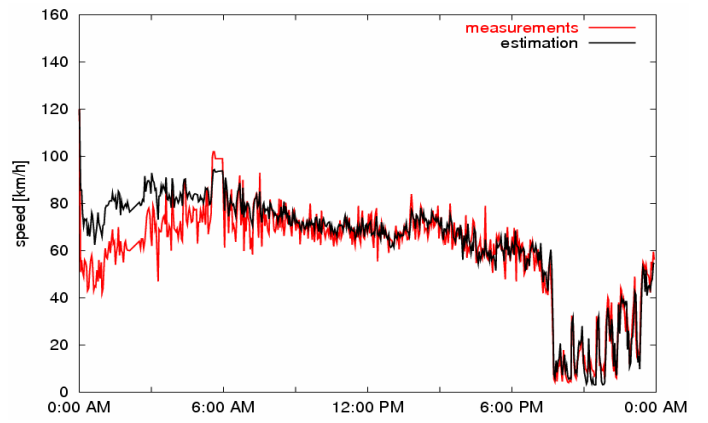
Figure 40: Speed at D11014, May 28
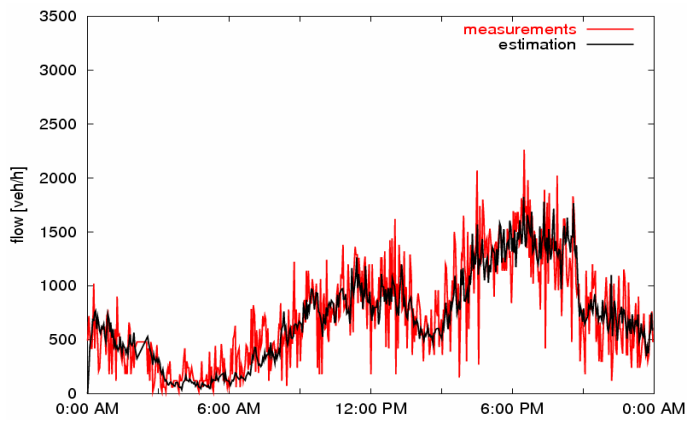
Figure 41: Flow at D11009, May 28
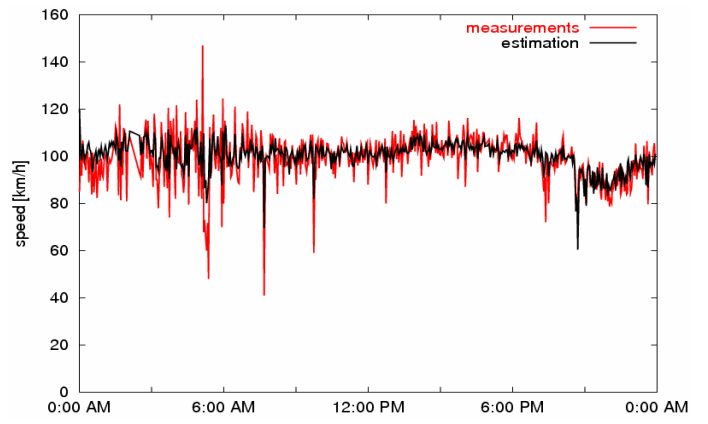
Figure 42: Speed at D11009, May 28
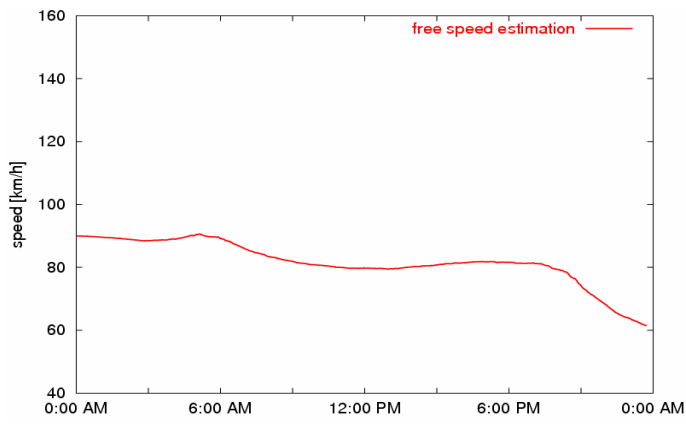
(a)
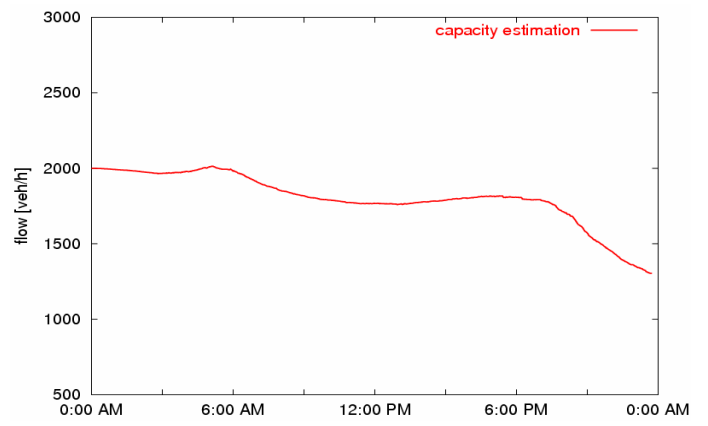
(b)
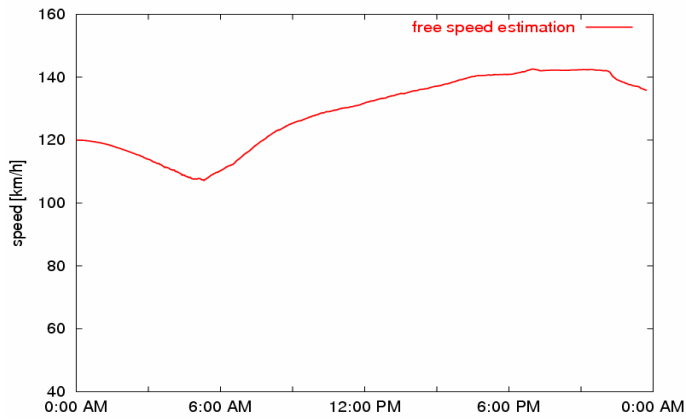
(c)
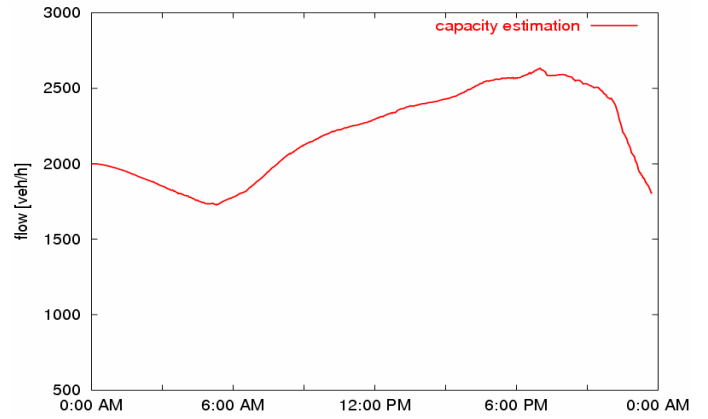
(d)
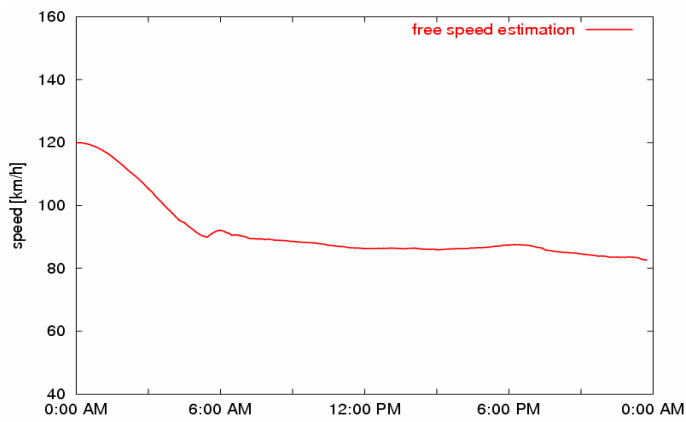
(e)
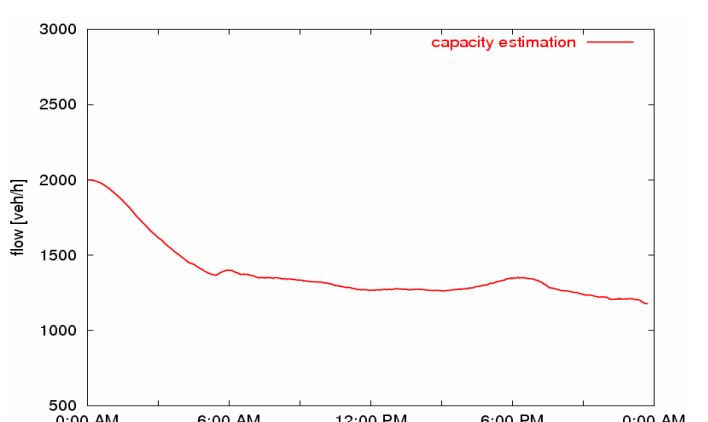
(f)
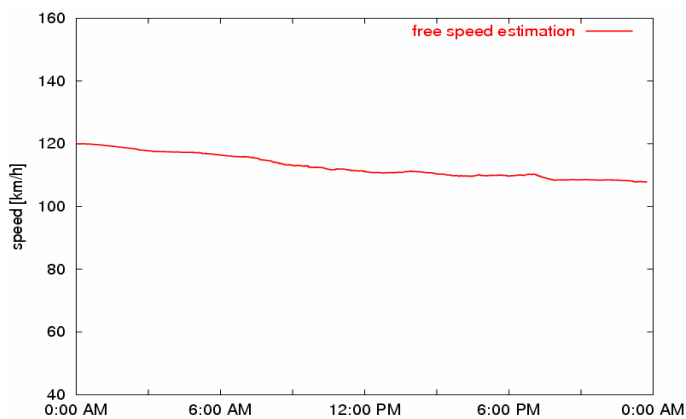
(g)
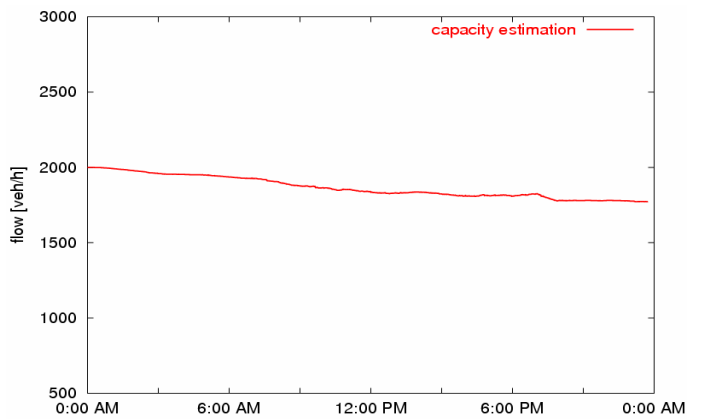
(h)

**Figure 43: Free speed and capacity estimates along A3 in Naples direction on May 28, 2006**

80
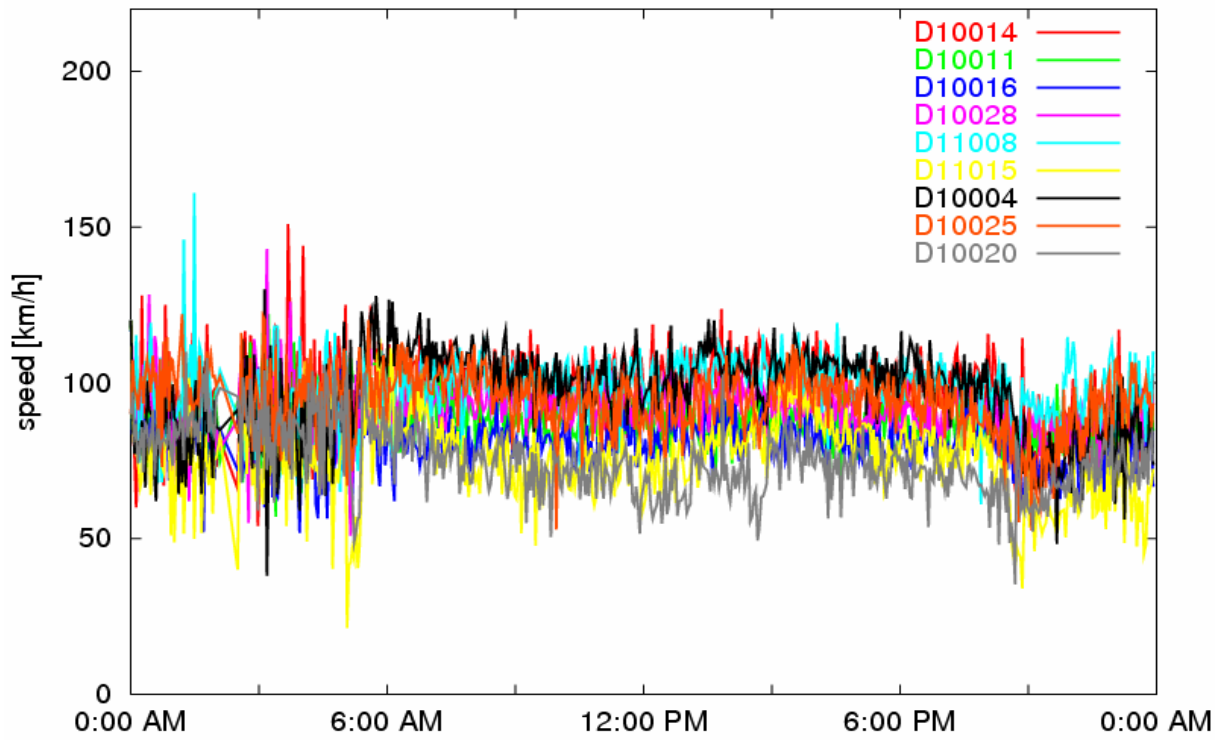
Figure 44: Speed measurements along A3 in Salerno direction on June 10, 2006
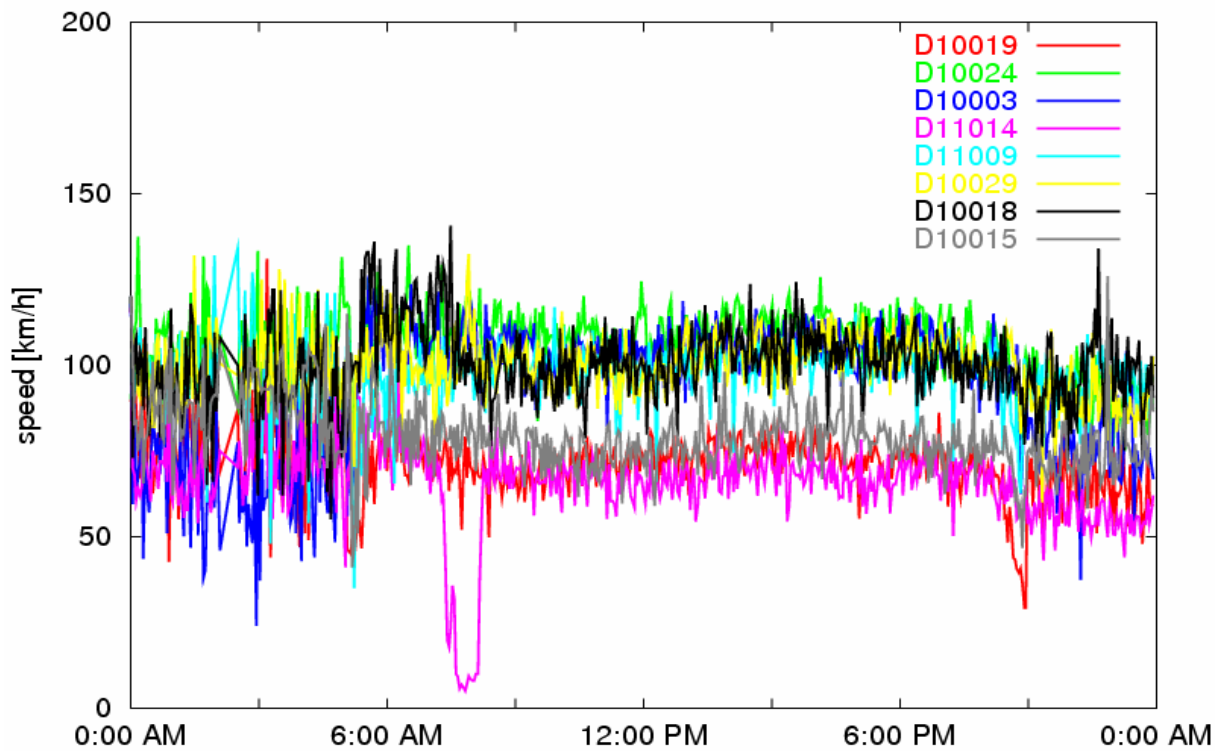
Figure 45: Speed measurements along A3 in Naples direction on June 10, 2006
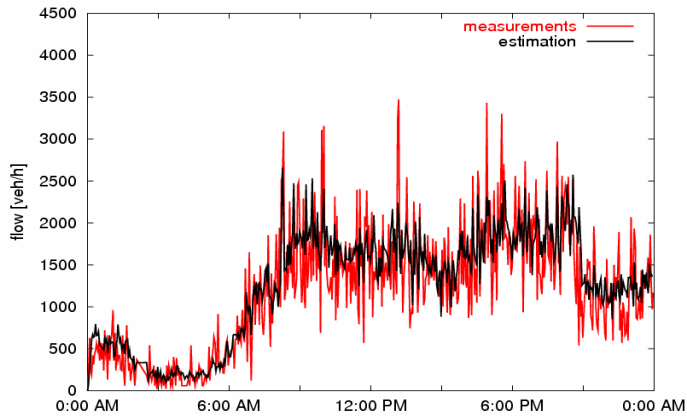
Figure 46: Flow at D10024, June 10
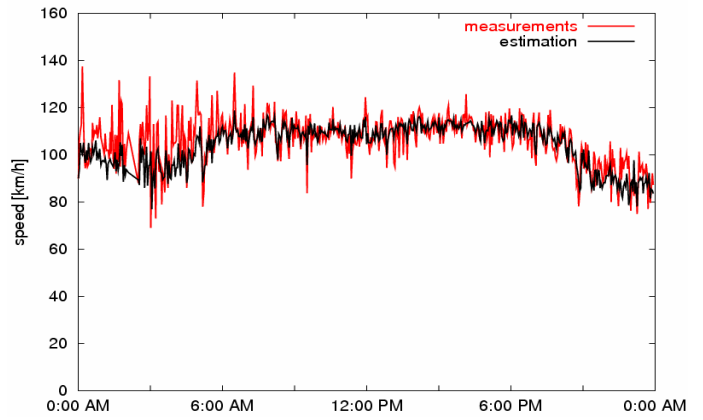
Figure 47: Speed at D10024, June 10
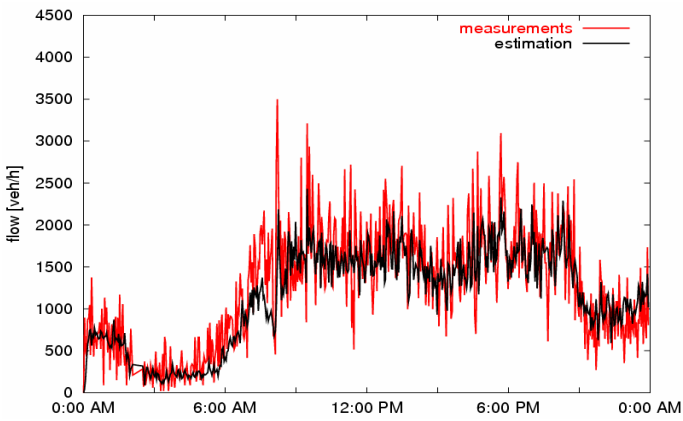
Figure 48: Flow at D10003, June 10
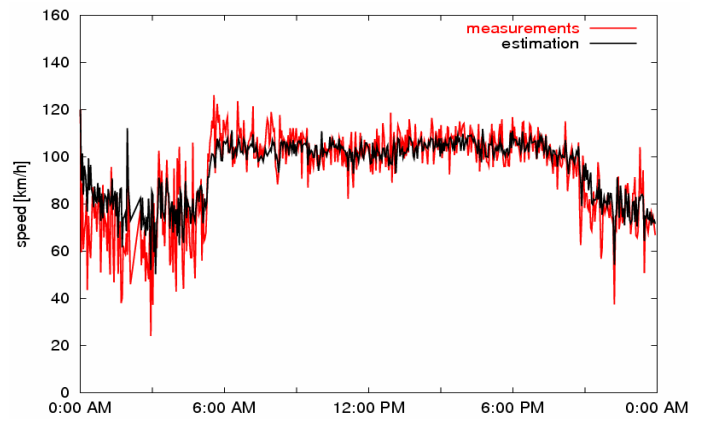
Figure 49: Speed at D10003, June 10
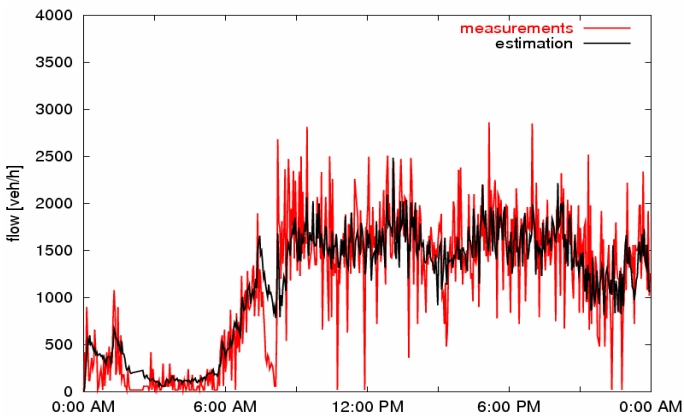
Figure 50: Flow at D11014, June 10
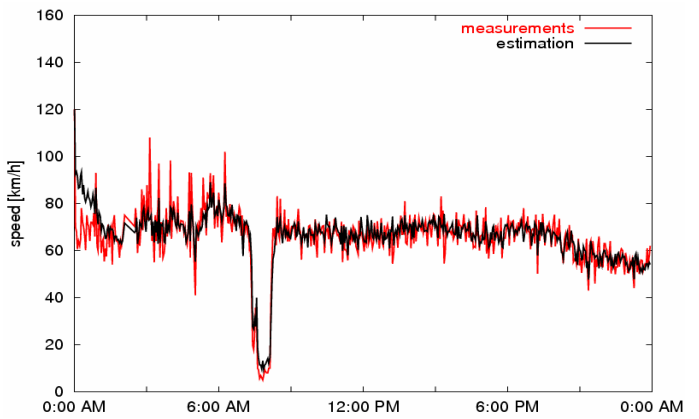
Figure 51: Speed at D11014, June 10
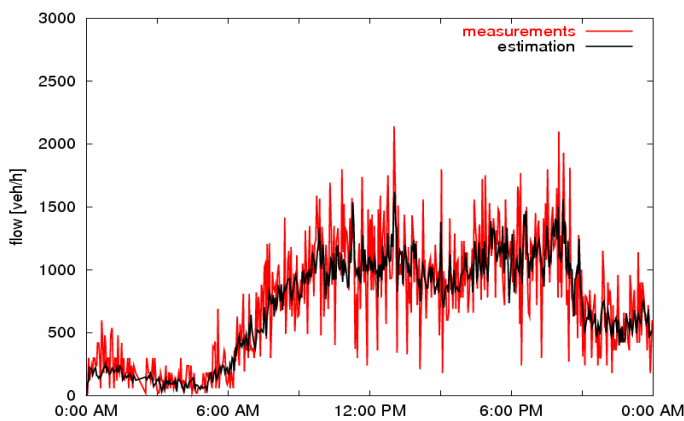
Figure 52: Flow at D11009, June 10
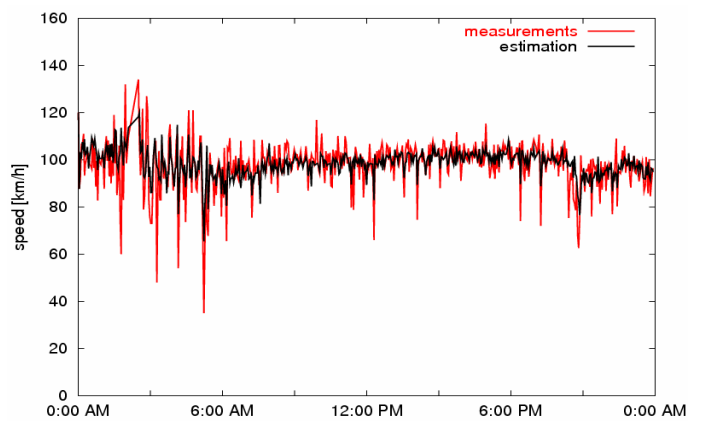
Figure 53: Speed at D11009, June 10

82
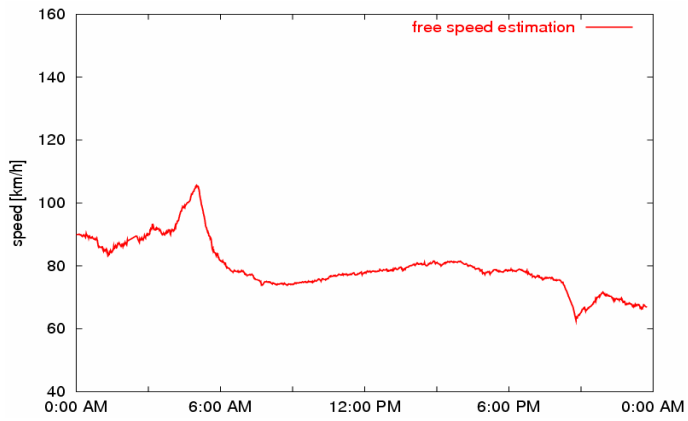
(a)
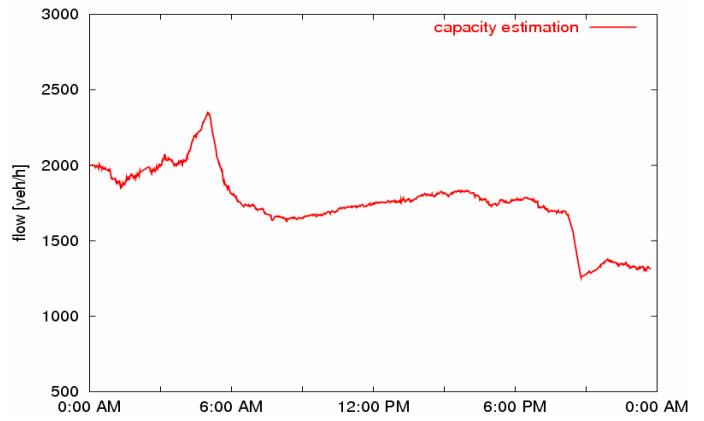
(b)
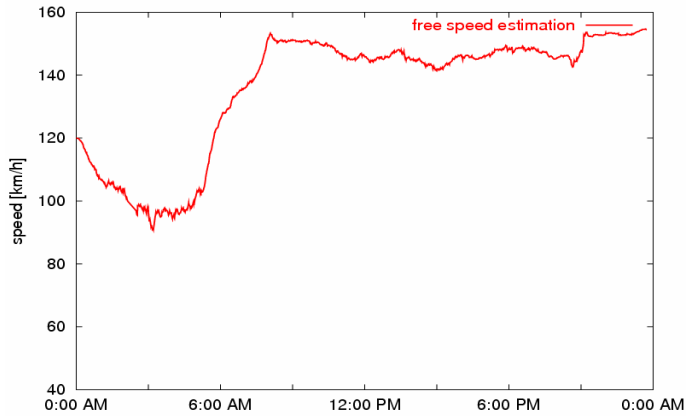
(c)
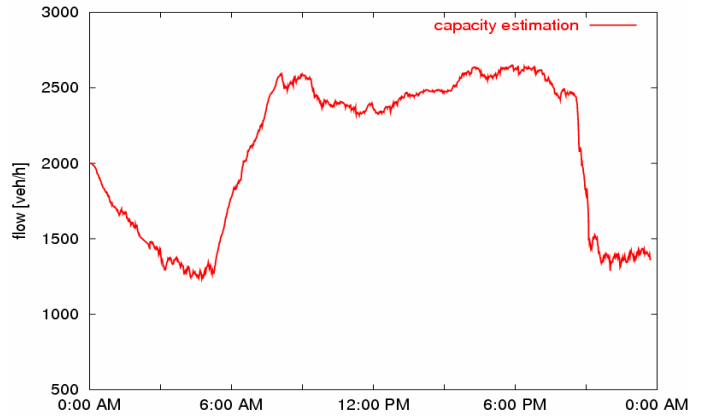
(d)
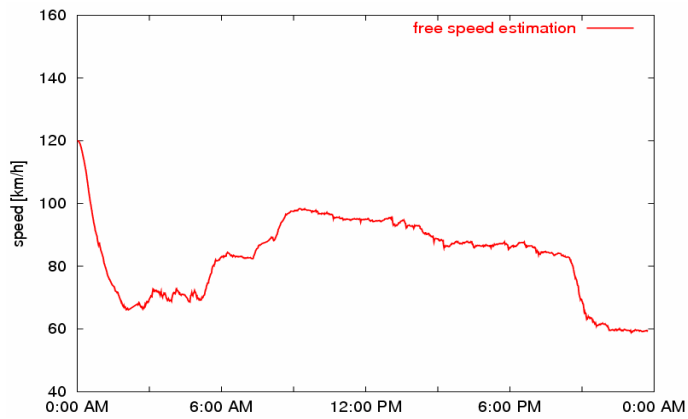
(e)
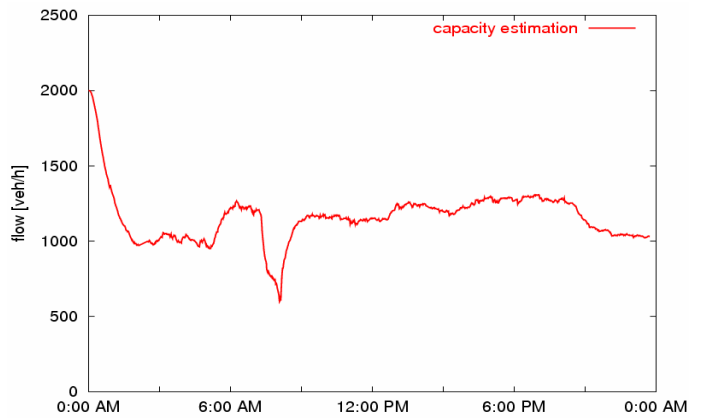
(f)
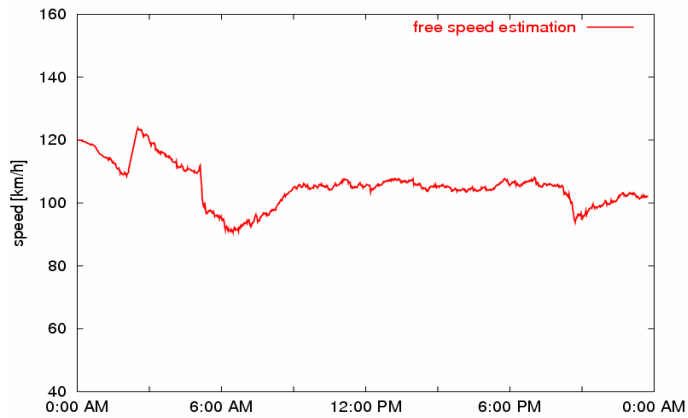
(g)
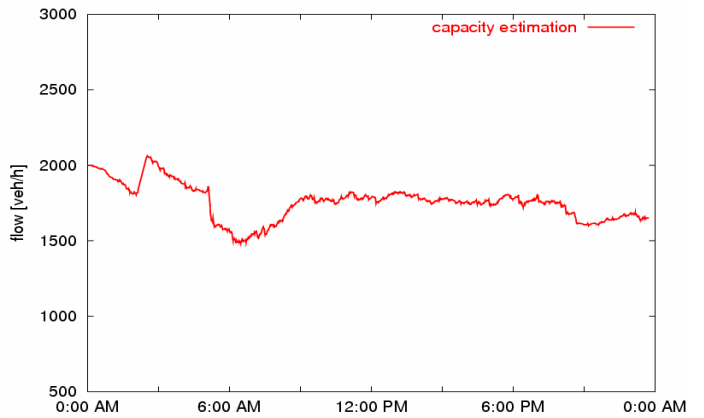
(h)

Figure 54: Free speed and capacity estimates along A3 in Naples direction on June 10, 2006

83
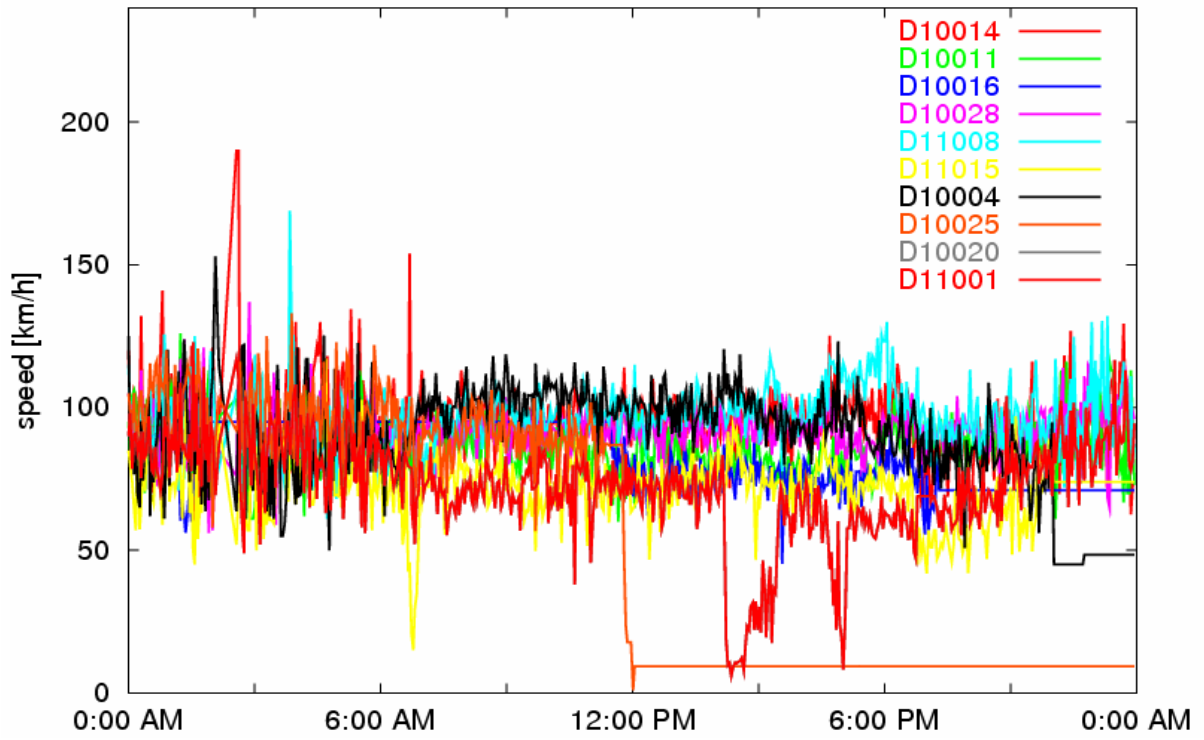
Figure 55: Speed measurements along A3 in Salerno direction on October 9, 2006
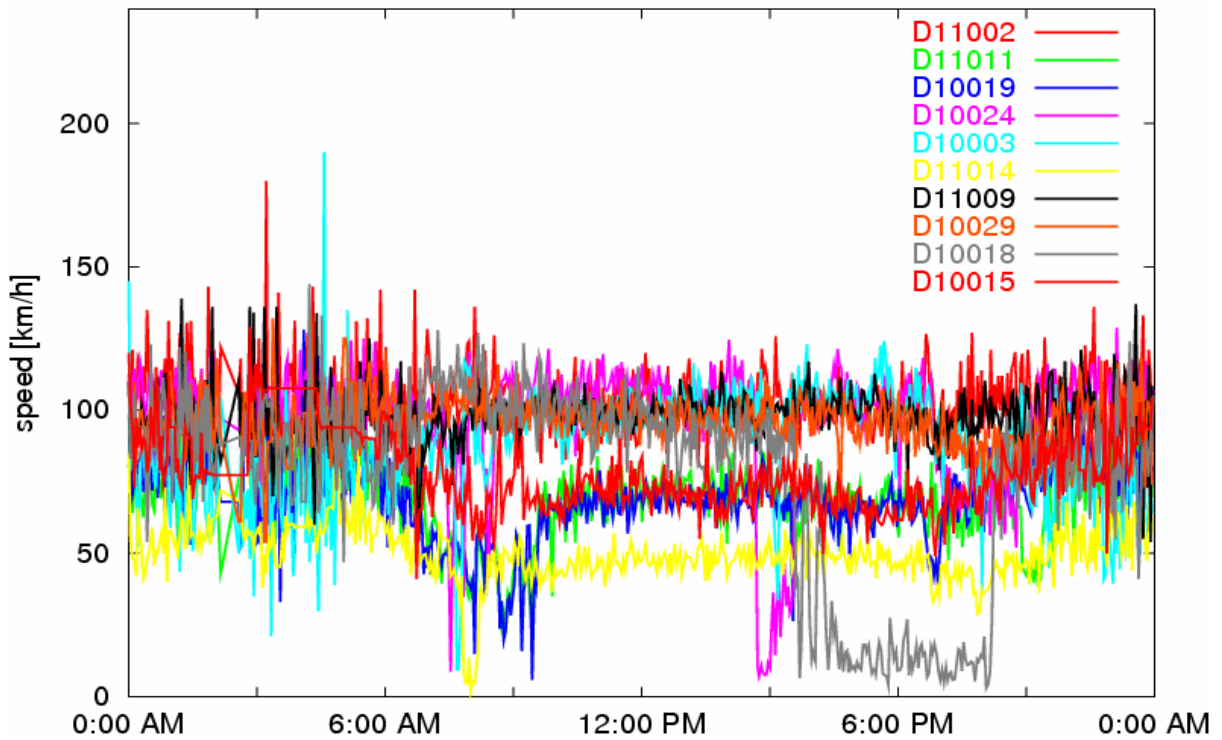
Figure 56: Speed measurements along A3 in Naples direction on October 9, 2006

84
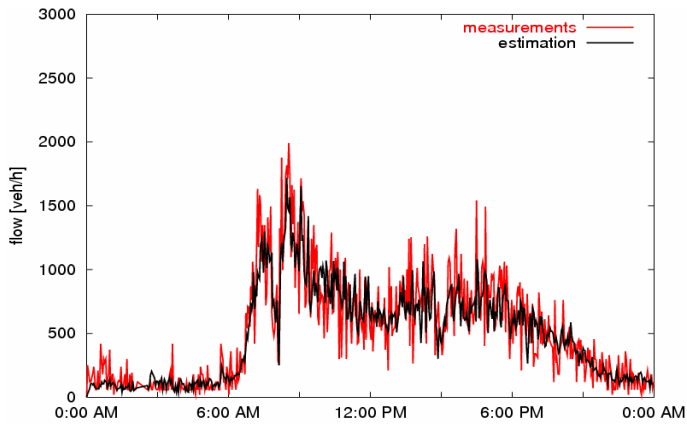
Figure 57: Flow at D11002, October 9
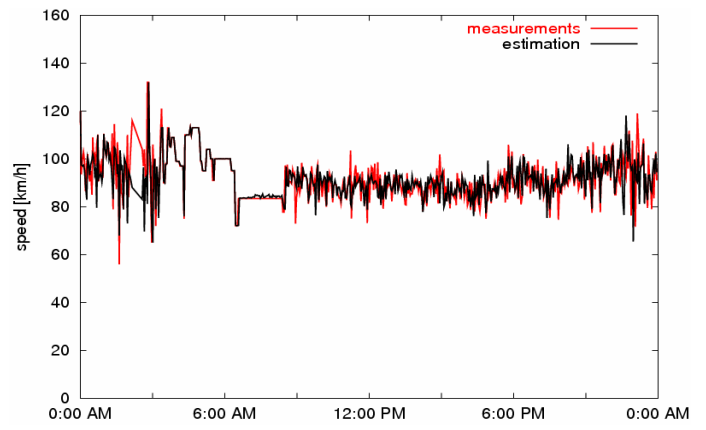
Figure 58: Speed at D11002, October 9
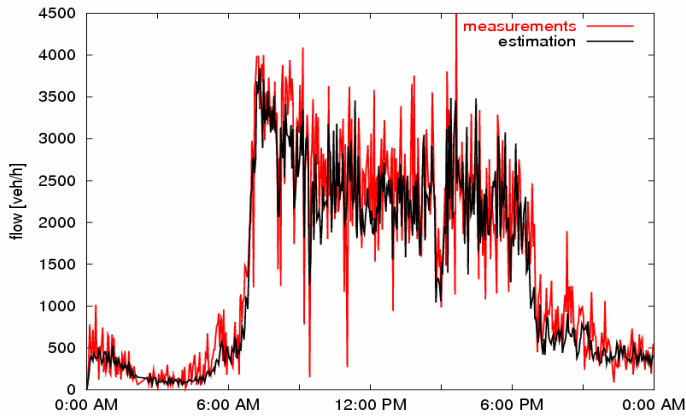
Figure 59: Flow at D10019, October 9
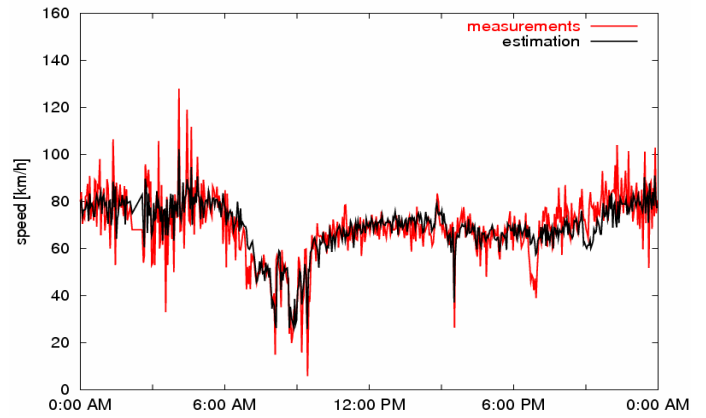
Figure 60: Speed at D10019, October 9
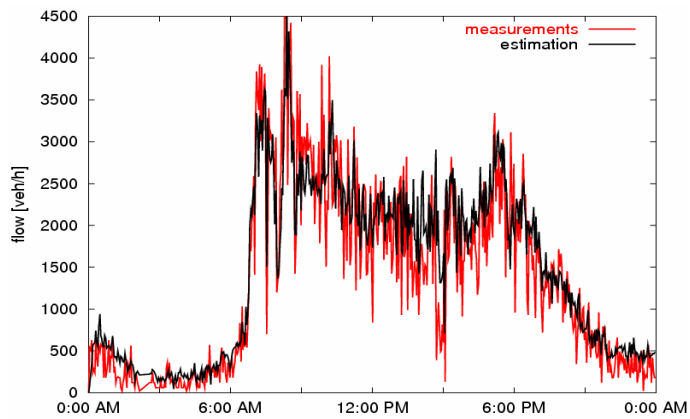
Figure 61: Flow at D10024, October 9
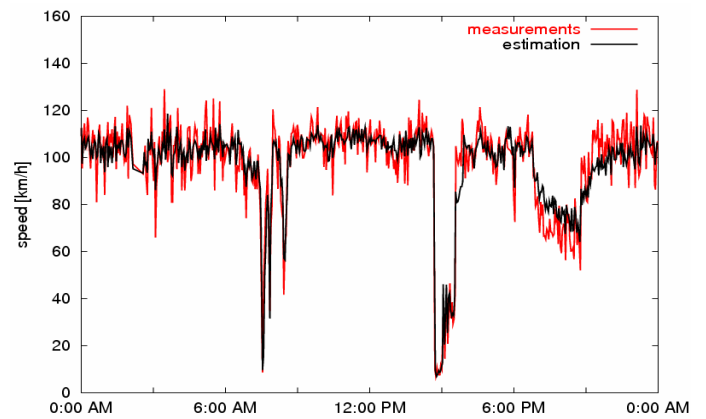
Figure 62: Speed at D10024, October 9
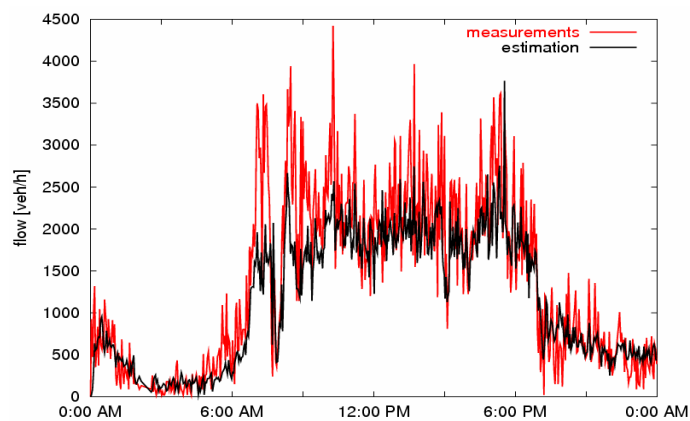
Figure 63: Flow at D10003, October 9
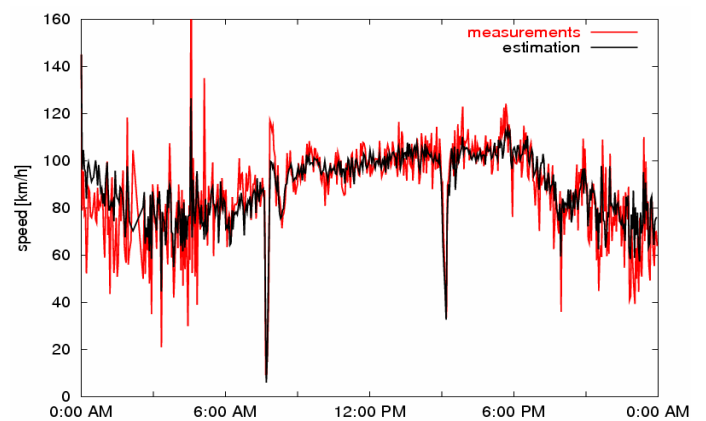
Figure 64: Speed at D10003, October 9
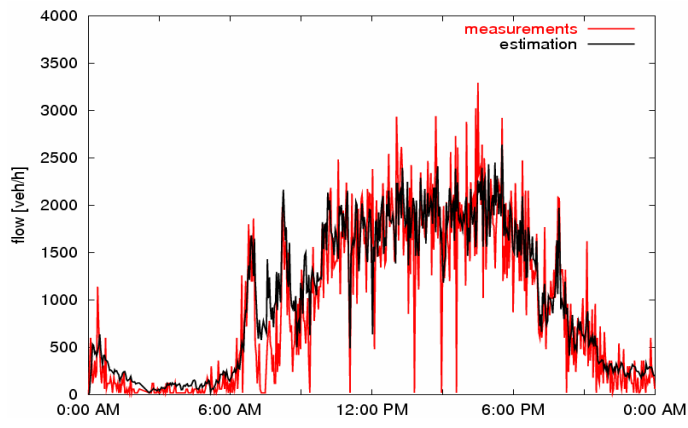
Figure 65: Flow at D11014, October 9
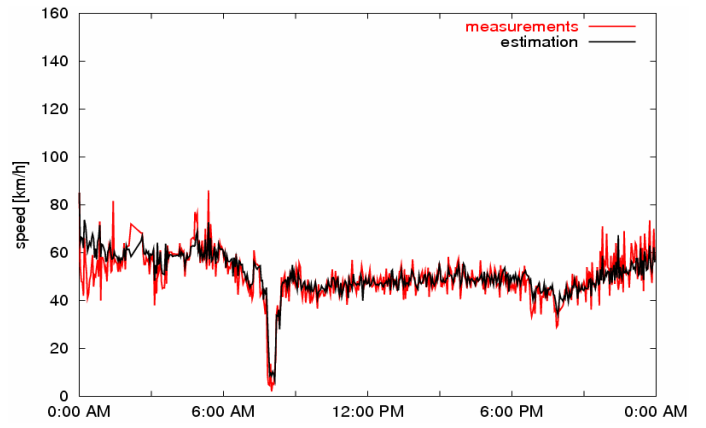
Figure 66: Speed at D11014, October 9
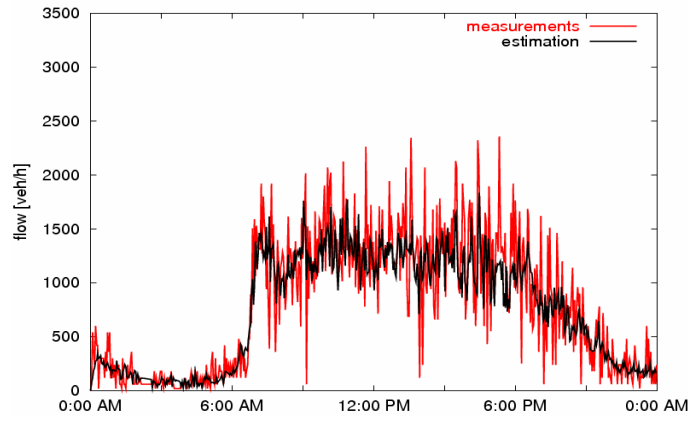
Figure 67: Flow at D11009, October 9
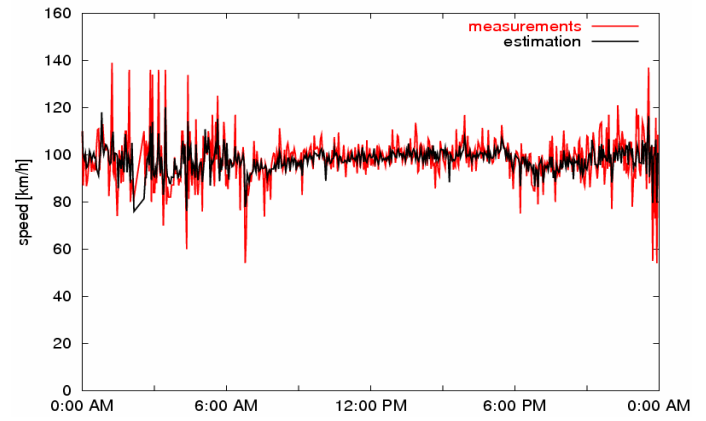
Figure 68: Speed at D11009, October 9
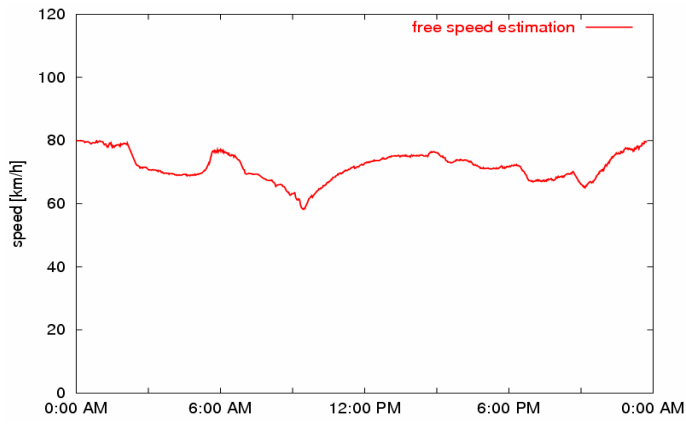
(a)
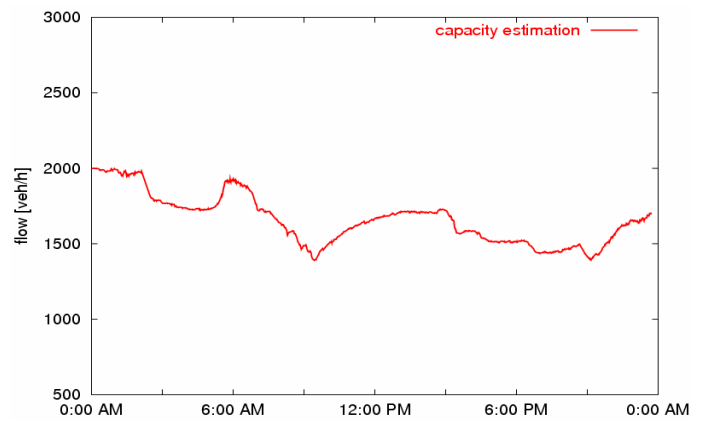
(b)
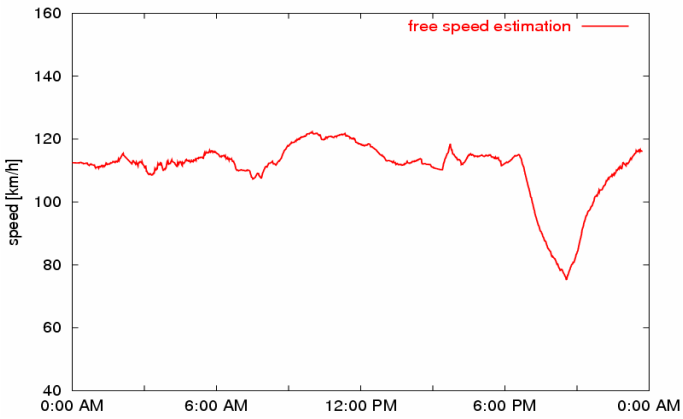
(c)
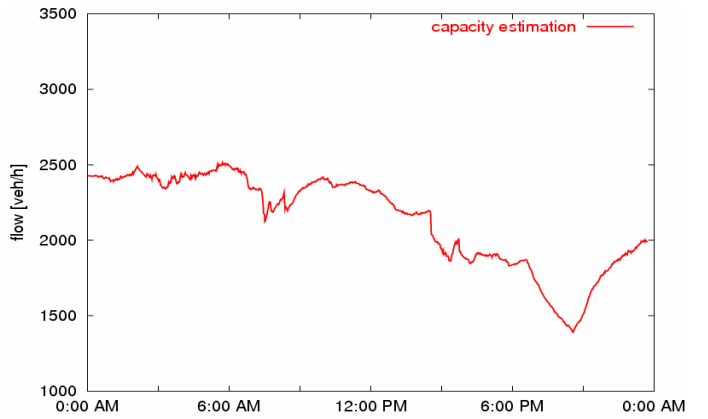
(d)
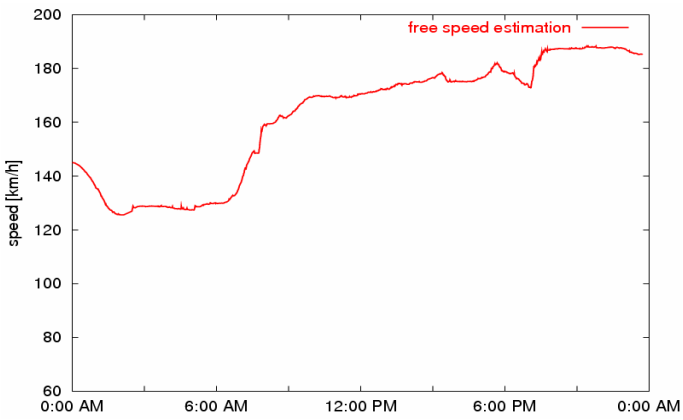
(e)
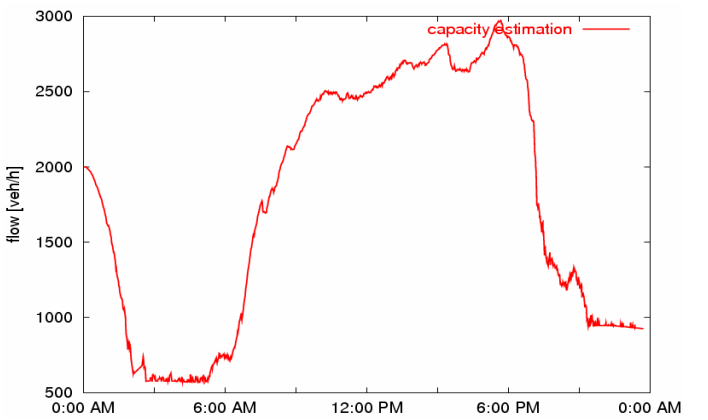
(f)
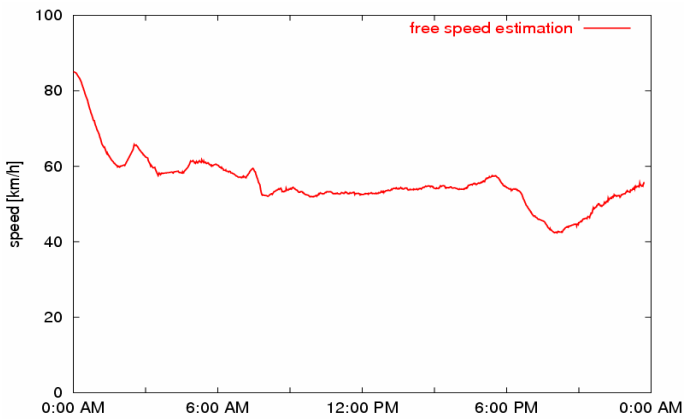
(g)
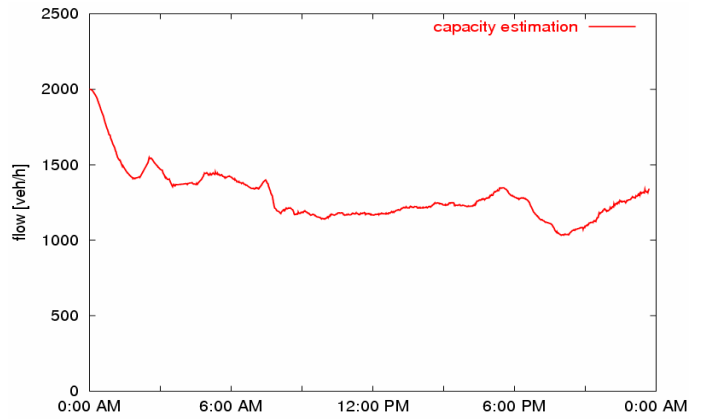
(h)

Figure 69: Free speed and capacity estimates along A3 in Naples direction on October 9, 2006

87
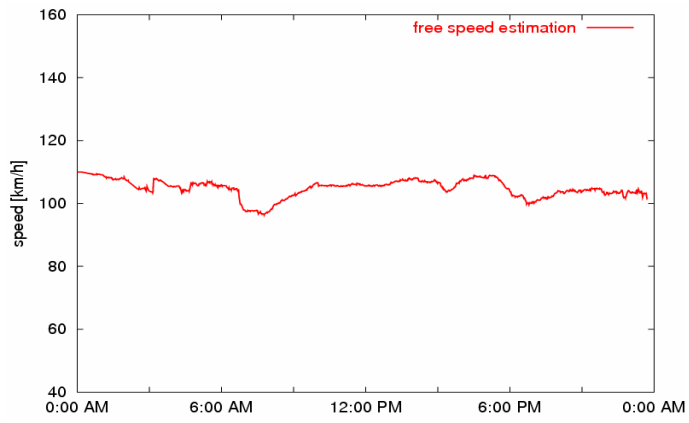
(a)
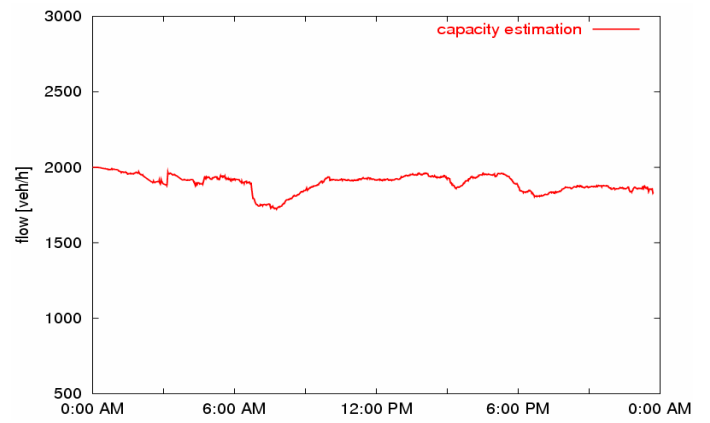
(b)
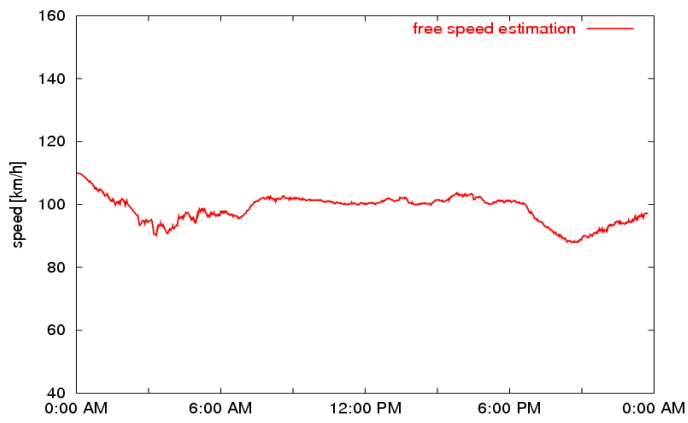
(c)
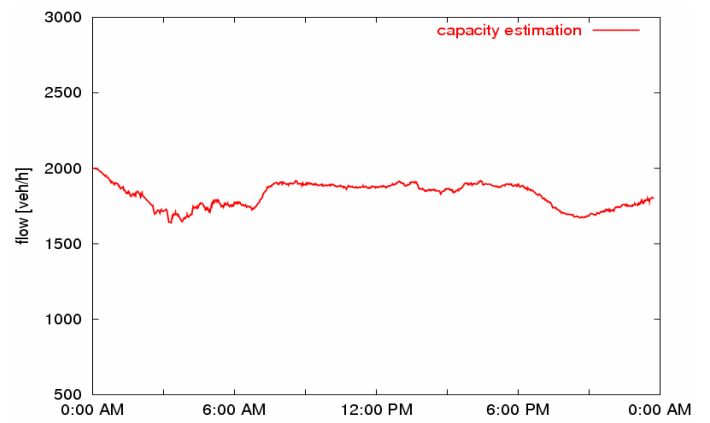
(d)

Figure 70: Free speed and capacity estimates along A3 in Naples direction on October 9, 2006
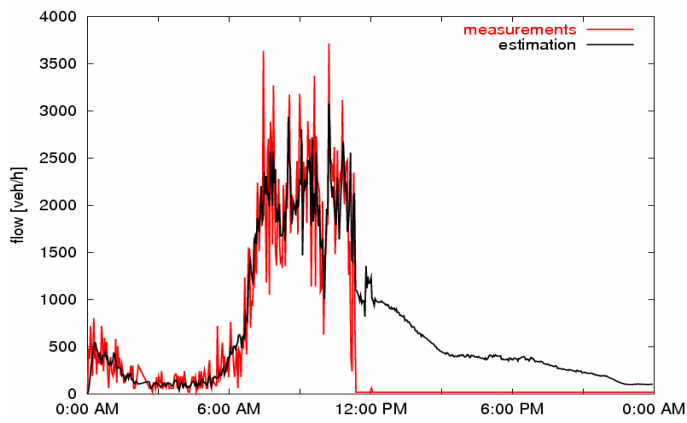
(a)
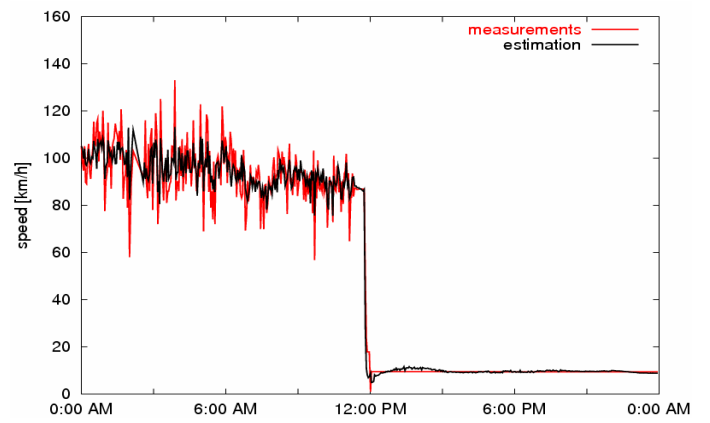
(b)
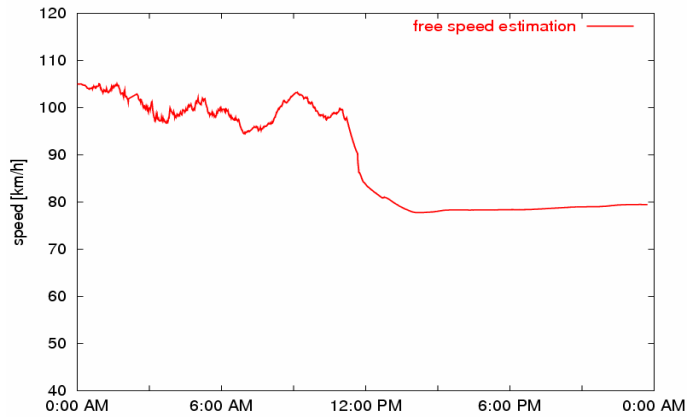
(c)
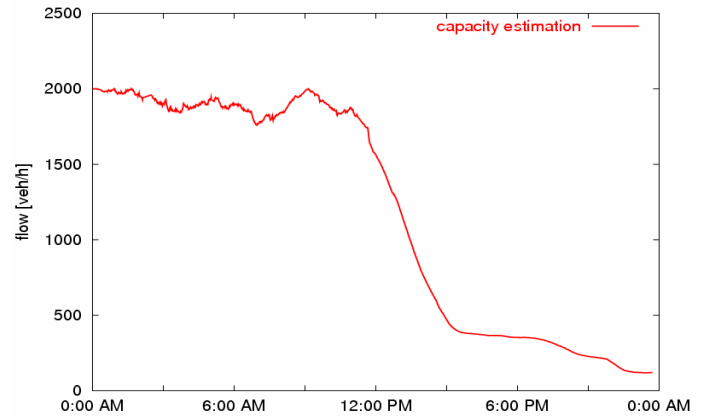
(d)
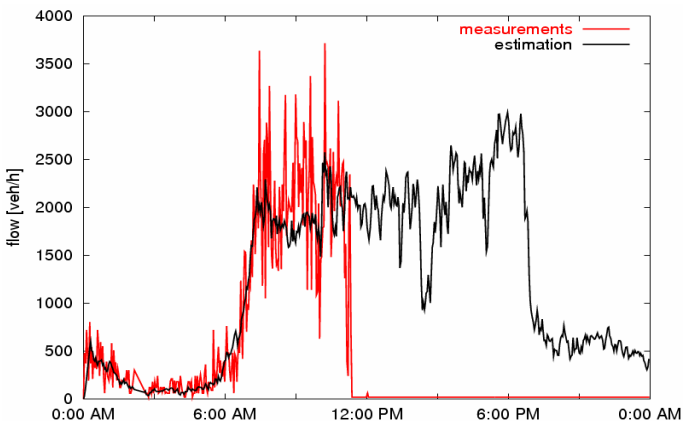
(e)
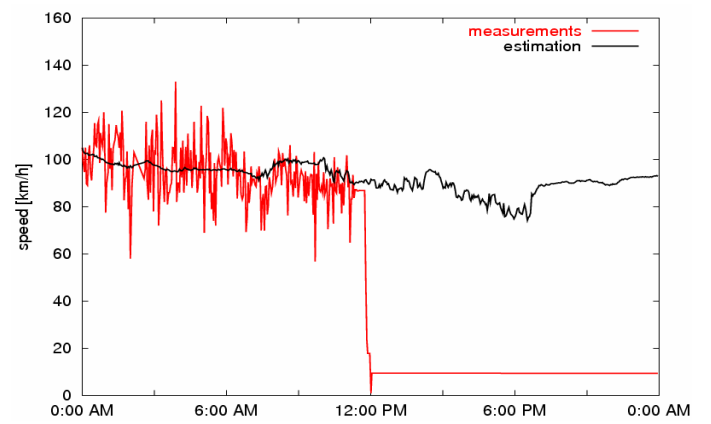
(f)
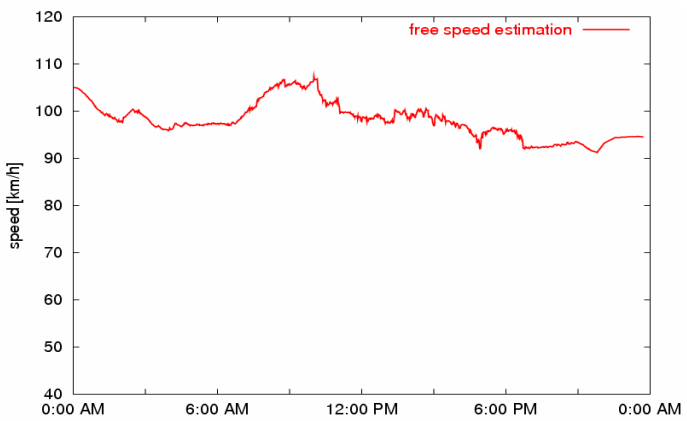
(g)
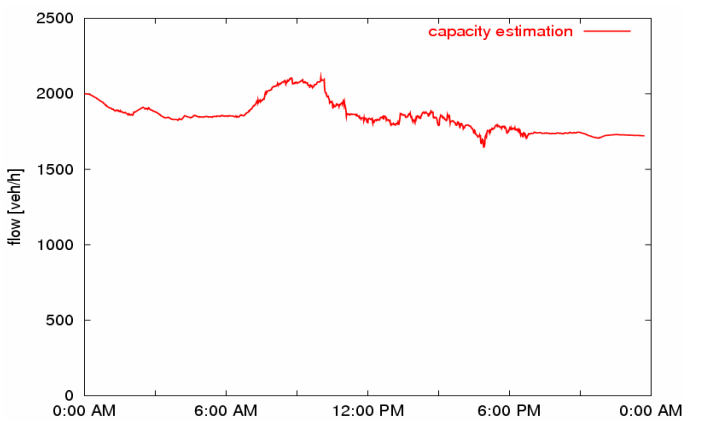
(h)

Figure 71: Detector fault at D10025 on October 9, 2006
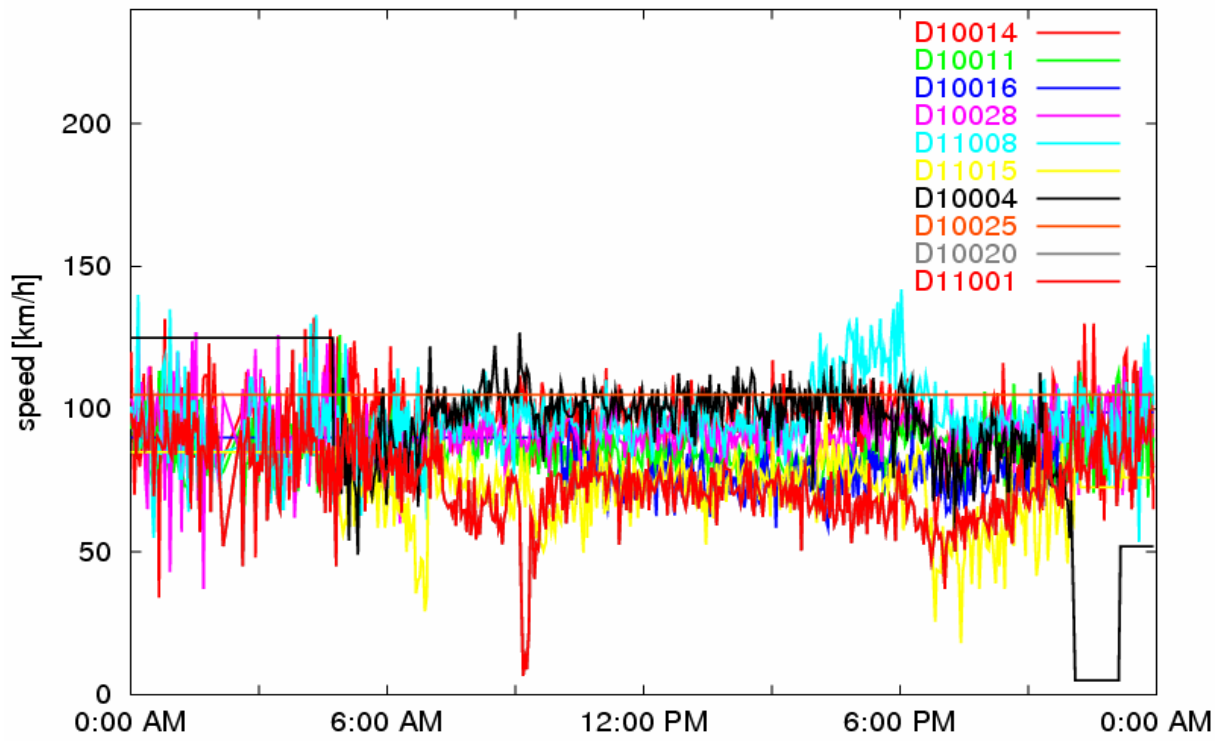
Figure 72: Speed measurements along A3 in Salerno direction on October 10, 2006

(b)
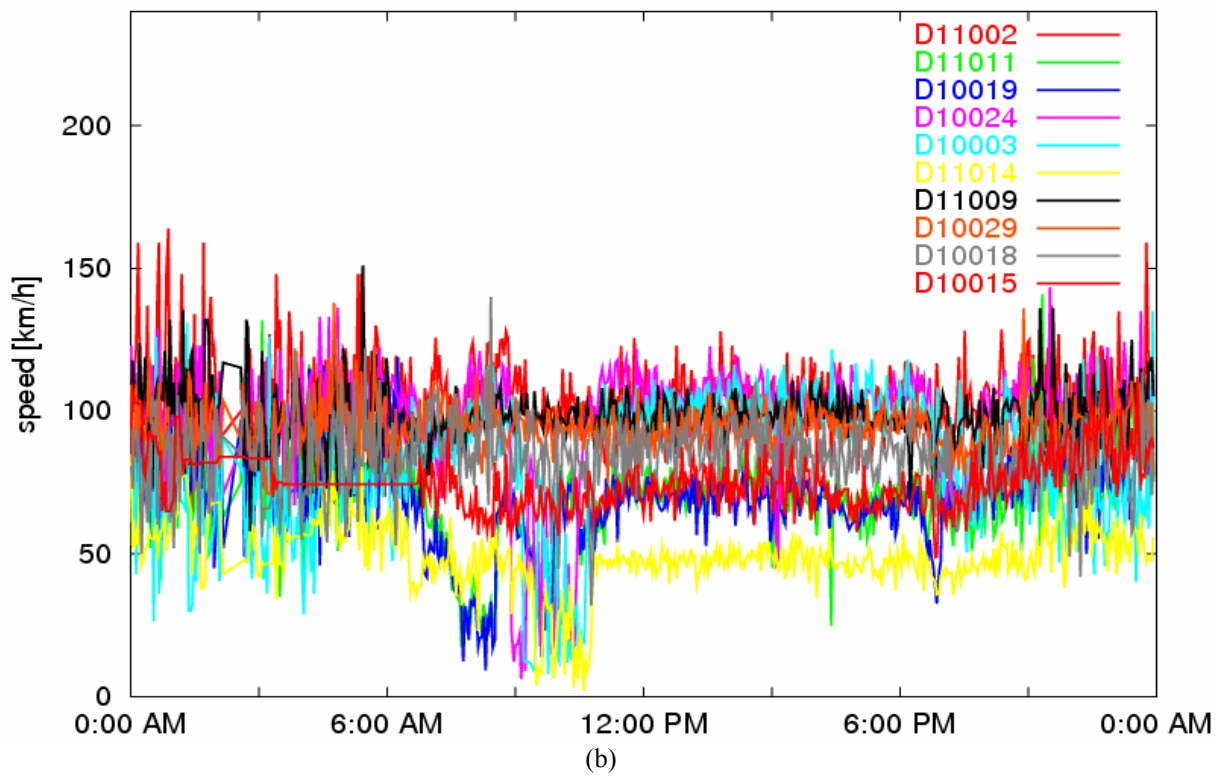
Figure 73: Speed measurements along A3 in Naples direction on October 10, 2006
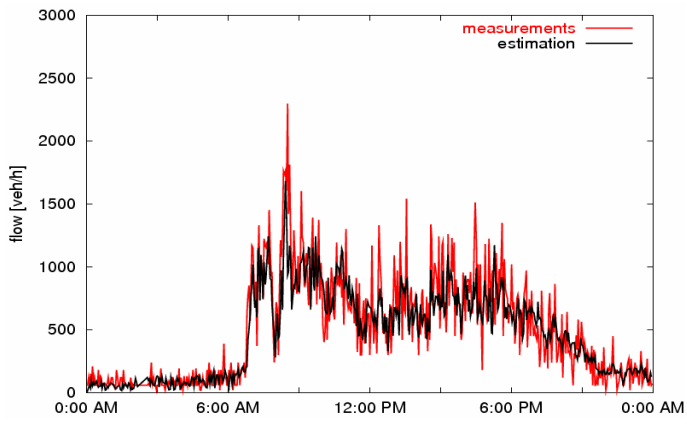
Figure 74: Flow at D11002, October 10
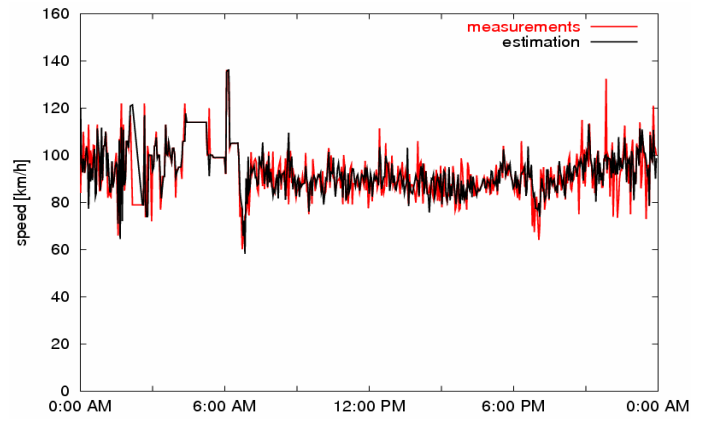
Figure 75: Speed at D11002, October 10
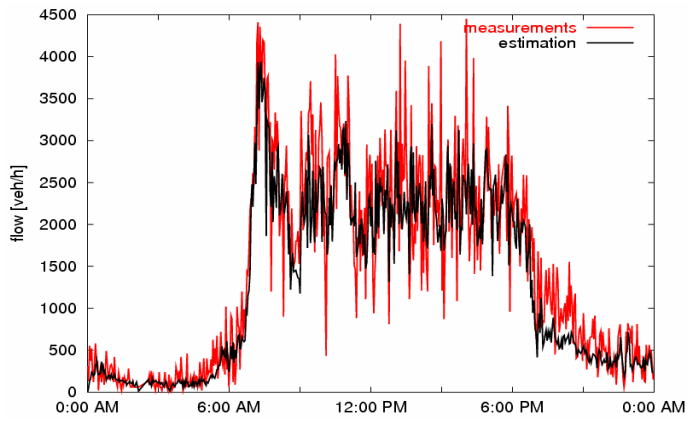
Figure 76: Flow at D10019, October 10
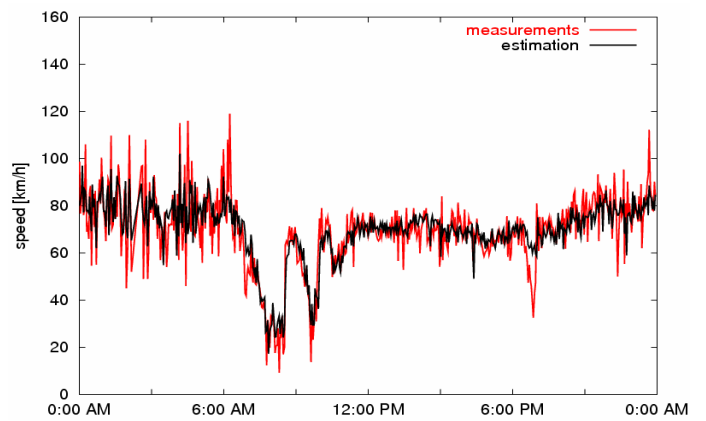
Figure 77: Speed at D10019, October 10
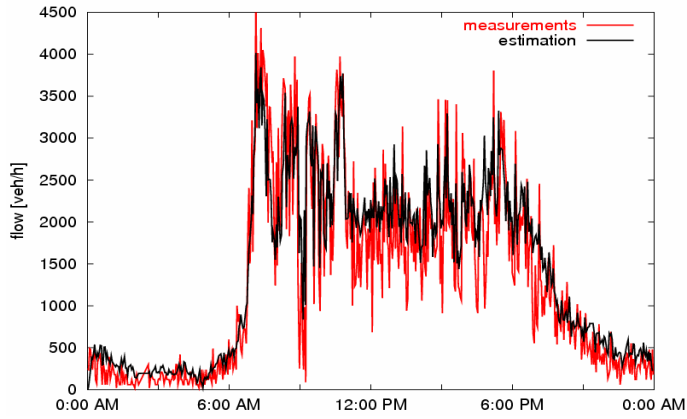
Figure 78: Flow at D10024, October 10
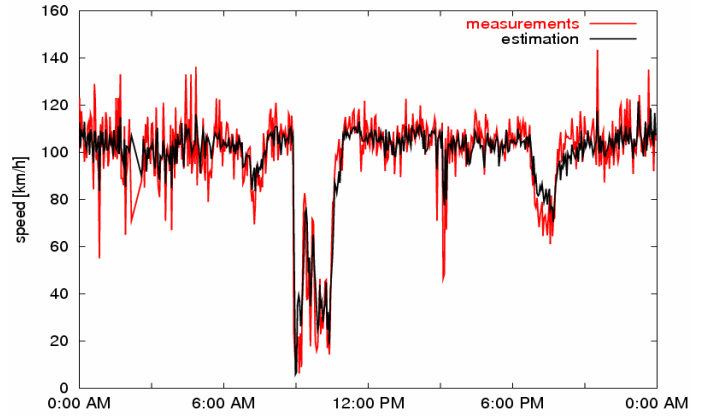
Figure 79: Speed at D10024, October 10
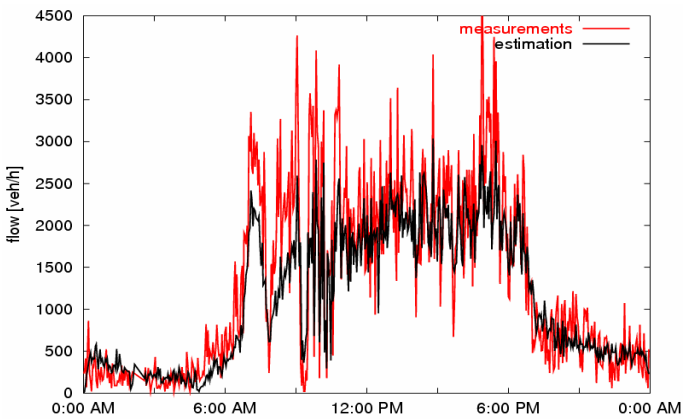
Figure 80: Flow at D10003, October 10
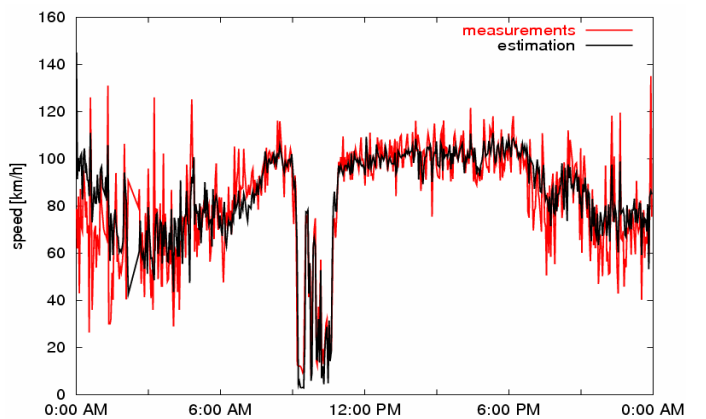
Figure 81: Speed at D10003, October 10

91
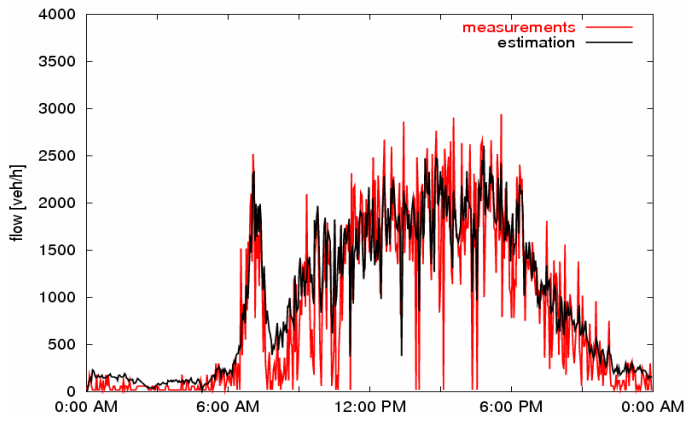
Figure 82: Flow at D11014, October 10
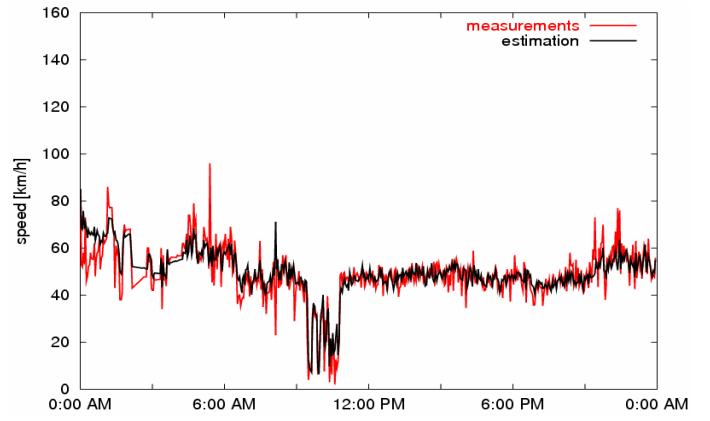
Figure 83: Speed at D11014, October 10
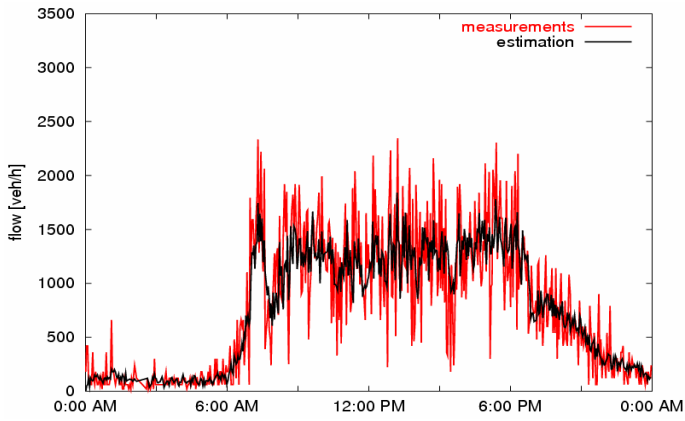
Figure 84: Flow at D11009, October 10
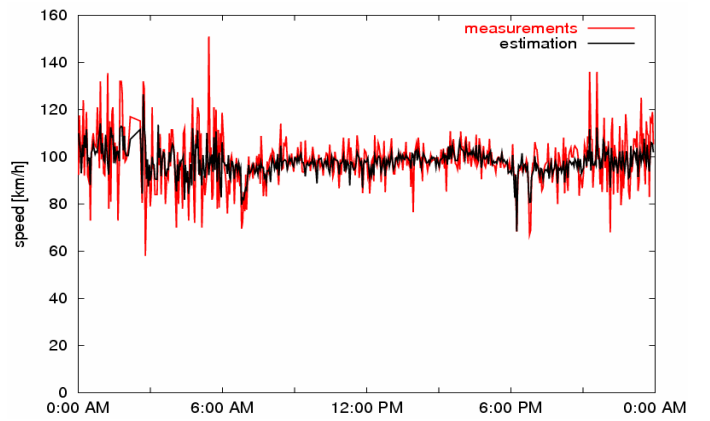
Figure 85: Speed at D11009, October 10
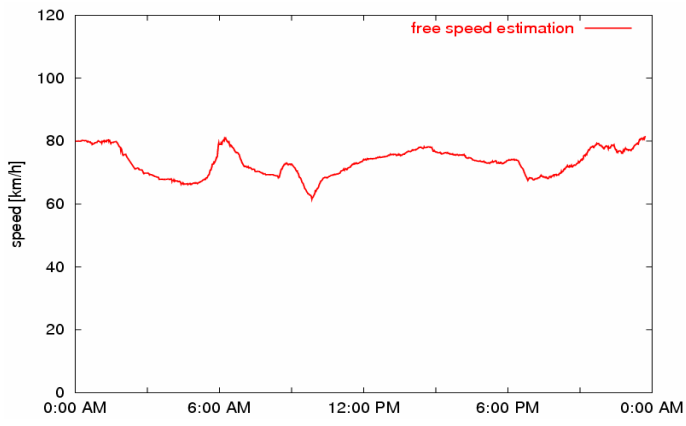
(a)
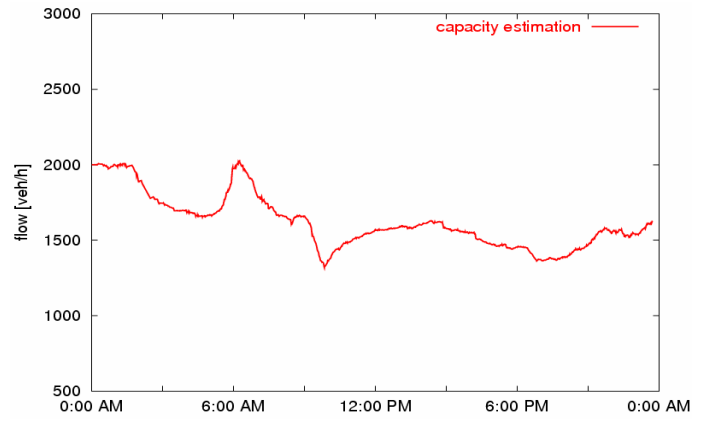
(b)
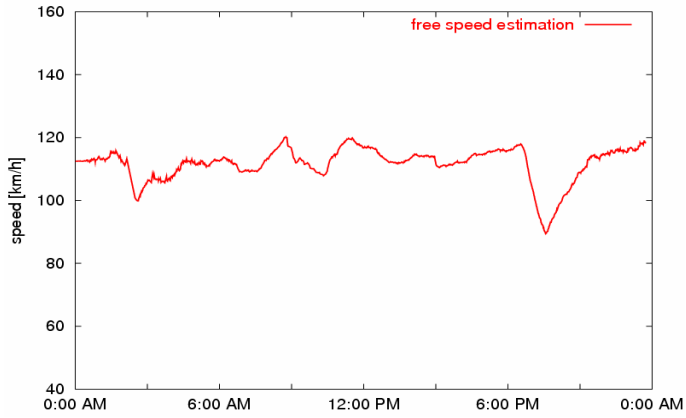
(c)
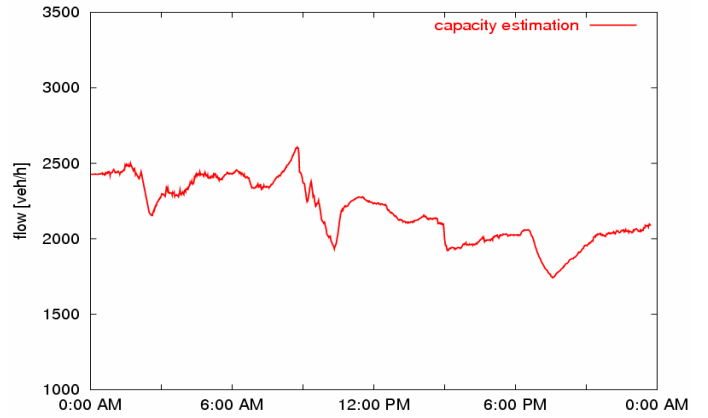
(d)
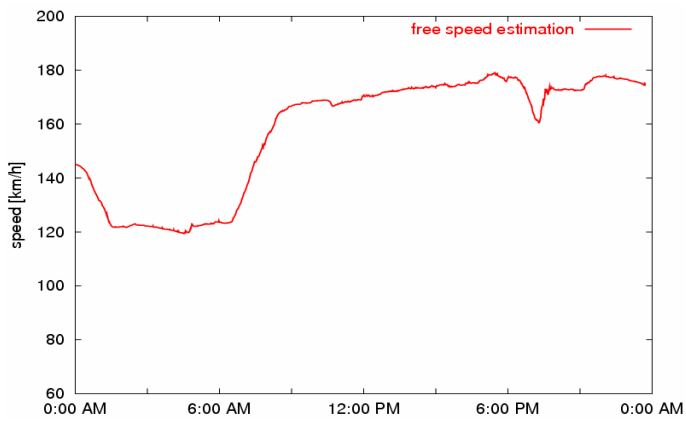
(e)
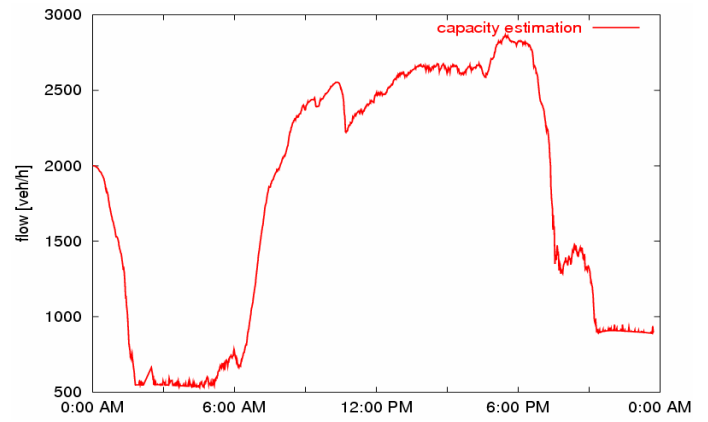
(f)
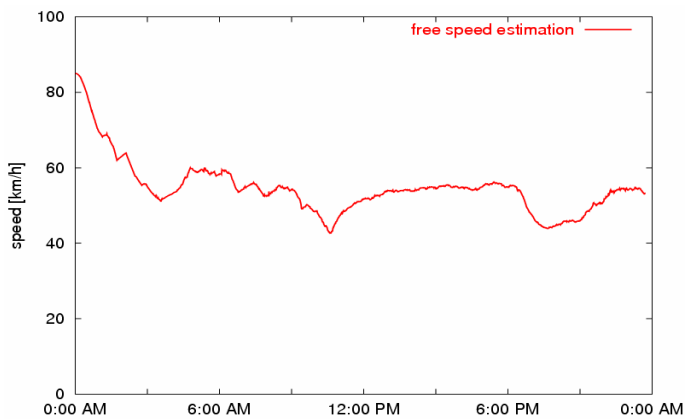
(g)
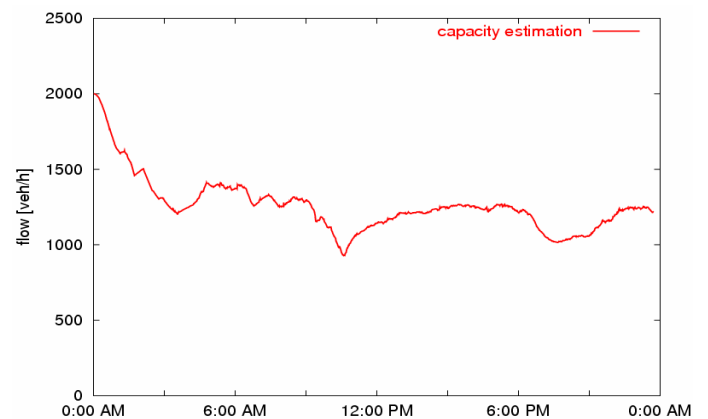
(h)

Figure 86: Free speed and capacity estimates along A3 in Naples direction on October 10, 2006

93
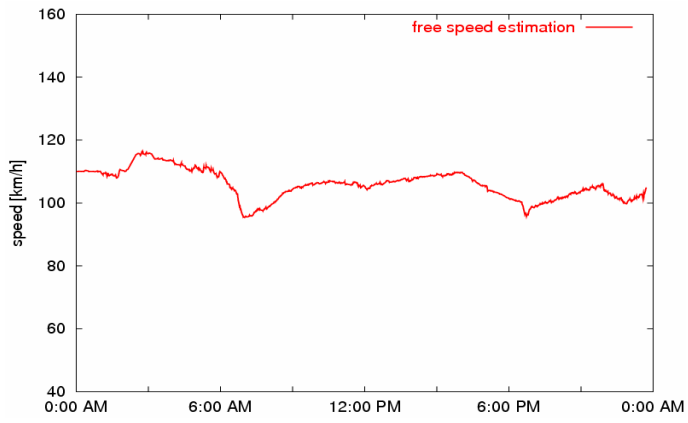
(a)
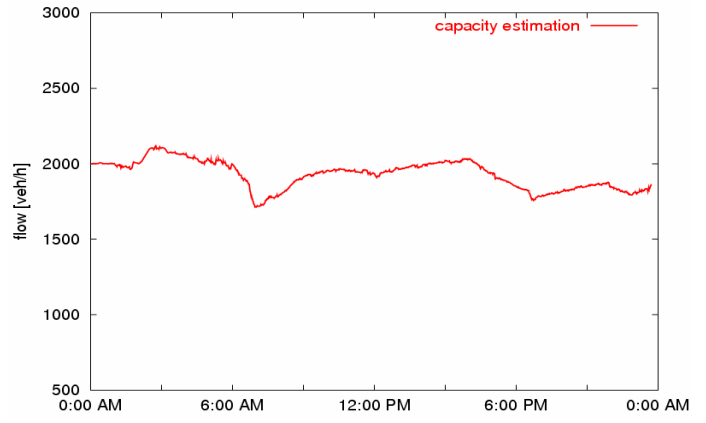
(b)
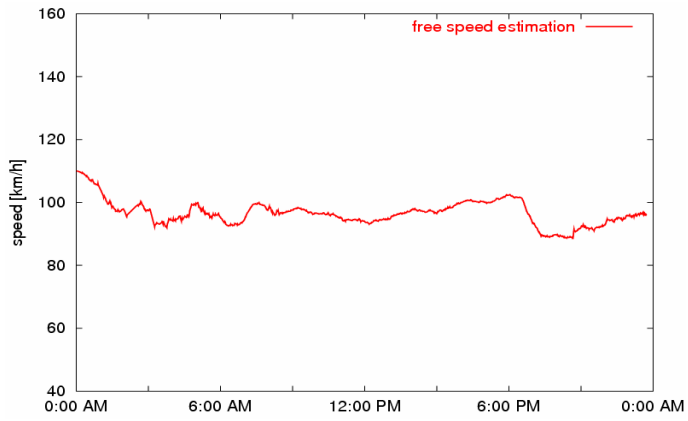
(c)
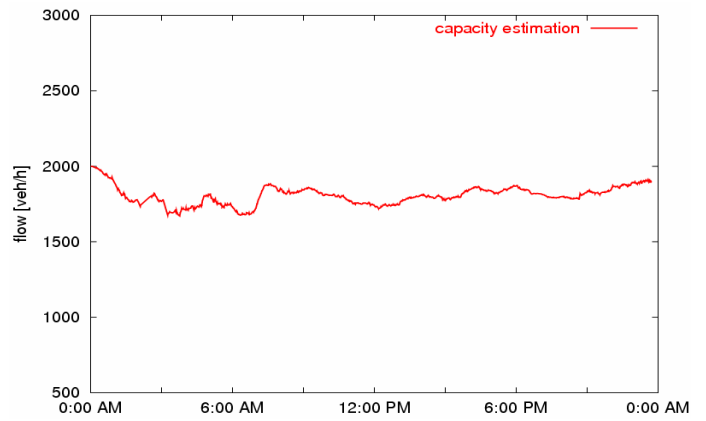
(c)

Figure 87**: Free speed and capacity estimates along A3 in Naples direction on October 10, 2006**
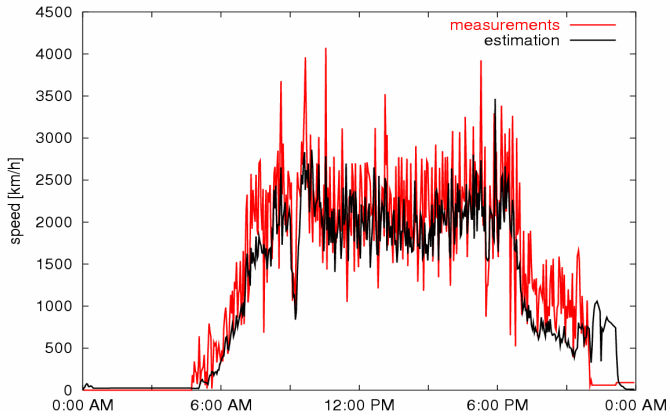
Figure 88: Flow at D10004, October 10
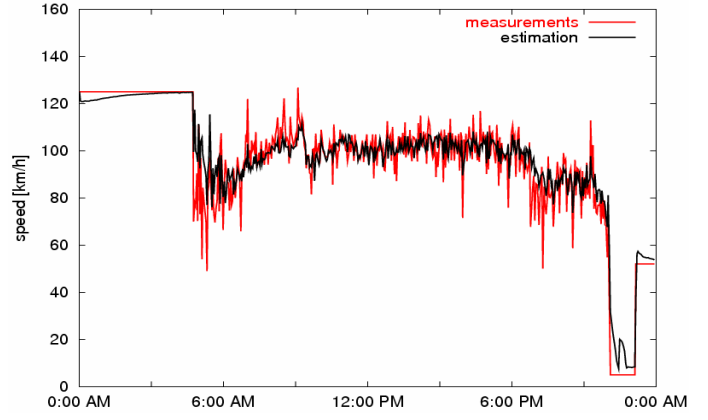
Figure 89: Speed at D10004, October 10
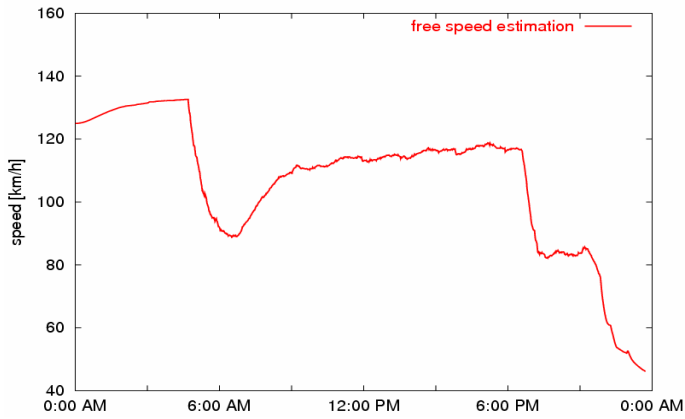
Figure 90: Free speed around D10004, October 10
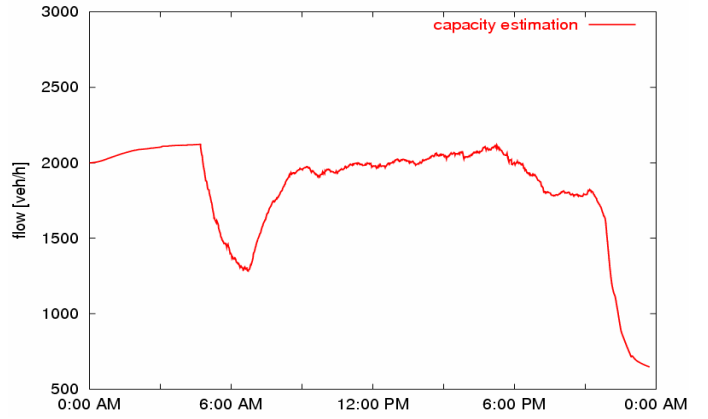
Figure 91: Capacity around D10004, October 10

Switching of D10004 from a faulty to correct status
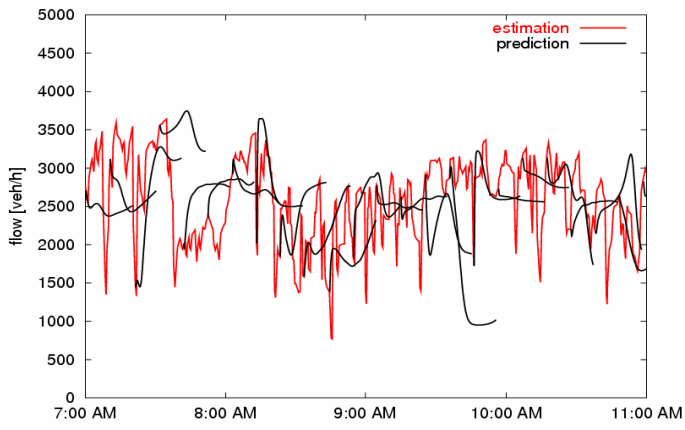
Figure 92: Flow around D10019, May 25
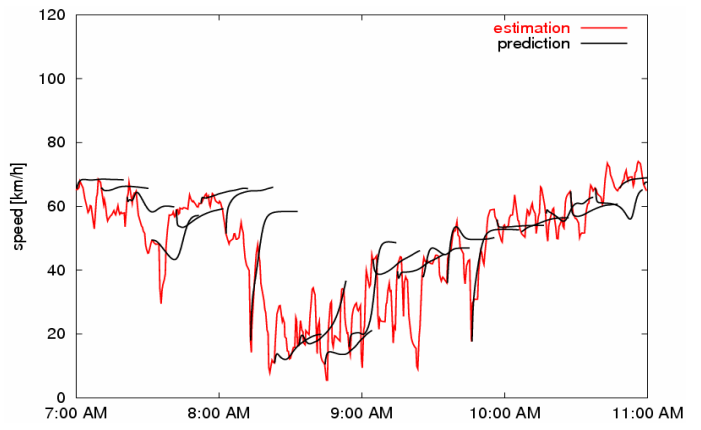
Figure 93: Speed around D10019, May 25
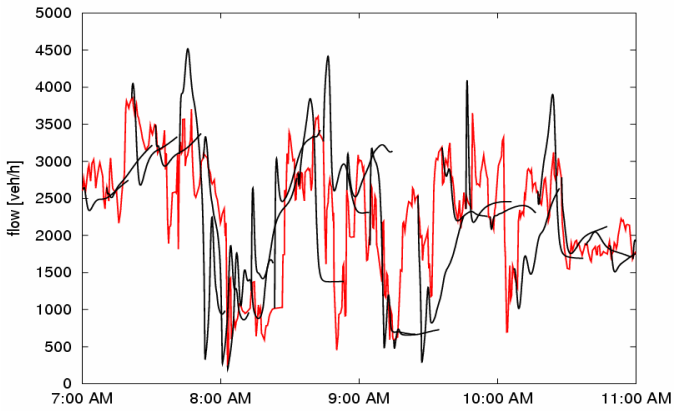
Figure 94: Flow around D10024, May 25
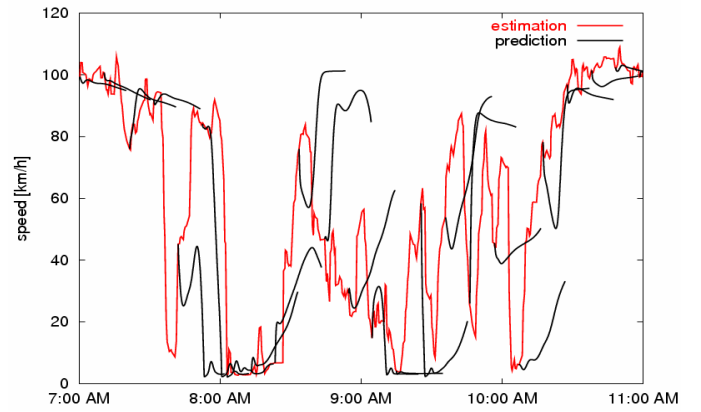
**Figure 95: Speed around D10024, May 25**
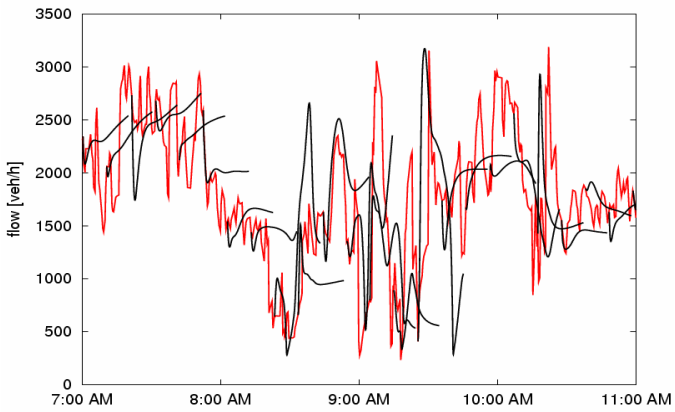
**Figure 96: Flow around D10003, May 25**
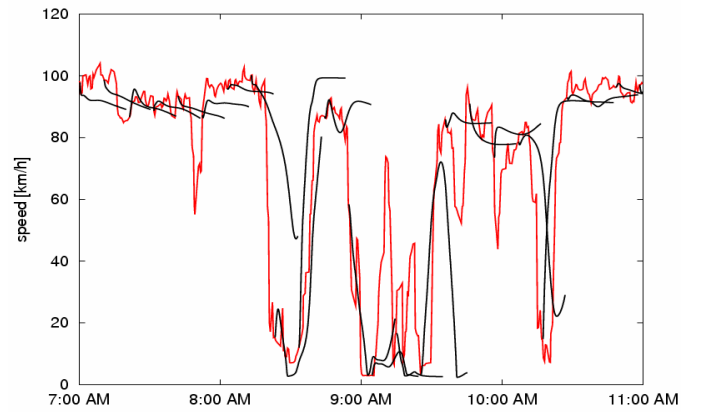
**Figure 97: Speed around D10003, May 25**
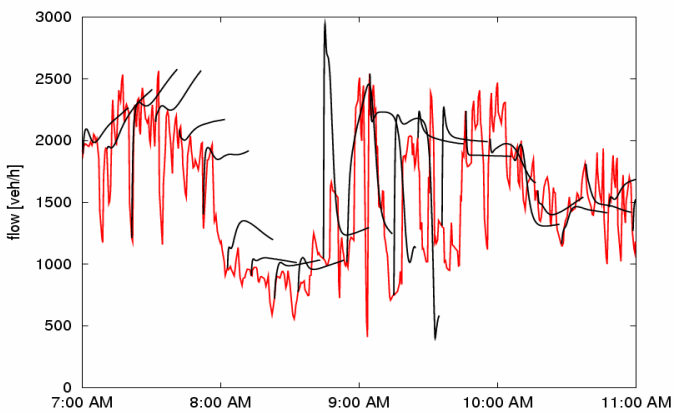
Figure 98: Flow around D11014, May 25
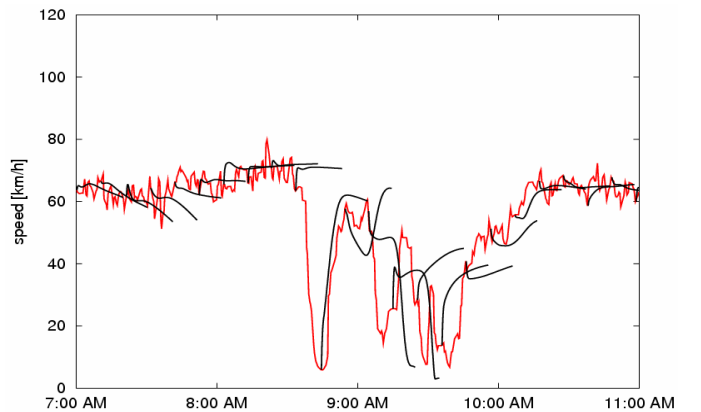
Figure 99: Speed around D11014, May 25

96
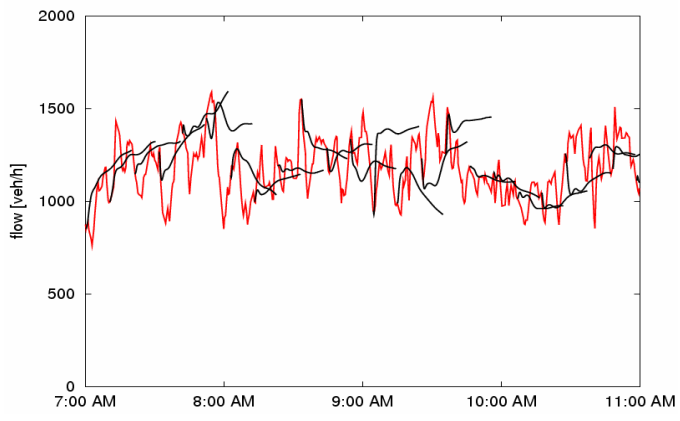
Figure 100: Flow around D11009, May 25
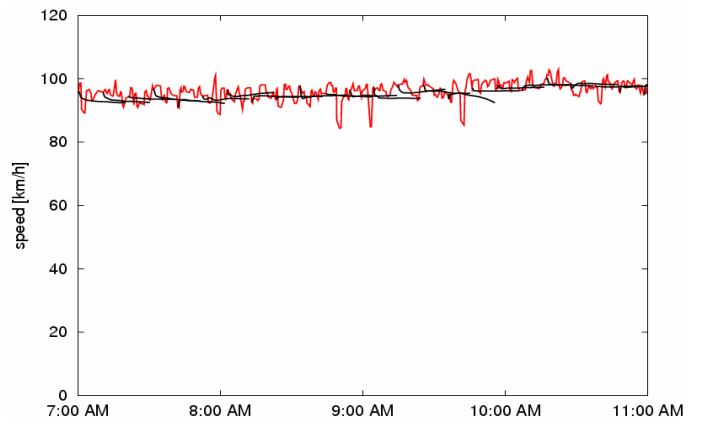
Figure 101: Speed around D11009, May 25
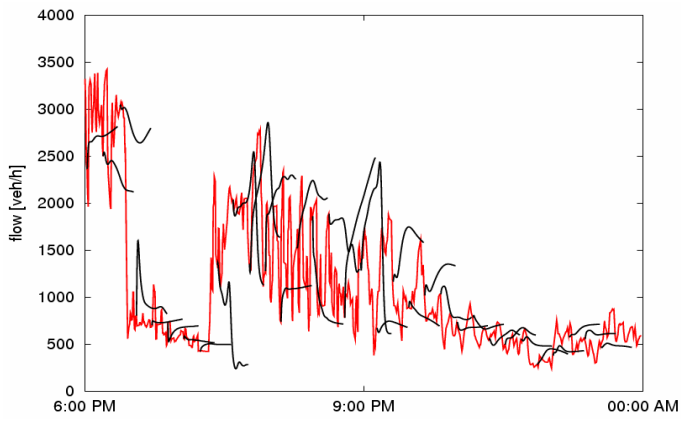
Figure 102: Flow around D10019, May 28
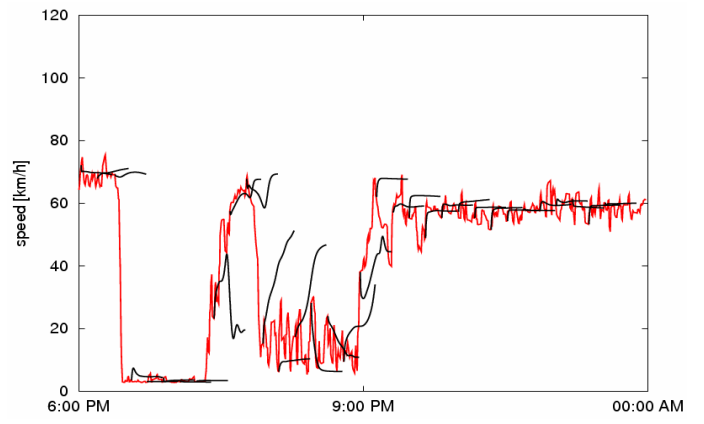
Figure 103: Speed around D10019, May 28
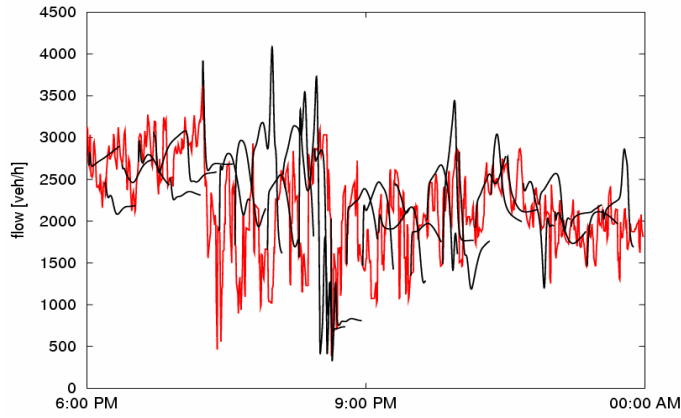
Figure 104: Flow around D10024, May 28
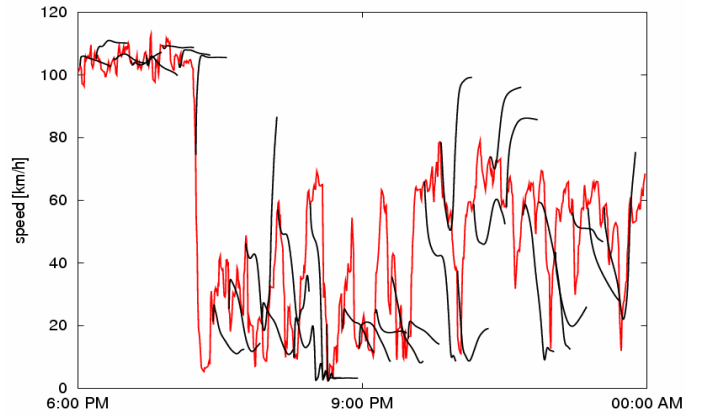
Figure 105: Speed around D10024, May 28
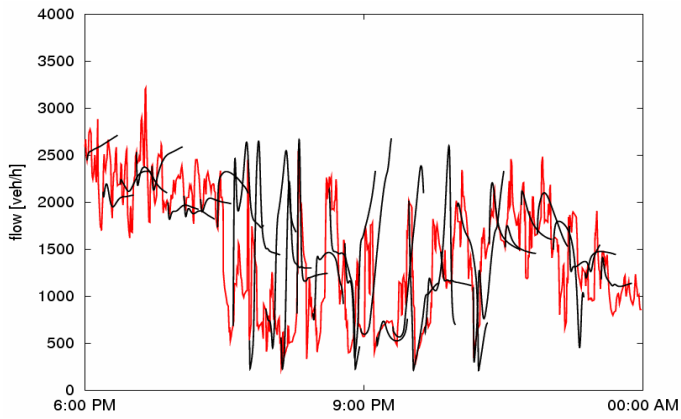
Figure 106: Flow around D10003, May 28
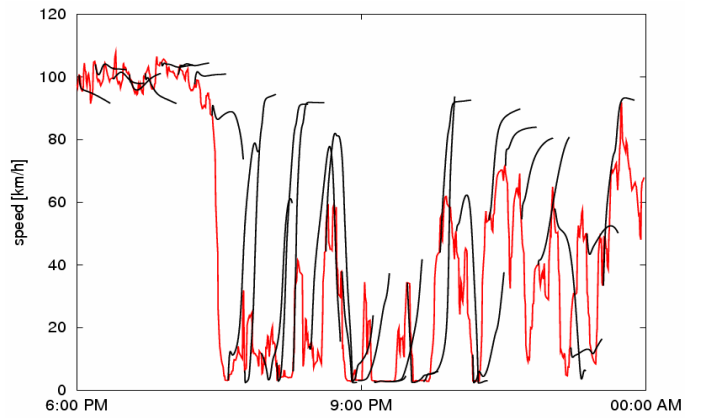
Figure 107: Speed around D10003, May 28
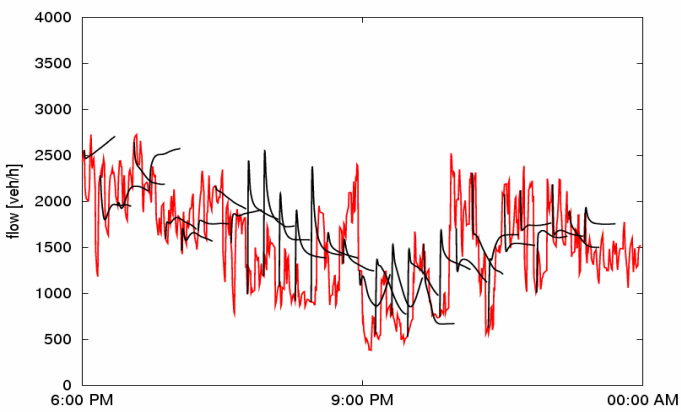

Figure 108: Flow around D11014, May 28
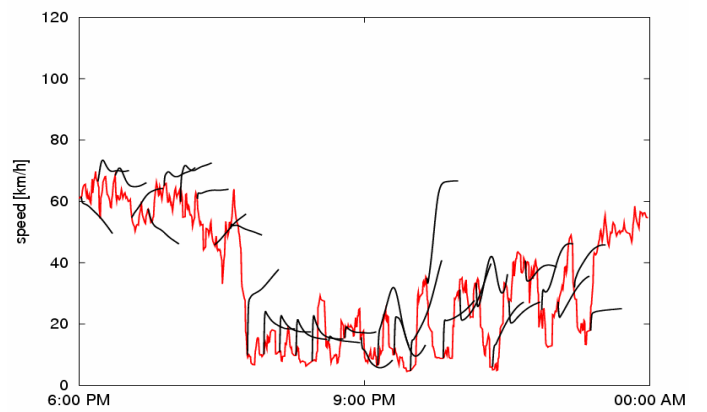
Figure 109: Speed around D11014, May 28

98
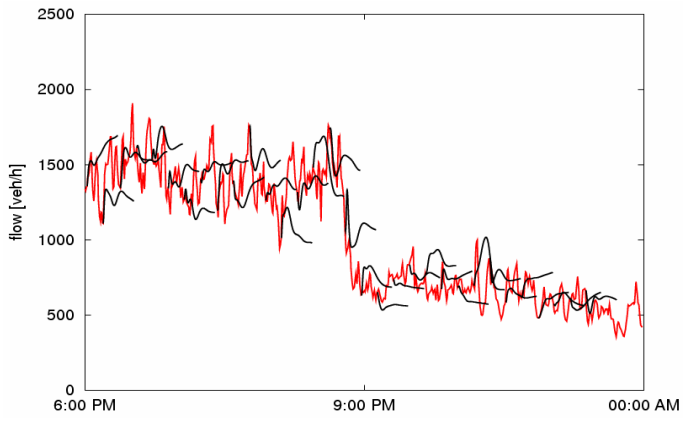
**Figure 110: Flow around D11009, May 28**
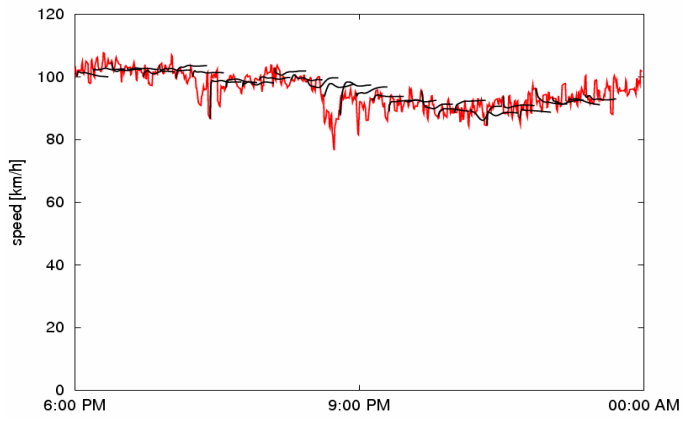
Figure 111: Speed around D11009, May 28

**Figure 112: An inner congestion**
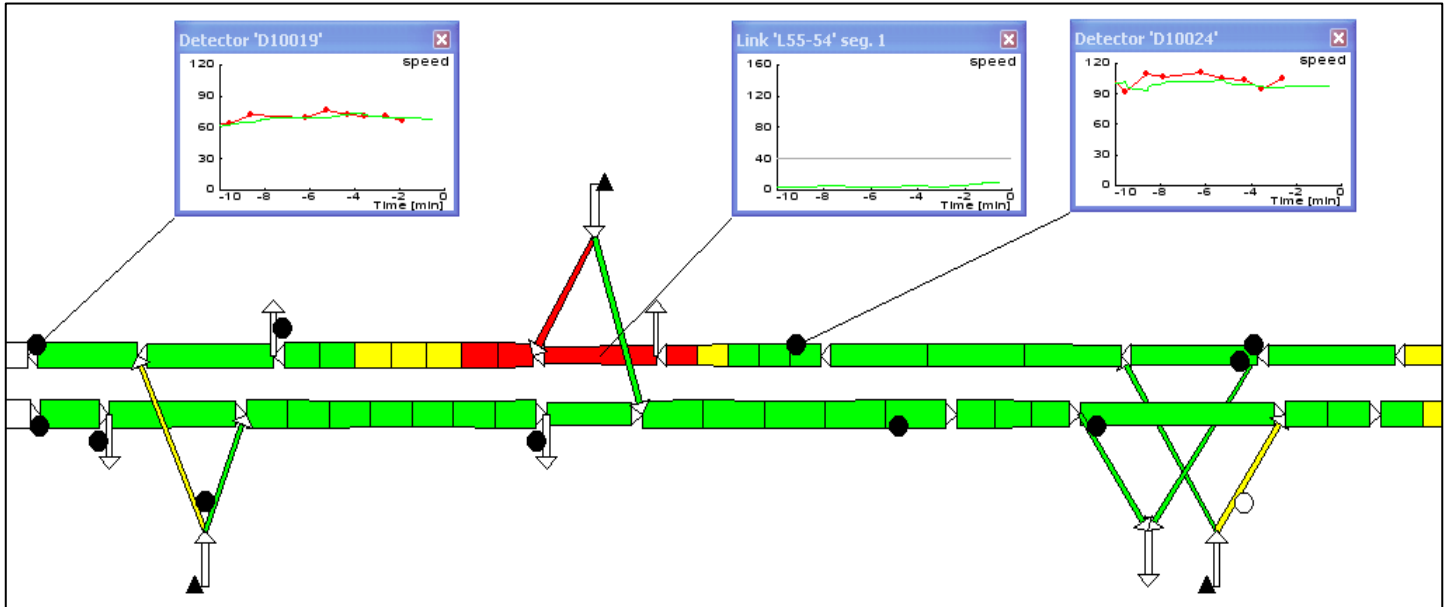
Figure 113: A GUI view of an inner congestion IN 1
(The grey line in the second window represents the speed threshold for congestion)
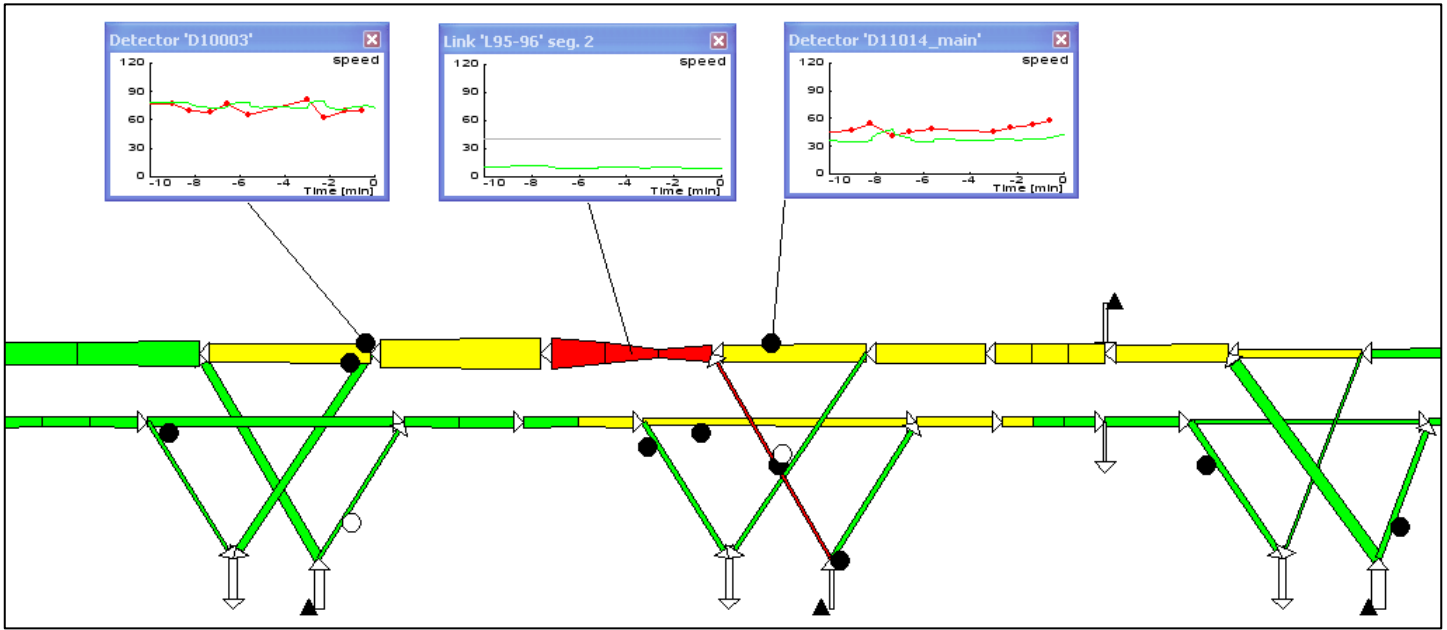
(a)
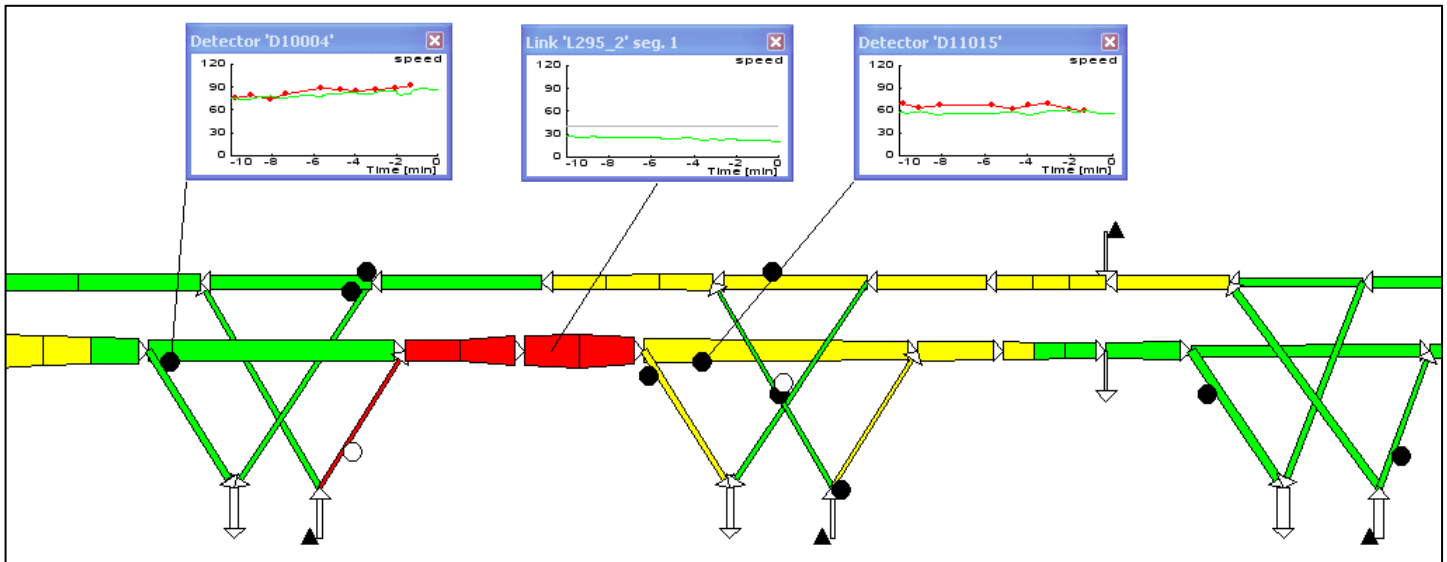
(b)

**Figure 114: Inner congestions: (a) IN 2; (b) IN 3**
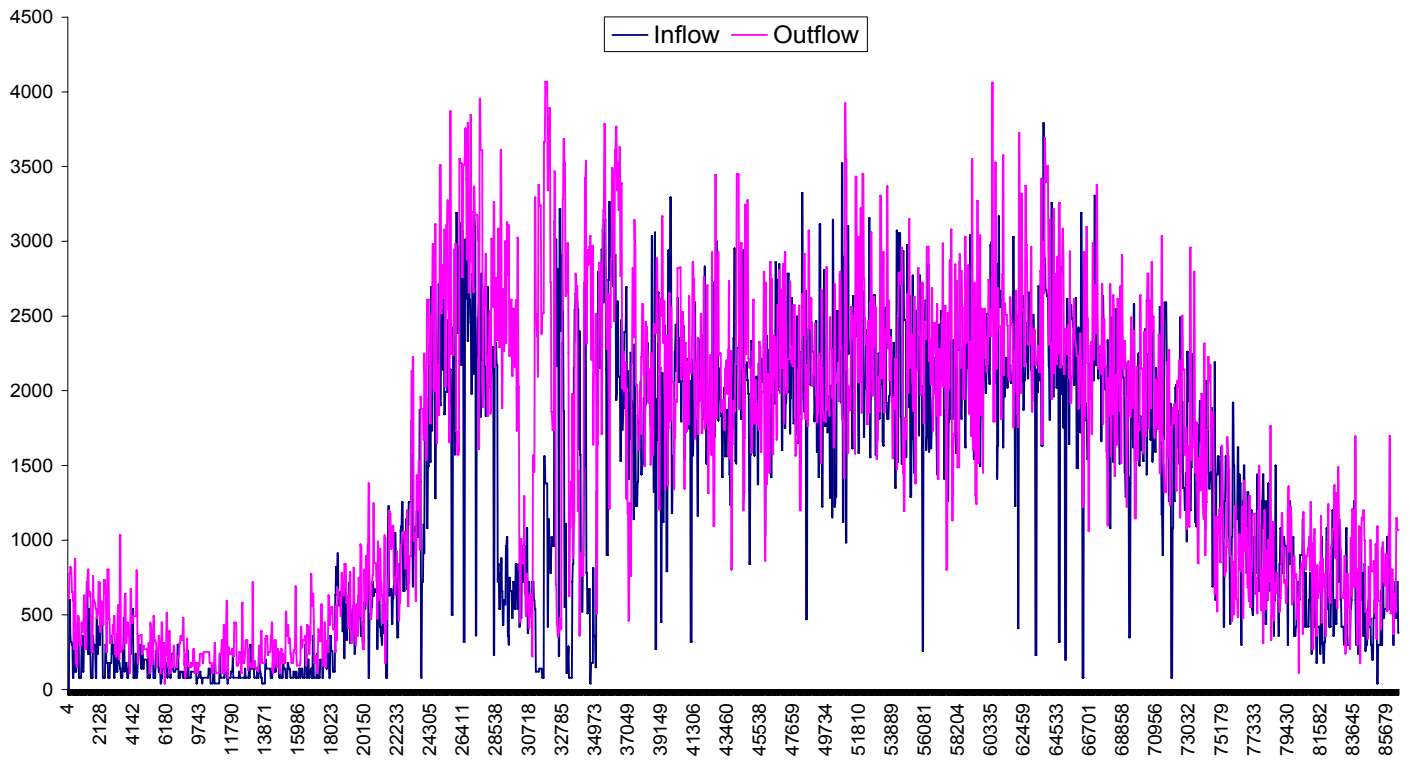
**Figure 115: Flow balance checking for IN 2 with data from May 25, 2006**
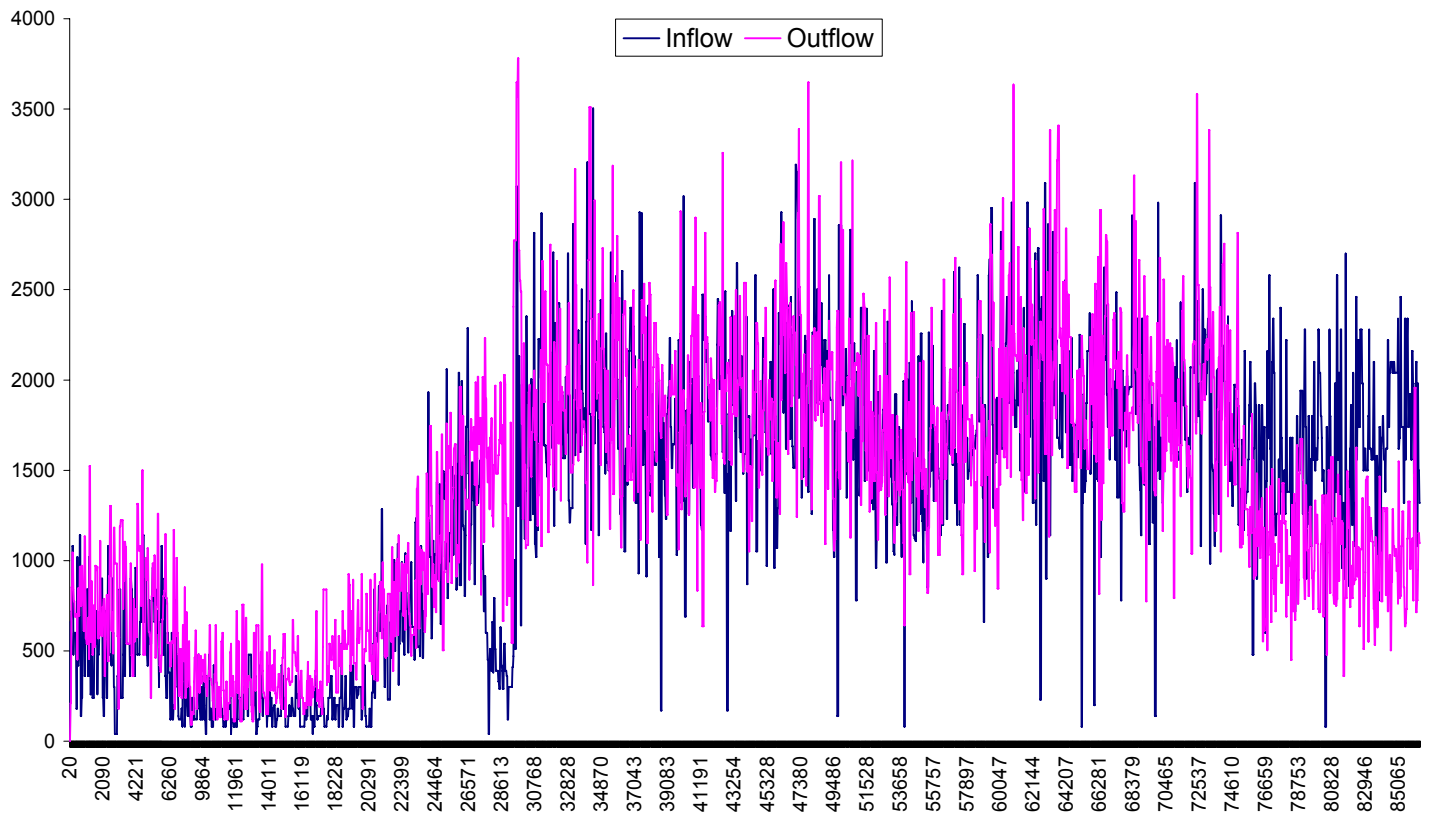
(a)
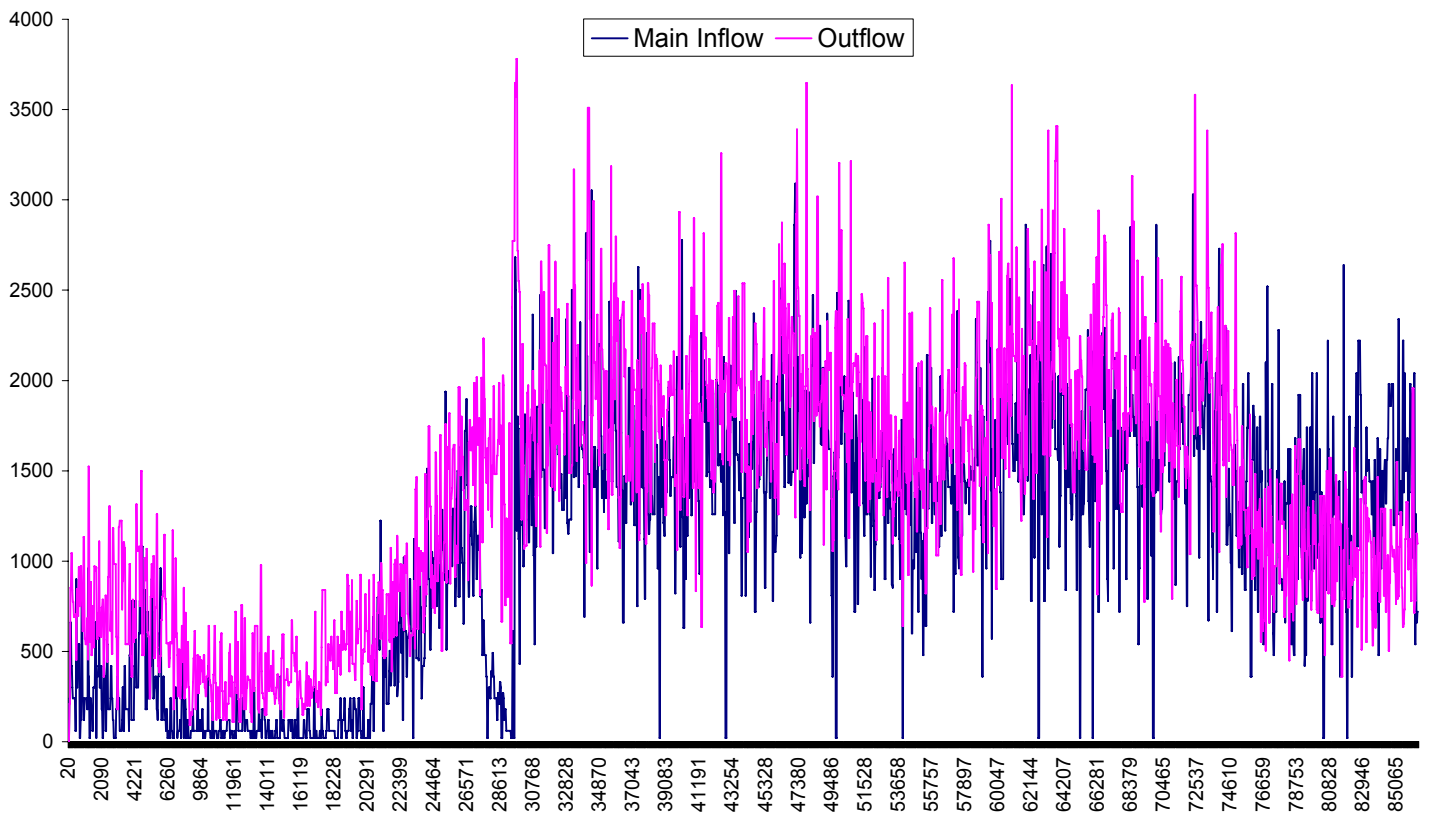
(b)

Figure 116: Flow balance checking for IN 2 with data from October 6, 2006

103
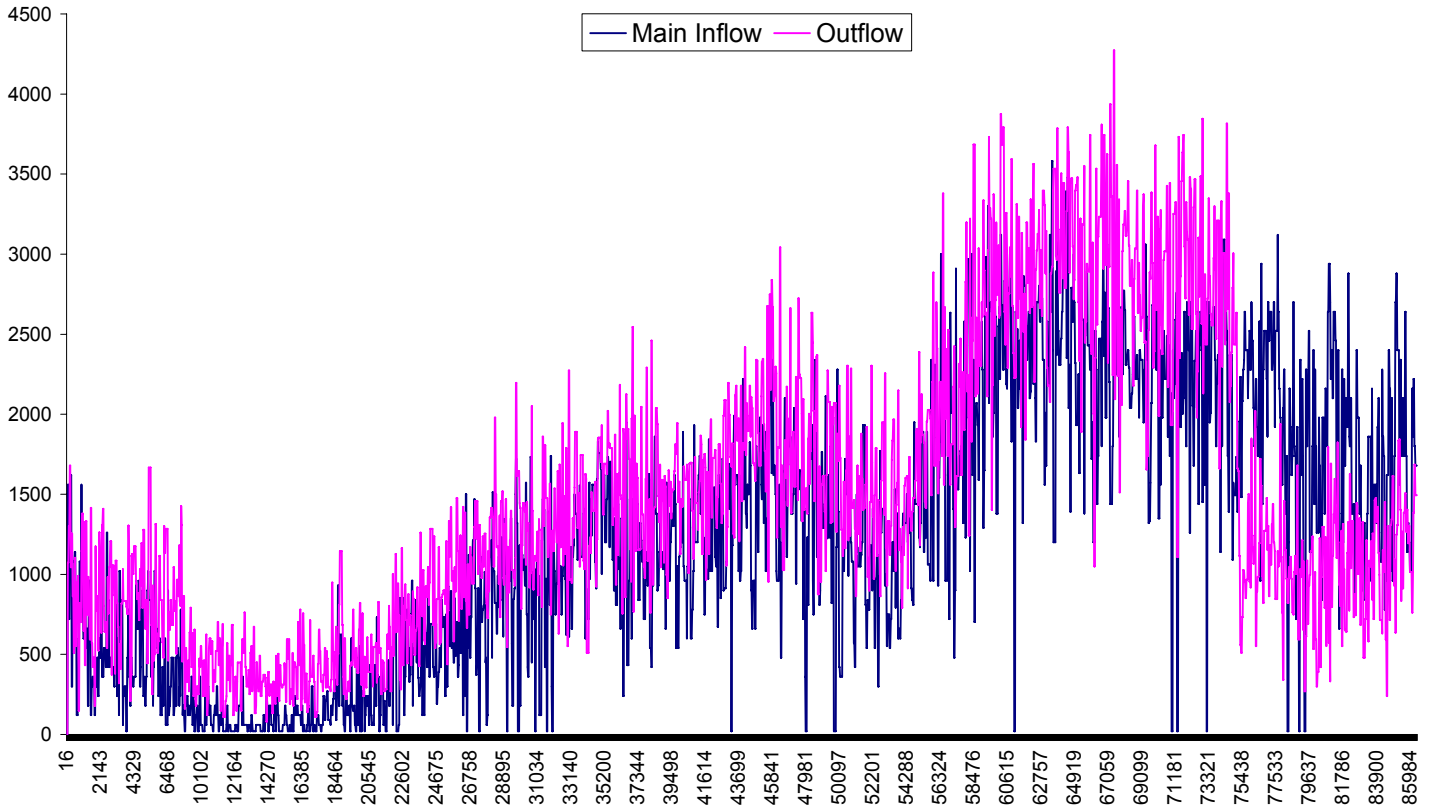
(a)
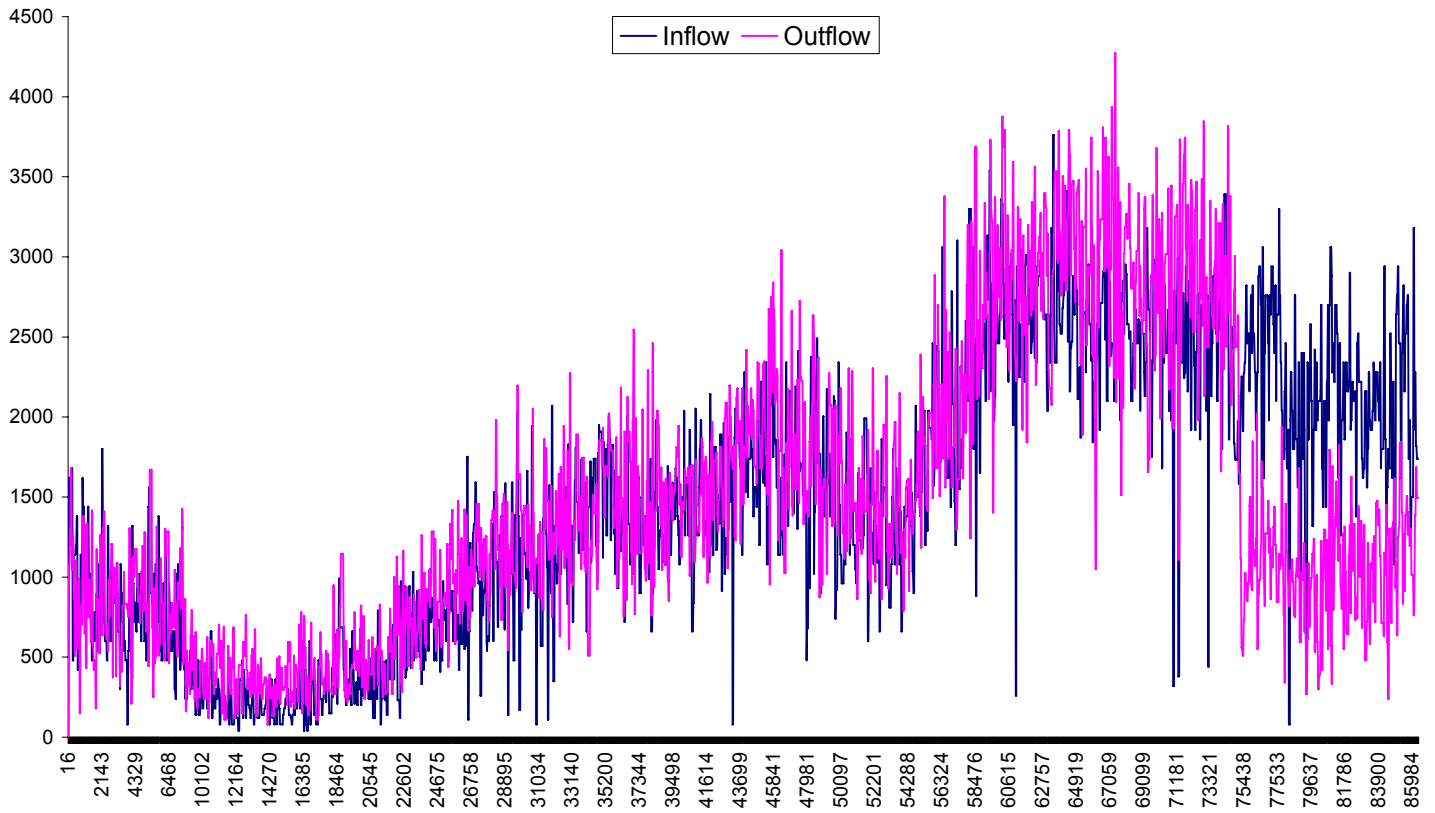
(b)

Figure 117: Flow balance checking for IN 2 with data from June 18, 2006

Table 1: Data checking results for IN 2 and IN 3

	IN 2		IN 3	
	Comparison 1	Comparison 2	Comparison 1	Comparison 2
May 25	√		×	×
May 28	√		×	×
June 9	√		×	×
June 10	×	√	×	×
June 16	√		×	×
June 17	√		√	
June 18	×	×	√	
June 19	×	×	√	
June 23	√		×	×
June 24	×	√	×	×
June 25	×	√	×	×
Sept. 15	√		×	√
Sept. 18	√		×	×
Sept. 20	√		×	×
Oct. 6	×	√	×	×
Oct. 8	√		×	×
Oct. 9	√		×	×
Oct.10	√		×	×
Oct.15	√		×	×
Oct.20	√		×	×

Table 2: Inner congestions IN 1 and countermeasures

	Basic RENAISSANCE turning rate SD setting	**Improved** RENAISSANCE turning rate SD setting
May 25	10:00 AM– 12:30 AM	09:43 AM – 10:41 AM
June 10	08:15 AM– 23:59 PM	08:15 AM – 08:45 AM
June 18	20:20 PM – 23:00 PM	20:30 PM – 21:10 PM
June 19	09:00 AM – 23:45 PM	07:20 AM– 08:20 AM
June 23	20:30 AM– 23:59 PM	20:00 PM– 20:30 PM
June 25	19:40 PM – 22:13 PM	none